Effect of Remodeling Root Surfaces by New Cementum Formation on Orthodontically Induced Tooth Root Resorption in Rats

by

Mahmoud Abdulsalam Alsulaimani

A thesis submitted in partial fulfillment of the requirements for the degree of

Doctor of Philosophy

Medical Sciences - Orthodontics

University of Alberta

ABSTRACT

Background: The etiology of dental root surface resorption associated with orthodontic tooth movement is not fully understood. However, under normal circumstances, the cementum layer covering the dental root surfaces provides a protective barrier against resorption.

Objective: To investigate the effect of cementum layer remodeling, induced either by cyclosporine A (CsA) or by low-level laser therapy (LLLT), on the amount of root resorption caused by orthodontic tooth movement.

Methods: Two different animal experiments were performed. The first experiment lasted two weeks and used three groups of female Sprague-Dawley (SD) rats as follows: six rats received daily 10mg/kg CsA subcutaneous injections; six rats received daily LLLT treatment delivered by gallium-aluminum-arsenide (GaAlAs) laser at an 830nm wavelength; and six rats received no treatment (control). *In vivo* micro-computed tomography (micro-CT) was used to analyze volumetric changes in the root hard tissue. The cementum thickness was also evaluated histologically. A follow-up split-mouth study was performed using nine female SD rats. The right side maxillary first molars received daily LLLT treatment using the same laser exposures as in the previous experiment for two weeks. The left side was not treated and served as the control. Immediately after LLLT treatment, orthodontic appliances were placed bilaterally to move the right and left molars mesially over four weeks. *Ex vivo* micro-CT was used to evaluate the volume of root resorption. The extent and severity of root resorption were then assessed histologically.

Results: In the first experiment, the cementum was significantly thicker (P=0.019) over the root surfaces in the LLLT group compared with the control and CsA groups. The follow-up experiment showed significantly less (P=0.028) root resorption volume due to tooth movement on the LLLT side compared with the control side. This protective effect against root resorption was more, on average, on the root surfaces that showed more cementum growth in response to our LLLT treatment.

Conclusion: Our LLLT treatment significantly increased the thickness of dental root cementum in rats. Moreover, remodeling of the rats' dental root surfaces using our LLLT treatment resulted in a significant decrease in the volume of root surface resorption following application of orthodontic force.

PREFACE

This thesis is an original work by Mahmoud Alsulaimani. The animal experiments protocol, of which this thesis is a part, was approved by Animal Care and Use Committee for Health Sciences at University of Alberta (animal use protocol number: 601, 2009).

Parts of this thesis first experiment have been published as: Alsulaimani M, Doschak M, Dederich D, Flores-Mir C. “Effect of low-level laser therapy on dental root cementum remodeling in rats”. Orthod Craniofac Res. 2015 May; 18 (2): 109-16. I was responsible for the data collection and analysis as well as the manuscript composition of this article. Doschak M and Dederich D contributed to manuscript edits. Flores-Mir C was the supervisory author and was involved with the manuscript composition.

Dedicated to all my family members, each of whom is the blessing and the true meaning of my life

ACKNOWLEDGMENTS

First and foremost, I would like to express an immeasurable appreciation towards my family for supporting me in completing this endeavor. Words cannot express how much grateful I am to my beloved wife **Tahani**, who is always by my side especially during the most difficult of times. I am, as ever, deeply thankful to her and to my lovely children, **Hisham**, **Hala** and **Aleen** for always making me inspired and hopeful especially during times of uncertainty. Nothing in this world is more inspiring than hearing my children says: "We love you dad more than infinity". I am also greatly indebted to my **Mom** and **Dad**, who have raised me up and helped me fulfill my dreams. I would never forget their sacrifices and prayers that have sustained me in distress and helped me get this far. I also would like to thank my **Brothers** and **Sisters** for always encouraging me to strive towards my goal.

Special thanks to my supervisors: **Dr. Carlos Flores-Mir** and **Dr. Douglas Dederich** for their guidance, advices, patience and valuable comments that contributed in making this research possible. I will always be grateful to them mainly because they believed in me and gave me the opportunity to continue my PhD program. I am also deeply thankful to my supervisory committee member: **Dr. Michael Doschak**, for his excellent guidance and constructive criticism that helped shape my thinking and reconstruct my research direction.

Many thanks to everyone in the Graduate Orthodontics Program for making my life in the program much less difficult than it could be. Special thanks to Dr. Giseon Heo for her valuable statistics guidance. Micro-CT imaging was done by great help from the Pharmaceutical Orthopaedic Research Lab team at University of Alberta. I also thank the HistoCore staff in Alberta Diabetes Institute at University of Alberta for their help in the histological processing. This study was funded by both Saudi Arabian Cultural Bureau in Canada and the University of Alberta.

TABLE OF CONTENTS

LIST OF TABLES

LIST OF FIGURES

LIST OF ABBREVIATIONS

AAC	Acellular afibrillar cementum
AEFC	Acellular extrinsic fiber cementum
ANCOVA	Analysis of covariance
ANOVA	Analysis of variance
ATP	Adenosine triphosphate
b-FGF	basic fibroblast growth factor
BGN	Biglycan
BMP	Bone morphogenetic protein
Ca^{2+}	Calcium ions
CAP	Cementum attachment protein
CIFC	Cellular intrinsic fiber cementum
CMSC	Cellular mixed stratified cementum
CO_2	Carbon dioxide
CsA	Cyclosporine A
CTGF	Connective tissue growth factor
ECM	Extracellular matrix
ERM	Epithelial rests of Malassez
Er:YAG	Erbium: Yttrium Aluminium Garnet
FGF	Fibroblast growth factor
GaAlAs	Gallium-aluminum-arsenide
GaAs	Gallium-arsenide

GO	Gingival overgrowth
HbO_2	Hemoglobin
H&E	Hematoxylin and eosin
HEBP	1-hydroxyethylidene-1, 1-bisphosphonate
HeNe	Helium-Neon
HERS	Hertwig's epithelial root sheath
Ho	Null hypothesis
H_2O_2	Hydrogen peroxide
IGF	Insulin-like growth factor
IL	Interleukin
J	Joules
LLLT	Low-level laser therapy
Micro-CT	Micro-computed tomography
MMP	Matrix metalloproteinases
Nd:YAG	Neodymium-doped: Yttrium Aluminium Garnet
NF-kB	Nuclear factor kappa B
NO	Nitric oxide
NSAID	Non-steroidal anti-inflammatory drugs
O_2^-	Superoxide anions
OITRR	Orthodontically induced tooth root resorption
OPG	Osteoprotegrin
PDGF	Platelet-derived growth factors

PDL	Periodontal ligament
PG	Prostaglandin
PP_i	Inorganic pyrophosphate
PTH	Parathyroid hormone
RANK	Receptor activator of nuclear factor kappa B
RANKL	Receptor activator of nuclear factor kappa B ligand
RGD	Arginine-glycine-aspartic acid
ROS	Reactive oxygen species
RVD	Root-Volume-Difference
RVDP	Root-Volume-Difference-Proportion
SD	Sprague-Dawley
SLRP	Small leucine-rich proteoglycan
SOD3	Superoxide dismutase 3
TGF-β	Transforming growth factor-β
TH	Thyroid hormone
TIMP	Tissue inhibitor of metalloproteinase
TNF	Tumor necrosis factor
TRAP	Tartrate resistant acid phosphatase
T-test	Student T-test
W	Watts
$\Delta\Psi_m$	Mitochondrial membrane potential

1 INTRODUCTION

Dental root external surface resorption is a common deleterious result of orthodontic tooth movement that can cause tooth mobility or even tooth loss. The pathology behind this negative side effect is partially unknown. However, based on several reports from the literature, we propose that tooth root surface remodeling by inducing new cementum formation might be an important preventive factor that influences the onset and the progression of orthodontically induced tooth root resorption (OITRR). If our hypothesis were correct, it would be a novel discovery. This study will help to provide a better understanding of the relationship between the remodeling activities of dental root cementum and the pathological consequences of OITRR. This could be an important contribution toward reducing one of the most potentially negative side effects in orthodontic treatment.

We hypothesize that the systemic administration of cyclosporine A (CsA) or the local application of low-level laser therapy (LLLT), will induce new cementum formation in sound rat tooth root surfaces and subsequently prevent OITRR. Although extrapolation from animal studies to humans is not directly feasible or completely accurate, our experiments can provide good insights as to possible mechanisms that may also work well in humans.

2 LITERATURE REVIEW

2.1 Orthodontically Induced Tooth Root Resorption

2.1.1 Prevalence and Complication of OITRR

Root resorption is a general term used to describe the physiological or pathological process resulting in structural loss of dental root cementum and/or dentin. In OITRR, the destructive processes affect the external surfaces of dental root, as a consequence of orthodontic tooth movement. It was first related to orthodontic treatment during the beginning of the last century and has become one of the major topics of orthodontic research since then (1).

OITRR is a common phenomenon. The frequency of teeth showing some grades of OITRR is quite high. All orthodontically moved teeth in both dental arches are susceptible to OITRR because of the fact that even a light orthodontic force can produce a considerable amount of root resorption due to the relatively long duration of conventional orthodontic treatment (2). The maxillary anterior teeth are the most common sites for OITRR and the worst resorption is often seen in maxillary lateral incisors and in teeth with abnormal root shape (3, 4).

Intra-oral radiographs do not accurately detect early stages and certain aspects of OITRR, in comparison to the more precise histological evaluation. For this reason, it is difficult to accurately assess the incidence, “number of new cases” and prevalence, “number of existing cases in a certain population”, of OITRR (5). However, in a prevalence study, it was shown that the frequency of incisors

showing some grades of root resorption increased from 15% before orthodontic treatment to 73% after treatment. The percentage of teeth with moderate root resorption increased from 1% before orthodontic treatment to 25% after treatment. Severe root structural loss (resorption beyond one third of root length) was a rare event with one instance before orthodontic treatment and 13 sites (2%) after treatment (6). Another prevalence study showed that one third of orthodontically treated individuals experienced more than 3mm of root resorption and only 5% had more than 5mm of root resorption (7).

The major effects of severe OITRR are related to an impaired tooth crown/root ratio that can result in morbidity that ranges from mild tooth mobility to tooth loss, if the remaining total root length is less or equal to 9 mm (8). Teeth with OITRR are asymptomatic and the pulp usually vital unless the pressure of the force reaches a high enough level to clinically compromise the tooth blood supply in the apical area (9).

2.1.2 Risk Factors of OITRR

The onset and progression of OITRR are associated with many different risk factors that are related to orthodontic tooth movement. These factors include: the magnitude of the dental root displacement, treatment duration (10), magnitude of the applied force (10, 11), direction of the applied force (12, 13), method of force application (continuous or intermittent) (13, 14), age (15), root morphology (16-18) and/or genetic factors (19).

Many different studies of the effect of orthodontic treatment-related factors on degree of pathology have suggested that root resorption is correlated with total root displacement, treatment duration and magnitude of orthodontic force (4, 10, 20). A greater degree of root resorption is directly related with the longer duration of teeth movement and also with the higher magnitude of applied orthodontic force (21).

The direction and method of force application are other treatment-related factors that influence the degree of OITRR. In orthodontics, torquing movement describes the root movement either buccally or lingually, whereas crown tipping describes the tooth crown tipping movement either mesially or distally. Torquing movements of the maxillary incisors root lingually are strongly correlated with the occurrence of OITRR. Intrusive tooth movements also cause higher degree of root resorption as they concentrate the pressure to a small area on the apex (12, 13, 22). In combination, intrusive movement and lingual root torque could be the major causes of OITRR in maxillary anterior teeth (12). On the other hand, bodily movements (i.e. translation), extrusion and crown tipping are associated with a lower risk of OITRR because the stress is distributed along a wide area on the root (12). Intermittent orthodontic force results in a lesser degree of root resorption than a continuous force application since the rest period in treatment with intermittent force could allow the traumatized cementum to heal and thus prevent further resorption (13, 14).

Other studies have been done to illustrate certain patient-related risk factors that may cause or facilitate OITRR. These groups of factors include: patient age, root morphology and genetic predisposition. Patients treated early, before 11 years of age, are found to have less OITRR than those who are treated later (15). Root morphology affects the stress distribution of orthodontic force. More stress concentrations are related to roots with short, bent and pipette shaped (markedly tapered at apical end), which lead to increased vulnerability of these sites to OITRR (16, 17, 23).

Stress is generally concentrated at the compressed root side following the application of orthodontic force. Therefore, any decrease in catabolic remodeling rate (turnover rate) that should happen at the cortical surface of the alveolar bone opposing the dental root during tooth movement may result in greater stress concentration at the root surface that could facilitate the process of OITRR. Genetic factors are found to be responsible for the variation in catabolic bone remodeling rate (turnover rate) among orthodontic patients, which may account for the variation in OITRR severity among different populations (19).

Finally, it is important to emphasize that none of the aforementioned studies had claimed that OITRR is caused directly or exclusively by only one of the previously discussed risk factors. Some authors believe that other etiological key factors have yet to be identified (5, 24).

2.1.3 Histopathology and Pathogenesis of OITRR

Three different degrees of OITRR severity are described histologically based on the extent of the injury and the subsequence prognosis of this resorption process (24). Surface resorption, involving only the outer layer of cementum, is fully regenerated or remodeled once the pressure caused by orthodontic force has been removed. Deep resorption, involving the cementum and the outer layers of dentin, is usually repaired with cementum material to restore the root shape and function. Root shortening is an irreversible form of OITRR resulting from a total destruction of the hard tissue component of the root apex. No regeneration is possible when the root loses the dentin layer beneath the cementum (24).

The detailed pathological events that influence the onset and the progression of the OITRR are not completely known. However, the process of root resorption requires two major etiological factors: a mechanical injury to the dental root protective tissues and a persistent inflammatory stimulation caused by the continuous orthodontic pressure (9). The pressure caused by orthodontic force could directly lead to mechanical damage of the protective layer that covers the dental root, which consists of cementum and the non-mineralized tissues covering the external surface of the root (precementum). Thereafter, multinucleated cells, odontoclasts, colonize the exposed root tissue and initiate the process of root resorption (9). At this stage, the resorption process will end spontaneously once the pressure caused by orthodontic force has been removed. Repair of root surface

will start after that with new cementum tissue formed during the following 2-3 weeks (9).

Figure 1: the histopathology of root resorption induced by orthodontic tooth movement. Photomicrograph (25) of the hyalinized zone (H) between alveolar bone (B) and root surface (T). Large black arrow represents the direction of tooth movement. Open arrow shows alveolar bone resorption; small arrows indicate thin line of bone between the resorbed bone and hyalinized tissue. Root resorption lacunae (R), mono and multi-nucleated cells (arrow heads) at the periphery of the hyalinized tissue.

A long lasting pressure produced by orthodontic force during tooth movement disturbs the blood supply in the periodontal ligament (PDL) that surround root, resulting in an ischemic necrosis next to the compressed root surface (24, 26). The sterile necrotic tissue then triggers biochemical signals that activate macrophage-like and multinucleated cells to eliminate necrotic tissues. This process of

eliminating necrotic tissues starts at the periphery of the hyaline zone (Figure 1) (25). The elimination process itself can extend to the adjacent cementum layer and, therefore, exposing the root surface (24, 26). Later, multinucleated cells migrate and settle in resorption lacunae at the surface of the unprotected root. The initiation of the resorption process increases the root surface area in order to decrease the pressure exerted through force application (24).

Mononucleated cells are found to be the initial cells involved in the necrotic tissue elimination phase (25). These initial cells stained negatively for tartrate resistant acid phosphatase (TRAP) which indicate that these cells are non-osteoclastic lineage, and resemble macrophages or fibroblasts, because osteoclast-like cells and their precursors stained positively for TRAP (27). At a later stage, the bulk of necrotic periodontal ligament (PDL) tissue and the adjacent root cementum layers are removed by giant multinucleated TRAP-positive cells without a ruffled border, as well as mononucleated macrophage-like cells (25-28). After that, multinucleated TRAP-positive cells with ruffled borders (also called odontoclasts) colonize the exposed root surface and also could be found in the deeper root resorption lacunae (25-28). TRAP-positive enzymatic reaction was also seen penetrating the dentinal tubules (28). These findings indicate that TRAP-positive cells, which derive from mononucleated phagocytic system, are important in the removal of the necrotic tissue as well as in the resorption of the root surface (25, 26).

Local biochemical mediators generate complex inflammatory interactions, which follow the application of orthodontic force. The biological remodeling activities, of the connective tissues surrounding the dental root, respond markedly to the increase in the expression of the proinflammatory cytokines, such as IL-1β, IL-6, IL-1α and TNF-α, that occur during tooth movement (29, 30). Orthodontic pressure was also found to increase the expression level of CD40 (a cell surface receptor that belongs to the tumor necrosis receptor family (TNF-R)) in the compressed periodontal ligament tissues, and thus facilitates the interaction with its counter-receptor, the CD40L. These interactions activate T-cells to produce inflammatory reactions that could facilitate the process of root resorption (31).

Repair processes of OITRR take place at the resorption lacunae in order to restore the integrity of the root surface as well as the functional relation with the adjacent periodontal membrane. It seems that the repair process of OITRR is similar to the cementogenesis process occurring during tooth development (32). The repair process is started early with invasion of fibroblast-like cells from the surrounding periodontal connective tissues into the periphery of the resorption lacuna, in the same time that active resorption by multinucleated cell (odontoclast) is taking place in the central part of the lacuna (32). Once the orthodontic force stops, new cementum is deposited and the structure of a new periodontal ligament (PDL) is re-established (32, 33). Initial attachment of PDL fibrils to the exposed dentinal and cemental collagen seems to be mediated by deposition of small amount of fibrillar cementum (32).

2.1.4 Diagnosis and Management Strategies of OITRR

The prevention of severe OITRR is essential toward achieving the desirable outcomes in contemporary orthodontics. Tooth mobility or even tooth loss is a clinical sign of severe OITRR when the remaining total root length is 9mm or less (8). It is important to use precautionary measures when treating patients exhibiting predisposing factors to OITRR such as abnormal root shape, dental anomalies, long roots, proximity of the root to the cortical plates or history of dental trauma (4, 34). Although there is no safe orthodontic force for teeth at higher risk regarding the susceptibility to OITRR, it is still recommended not to use high force levels (4, 35). Intermittent force and longer intervals between activations are also strongly recommended (35). Moreover, the duration of the treatment has to be shorter than usual. On the other hand, the aforementioned precautions should to be taken in consideration with regular patients undergoing an orthodontic treatment that is going to be longer than usual (4, 10, 34).

It is important to monitor teeth at risk for severe OITRR more often if the teeth exhibit early signs of root resorption (17). The standard method that is currently used to detect root resorption during orthodontic treatment is conventional intra-oral radiographs. However, it is not sufficiently sensitive to detect early stages of OITRR. It was found that periapical radiographs could not detect OITRR that otherwise could be verified histologically within the first 7 weeks of orthodontic

treatment. Moreover, it is difficult to detect resorption on the lingual and buccal surfaces of the roots by using the conventional intra-oral radiographs (1, 17).

The current accepted standard procedure to monitor OITRR is a periapical radiographic examination starting after 6 months of active fixed appliance treatment. However, for teeth at higher risk of severe resorption, a 3 month radiographic follow-up is recommended (17, 18). Once identifying teeth at higher risk of severe resorption by detecting an early sign of OITRR, the early mentioned precautions should be followed which could necessitate the interruption of the active treatment temporarily for 2 to 3 months by using passive archwires (35, 36). Moreover, when severe resorption is identified, the active treatment should stop and a modification of the treatment plan should be discussed with the patient by offering alternative options with minimal intervention such as prosthetic solutions to close spaces, interdental proximal reduction (IPR) instead of extraction, and early fixation of resorbed teeth should be attempted (35).

Root resorption does not usually progress after appliance removal. Therefore, interruption of active treatment is required to terminate the destructive process and allow cementum repair (17). The repair processes could start early during the first week of retention (37). However, the rate of the repair process increase during the first 4 weeks after the termination of the orthodontic force, and then slows down and reaches a steady phase for the following 5-6 weeks (1). However, if severe OITRR does progress after the appliance removal, sequential root canal

therapy with calcium hydroxide might offer some protection (35). Filling the root canal with gutta-percha as a final step should be delayed until root resorption completely stops (11).

2.1.5 Effect of Several Pharmacological Agents on OITRR

Several distinct drugs are being used as adjunct to orthodontic tooth movement in order to control pain and/or infections that could occur during the course of treatment. On the other hand, it is common to find a patient receiving a medication, for the prevention or treatment of various diseases, during orthodontic treatment (38). On that basis, many studies have examined the modifying effect of several pharmacological agents on OITRR.

Thyroid hormone (TH) administration at low doses seems to provide a protective role for the root surface during orthodontic treatment by decreasing the frequency and dimensions of OITRR without altering the rate of tooth movement nor reducing bone density (39-41). This protective effect was explained anecdotally by the ability of TH to increase the resistance of the cementum layer against resorption (41).

Systemic administration of tetracyclines, doxycycline at sub-antimicrobial dosage significantly decreased OITRR without altering the rate of tooth movement (42). This protective effect of doxycycline was explained by the ability of tetracyclines to exert an anti-inflammatory effect by inhibiting the activity of

metalloproteinases, such as collagenase and gelatinase, which in turn can prevent collagenolysis which is an essential step in the pathogenesis of periodontal disease (42, 43). The anti-inflammatory effect of tetracyclines can be demonstrated also by inhibiting the production of some pro-inflammatory cytokines (44).

Non-steroidal anti-inflammatory drugs (NSAID) are sometimes prescribed for pain control that usually accompanies an orthodontic treatment. Nabumetone was shown to be useful in reducing OITRR without interfering with the rate of orthodontic tooth movement (45). Another NSAID, Celebrex also offers a slight protection against OITRR without impeding the rate of tooth movement (46).

Bisphosphonates are potent blockers of bone resorption that are characterized by their high affinity for calcified tissues. Six different types are commercially available today for treatment of bone disease (47). Each bisphosphonate has its own chemical and biological characteristics. Topical administration of a bisphosphonate, risedronate, caused a significant decrease of OITRR without affecting the repair process of root resorption (48). Local administration of another bisphosphonate, clodronate inhibited OITRR and caused significantly smaller resorption area, in the meantime, it alters the rate of the tooth movement (49). On the other hand, 1-hydroxyethylidene-1, 1-bisphosphonate (HEBP) has been reported to affect not only the resorption of calcified tissues but also the mineralization process of these tissues (50). A single injection of HEBP is sufficient to induce a series of dental root cementum surface alteration such as,

inhibiting the formation of acellular extrinsic fiber cementum (AEFC), and deposition of atypical hyperplastic cementum (51). These cementum alterations caused by the single injection of HEBP was enough to increase the susceptibility of the root surface to resorption during orthodontic tooth movement experiment (51).

The process of dental root resorption caused by orthodontic tooth movement is known to be directly related to the activity of pro-inflammatory cytokines such as interleukin-1 (IL-1) and tumor necrosis factor α (TNFα). Inhibition of these cytokines activity by injection of their soluble receptors was found to decrease OITRR, however, they did not seem to be suitable treatment choices as they also directly delayed the rate of tooth movement (52).

Echistatin is arginine-glycine-aspartic acid (RGD) containing peptide, which is a compound that interacts with integrin αvβ3 receptors located on the surface of the multinucleated osteoclasts that resorb the calcified tissues. This interaction inhibits the resorption of calcified tissues by disturbing the adhesion abilities of these osteoclasts to the resorption sites. Intravenous administration of echistatin was found to decrease OITRR significantly in rats. However, this short-period study was not conclusive in evaluating the effect of this treatment on long-term tooth movement rate (53).

Excessive fluoride intake affects the mineral component of the dental hard tissue

structure. Fluoride is known to replace the hydroxyl group of the hydroxyapatite crystal in the dental calcified tissues to form fluoroapatite (54). Fluoroapatite is more resistant to demineralization than hydroxyapatite (55). It was found that fluoride concentrates in cementum more than the other surrounding calcified tissues (56). Moreover, fluoride concentration in cementum is directly related to the amount of fluoride exposure (57). Therefore, a high dose of fluoride in fluoridated water reduces the size of OITRR on rats. Although, the resorption site were smaller when fluoride was administered, however the effect was not significant (58). The author explained that as the anabolic effect of fluoride on opposing bone mass might counteract the beneficial effect of fluoride on reducing cementum solubility(58).

Nitric oxide (NO) is a free radical involved in the regulation of many physiological processes including bone cells function. NO concentration plays a role in bone resorption as well as bone formation by stimulation of osteoblast and/or osteoclast activity (59, 60). Injection of L-arginine (NO precursor) in rats resulted in increase in NO production, which increased bone remodeling as well as orthodontic tooth movement. It was found that that OITRR in the L-arginine group was less than the control group. However, only one animal from each study group was used to evaluate OITRR in this experiment (61).

Prostaglandins (PGs) are a lipid compound associated with wide range of biological activities. The precursor for PGs is arachidonic acid, which is released

from the phospholipids of the cell membrane by the action of phospholipase enzymes then metabolized by cyclooxygenase enzymes to produce PGs (62). During orthodontic tooth movement, PGs play an important role as mediators of bone remodeling (63, 64). Local administrations of prostaglandin E1 (PGE1) or prostaglandin E2 (PGE2), in different animal models, accelerate the rate of orthodontic tooth movement by increasing bone remodeling activities (64, 65). However, several studies demonstrate that prostaglandin E2 injection significantly increased the amount of OITRR (66, 67).

2.2 Dental Cementum

2.2.1 Cementum Nature

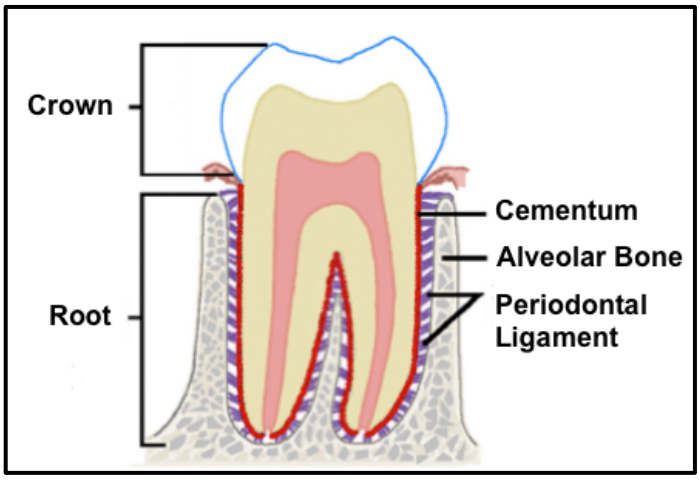

Figure 2: the basic anatomy of the dental attachment apparatus (68).

Fully developed tooth is composed of two main anatomical parts: crown and root. The crown is the visible part of the tooth in the oral cavity while the root is the anchor part, which is buried in alveolar bone (Figure 2) (68). Dental root is

covered by a thin mineralized connective tissue layer, known as cementum, and attached to alveolar bone through a soft connective tissue, referred to as the periodontal ligament (69). The periodontal ligament fibers are inserted in bone on one side and radicular cementum on the other side. The inserted portions of these collagen fibers are referred to as Sharpey's fibers (69).

The cementum layer connects the inert root surface, biologically and structurally, with the cellular and collagenous structure of the periodontal ligaments around the root (69, 70). Therefore, cementum is a component of the dental root structure, but functionally it belongs to the periodontium, which is the dental attachment apparatus (Figure 2) (68). The major role of the periodontium is to support the tooth in the jaw and it consists of cementum, periodontal ligament, gingiva, and alveolar bone (69, 70). Cementum has also important adaptive and reparative roles in maintaining the integrity of the root surface and thus preserves the proper dental occlusal relationship (69).

Cementum is a non-uniform mineralized connective tissue. Different types of cementum are associated with different location, function, rate of formation, chemical composition, and degree of mineralization (69). In fully developed human teeth, cementum is firmly attached to the radicular dentin and covers the entire surface of the root. Cementum thickness increases towards the apex and may extend partially into the apical foramen. The cementum thickness is about 50 μm at the cervical margin and increases in thickness as it approaches the root apex

to reach around 200 μm (69, 71). In the posterior teeth, cementum thickness is greater on the distal than on the mesial root surfaces due to the effect of the natural mesial drift of these teeth, which results in more pressure exerted on the mesial root surfaces (72). The external surface of human cementum is covered by a non-mineralized layer, 3-5 μm thick, known as precementum (69). The relationship between cementum and enamel define what is called cementoenamel junction. In about 30% of human teeth the cementum and enamel meet with no overlap as a butt joint; 10% have a gap between cementum and enamel exposing root dentin; and in about 60% the cementum slightly overlaps the enamel. These variations in the relation were obtained from studies analyzing ground sections, however, other studies using scanning electron microscope reported that all these variations in the cementoenamel junction could present within the same tooth when visualized circumferentially (71).

2.2.2 Cementum Origin and Development

The precise origin of cells and trigger factors that are responsible for cementum formation are still uncertain. However, the circumstances required for cementum formation are well established (73). Cementum development has been subdivided into a prefunctional stage, which occurs during root formation, and a functional stage, which begins when the tooth reaches occlusion and continues after that throughout life (71). During tooth development, each tooth germ comprises an enamel organ and a dental papilla surrounded by a loose connective tissue known as dental follicle. The external layer of enamel organ forms the outer enamel

epithelium while the inner layer, lining the dental papilla forms the inner enamel epithelium (74). The inner and outer enamel epithelium form the cervical loop that grows coronoapically into the Hertwig's epithelial root sheath (HERS), which outlines the future root by enclosing the dental papilla. The inner enamel epithelium of root sheath induces the differentiation of peripheral cells of the dental papilla into odontoblasts, which form the radicular dentin (74). HERS undergo apoptosis once the radicular dentin is formed. The fragmented root sheath leaves clusters of cells, known as the epithelial rests of Malassez (ERM), which persist in the mature periodontal ligament (PDL). Cementum is formed over the outer surface of the radicular dentin adjacent to the disintegrated outer enamel epithelium of the root sheath. The connective tissues of PDL, surround the forming root, are derived from the dental follicle cells (74).

Cementum matrix is deposited by specialized cells called cementoblasts. Several theories have suggested the origin of cementoblasts as well as the nature of the molecules that trigger the progenitor cell migration and differentiation. Currently, it is widely accepted that the cementoblasts are derived from the infiltrating dental follicle cells (69). However, some have suggested that cementoblasts originate from epithelial cells of Hertwig's root sheath when they undergo an epithelial-mesenchymal transformation (69, 75). However, it may be the case that there are two types of cementoblasts: those originating from the dental follicle cells which form the cellular cementum; and those originating from the epithelial cells of Hertwig's root sheath, through epithelial-mesenchymal transformation, which

form the acellular cementum (76). Anyway, the interaction between the dental follicle and the Hertwig's epithelial root sheath subsequent to the radicular dentin formation is an essential step for cementoblasts migration and differentiation (69). Hertwig's epithelial root sheath cells may produce the basement membrane containing chemotactic molecules, which trigger the migration and the differentiation of cementoprogenitor cells. These basement membrane molecules are extracellular matrix proteins include growth factors, enamel proteins and adhesion molecules, such as a collagenous-like protein, referred to as cementum attachment protein (CAP) (76).

Cementum grows in thickness throughout life, with a rate about 3 μm per year, and is capable of performing reparative activities when subjected to injury. Therefore, new cementoblasts must be continuously recruited from specialized cementoprogenitor cells within the same root-related portion of the mature and intact periodontal ligament (69). These progenitor cells exhibit some features of stem cells and present in paravascular locations within the periodontal ligament (76). However, when the pool of available progenitor cells in the periodontal ligaments is decreased, the cementoblasts could also be derived from stem cells present in other locations such as, gingiva, or alveolar bone around the dental root. This may be the case following an injury of the periodontium, when the demand for new progenitor cells is more than what are available in the periodontal ligaments (77). On the other hand, epithelial cell clusters with ultrastructural characteristics similar to those of epithelial rests of Malassez (ERM) have been

found in areas of cementum repair following orthodontic root resorption. (78). These epithelial cell clusters could have a role in repair/regenerative cementogenesis by producing matrix proteins, similar to what have been expressed during tooth development, subsequent to their migration into the resorption site (79). For this reason, it has been suggested that the interaction between ERM with specific periodontal ligament cells may generate new cementoblasts by recapitulating epithelial-mesenchymal interactions during dental root developmental events. Moreover, by recapitulating the early epithelial-mesenchymal transformation of HERS into cementoblasts, the ERM may directly give rise to new cementoblasts (80).

As mentioned above, the processes of cementoblasts migration and differentiation are controlled by several molecular factors either during cementum development and/or maturation and/or regeneration (73). Several adhesion molecules, responsible for the attachment and the maturation of appropriate cells on the root surface, have been identified during different stages of root development such as bone sialoprotein, osteopontin, laminin, fibronectin, type I collagen, cementum attachment protein and proteoglycans. Moreover, certain growth factors have been linked to the cells activities during cementum development and maturation including growth hormone, transforming growth factor-β and insulin-like growth factor-I. However, the factors recognized as having a role in the cementum development and maturation are not necessarily associated with the regeneration of this tissue (73). Extracellular matrix proteins such as bone sialoprotein and

osteopontin, in addition to platelet-derived growth factor and collagen type I and III, have been suggested to play an important role in cementoblasts migration and differentiation during cementum regeneration (73).

During root development, once the cementoprogenitor cells reach the root surface they differentiate into cementoblasts over the newly deposited and not yet mineralized radicular dentin mantle. Cementoblasts thereafter extend numerous tiny cytoplasmic processes into the non-mineralized dentin matrix in order to position the initially secreted collagen fibril of the cementum matrix among those of the dentinal matrix (69). Mineralization of the peripheral layer of mantle dentin is delayed and does not reach the outer surface until the collagen fibrils of dentin and cementum have had the time to blend together and form what is called dentinocemental junction. After that, mineralization progresses outward through the surface layer of dentin, across the dentinocemental junction and reach cementum layer (71). Dentinocemental junction has a biological and clinical importance since pathological alteration of this layer may influence the nature of the exposed root surface and thus the quality of the new junction during repair process when new cementum is deposited (71). Fortunately, as a result of root resorption, repair cementum adheres well to the root surface when the resorptive process precedes new cementum matrix deposition. This could mean that odontoclasts not only remove the hard tissues but also precondition the root surface and thus facilitate the blend between the matrix of reparative cementum and dentin prior to mineralization, thereby recapitulating the developmental

events (71). In rodent teeth, on the other hand, dentinocemental junction between dentin and acellular extrinsic fiber cementum is weak and an intermediate layer, rich in glycoprotein in addition to collagen fibrils, has often been observed in the cervical third of the tooth. The origin of this intermediate layer is uncertain (69).

2.2.3 Cementum Types

Three major different types of cementum are identified in human teeth based on the presence or absence of cells and collagen fibers in addition to the source of the collagen fibers. The acellular afibrillar cementum (AAC) covers teeth at and along the cementoenamel junction. It consists of mineralized matrix, but lacks collagen fibrils and embedded cells, which indicate that this type has no function in tooth attachment (69). It is deposited as isolated patches over enamel (cementum islands) and dentin (cementum spurs), and it is sometimes covered by acellular extrinsic fiber cementum and/or by junctional epithelium. The formation of AAC begins at the end of enamel maturation and continues for an unknown period of time. The cells responsible for depositing this cementum are still controversial, as either they are connective tissue cells, when they come into contact with the enamel surface, or may be epithelial cells of Hertwig's root sheath (69).

The acellular extrinsic fiber cementum (AEFC) is normally confined to the coronal half of the root covering the cervical and the middle portions of the root surfaces, but may extend further apically in anterior teeth (80). It consists of a

highly dense fringe of extrinsic collagenous fibers implanted into dentinal matrix and oriented perpendicular to the root surface. The highly dense extrinsic fibers elongate and extend with the periodontal ligament fibers, which indicate that this type has the significant function for tooth anchorage to the surrounding alveolar bone (69). The formation of AEFC begins shortly after crown formation and before the formation of cellular intrinsic fiber cementum on more apical root portion. AEFC is formed by cementoblasts that differentiate in closest proximity to the advancing root edge only about 20-30 μm coronal to the first deposited dentinal matrix. AEFC continues to grow constantly and slowly forming incremental growth lines throughout life, with a rate between 0.005 and 0.01 μm/day, as long as the adjacent periodontal ligament remains undisturbed. The direction of the extrinsic (Sharpey's) fibers can change as a result of post-eruptive tooth movements. These changes are accentuated by individual AEFC layers interfaced and by incremental growth lines (69, 80).

The cellular intrinsic fiber cementum (CIFC) covers the apical portions of the root surfaces, and has an important adaptive and reparative function. It consists of cementocytes entrapped in the mineralized cementum matrix as well as intrinsic collagen fibers that form discrete bundles oriented mainly parallel to the root surface (69). CIFC plays an important role in repairing a resorptive defect of the root surface due to its ability to grow much faster than the other cementum types (69). The cementoblasts deposited the cementum matrix around themselves close to the advancing root edge. Once the matrix mineralizes, the cementoblasts are

entrapped and become cementocytes, which occupy lacunae that are interconnected through canaliculi. The density of cells entrapped in CIFC is lower than in bone tissue and the system of interconnecting canaliculi, which might serve to maintain nutritional supply and cell contacts, is more sparse. In rare cases, the intrinsic cementum is formed by pure matrix deposition and completely lacks entrapped cementocytes, which form what is called acellular intrinsic fiber cementum (69). On the other hand, cellular mixed stratified cementum (CMSC) is a mixture of consecutively overlapped layers of CIFC and AEFC. The intrinsic part of CMSC may have an adaptive function, while the extrinsic part could serve in the tooth anchorage. This cementum could be found on apical root portions, furcations and in the areas of cementum repair of previously resorbed roots (77, 80).

2.2.4 Cementum Structure

The non-uniform nature of cementum in addition to its limited distribution makes it a difficult connective tissue to study biochemically (69). Unlike bone, dental cementum is avascular, non-innervated, and does not undergo continuous physiological remodeling. Moreover, deposition of cementum layers does not follow the lamellar arrangement found in bone. However, biochemical studies have suggested that acellular cementum is a unique tissue, while cellular cementum and bone share some compositional features (80). Volumetrically, cementum comprises approximately equal proportions of water, organic matrix and inorganic mineral. The inorganic mineral component of cementum is the

same as in other calcified tissues, which is composed of hydroxyapatite crystals with small amounts of amorphous calcium phosphate; however the mineralization degree of cementum is less than radicular dentin from the same tooth. Moreover, acellular extrinsic fiber cementum (AEFC) is more mineralized than the other cementum types (69). The mineral crystal arrangement in cementum exhibits a large specific surface area of the mineral component and a subsequence great capacity for adsorption of fluoride and other elements over time, however, this arrangement also make cementum more vulnerable to decalcification compared with the dental enamel in the presence of acidic conditions (69).

In general, about 50% of the dry mass of cementum is mineralized inorganic component whereas the remaining part is organic matrix consists mainly of collagens and, to a lesser degree, glycoproteins and proteoglycans. Up to 90% of the organic matrix is composed of type I collagen and about 5% is type III collagen. Collagen components play structural and morphogenic roles by providing a scaffold for mineral crystals and also supporting the inserted Sharpey's fibers from the periodontal ligament (69, 81). The remaining components of cementum organic matrix are glycoproteins (non-collagenous proteins) and proteoglycans. The main non-collagenous proteins are bone sialoprotein (BSP) and osteopontin (OPN). Both are found in acellular afibrillar cementum and acellular extrinsic fiber cementum more than in cellular intrinsic fiber cementum. They bind to the collagenous matrix and the hydroxyapatite crystals and participate in the cell attachment and the mineralization process (69).

Other glycoprotein found in the cementum organic matrix is osteonectin, which might be involved in the mineralization process. Fibronectin and tenascin are glycoproteins found at the attachment site of the periodontal ligament to the cementum surface but not in the cementum layer itself (69). Other non-collagenous proteins have been suggested to be present in the cementum organic matrix include enamel matrix protein, dentin matrix protein 1 and osteocalcin (69, 76).

The aforementioned components are also found in bone; however, some other molecules are only found in cementum. Some cementum specific proteins have been identified include cementum-derived growth factor (CGF), which is an isoform of insulin-like growth factor-I (IGF-I) (82); and cementum attachment protein (CAP), since antibodies to CAP immunostain only cementum and not dentin or the periodontium (83). No evidence was found regarding the expression of the aforementioned proteins by cementoblasts; however, other proteins are only produced by cementum cells, and not by any other mineralized tissue forming cells, such as GLUT-1 monosaccharide transporter and cementoblastoma-derived protein (CP-23) (76). Moreover, proteoglycans including: fibromodulin and lumican, which play a role in tissue formation and mineralization, are found more abundantly in cementum than in bone (80).

Finally, despite the fact that certain aspects of cementogenesis and cementum biology is different from those of bone, some diseases that affect bone could alter

the properties of cementum as well. For example, hypercementosis is usually associated with Paget's disease; no cementum formation can result from hypophosphatasia; decreased cementum is associated with hypopituitarism; and defective cementum is seen in patients with cleidocranial dysplasia (73).

2.2.5 Possible Role of Cementum in Periodontal Regeneration

The objective of regenerative periodontal therapy is to restore the structure and function of previously damaged periodontium. However, achieving proper periodontal regeneration requires an appropriate sequential reconstruction of the four different components of the periodontium, i.e., dental cementum, periodontal ligament, alveolar bone and gingiva. Therefore, the new attachment of the periodontal connective tissue fibers to the previously damaged root surface is a critical step toward achieving periodontal regeneration. Cementum plays an important role in this process, because it invests and securely attaches the periodontal ligament fibers to the root surface. Thus, new cementum formation must occur for periodontal regeneration to take place (77, 80).

The extracellular matrix of cementum itself has been proposed to have the potential to mediate cell migration and adhesion and to regulate the differentiation of precursor cells into cementoblasts and subsequent formation of cementum matrix and fiber insertion. Furthermore, the cementum matrix is a rich source of growth/differentiation factors such as the transforming growth factor-β, fibroblast growth factors and cementum-derived growth factor as well as a group of other

polypeptides; including osteopontin, bone sialoprotein and cementum attachment protein (CAP). Therefore, it is assumed that cementum components have the abilities to contribute in the regulation of the periodontium homeostasis and regeneration by providing the appropriate environment for the recruitment, proliferation, and differentiation of needed periodontal cells, at the same time excluding unneeded cells (71, 77, 80, 84).

The possibility of replanting a tooth, into its socket, following avulsion has been clinically established. Ideally the tooth should be replanted into the socket as soon as possible in order to maintain the viability of the cementum layer and then re-establish the periodontal fibers attachment (85, 86). However, if the avulsed tooth is replanted without viable cementum, unfavorable prognosis is usually followed, which could be demonstrated as replacement or external root resorption (77, 85, 86). Replacement resorption (ankylosis) occurs as a result of cementum death, which is then replaced by bone deposition directly on the root surface, causing a pathological fusion between root dentin and the alveolar bone (85, 86). External root resorption is caused by attracting osteoclasts to the root surface as a result of chemotactic process that follows the injury to the cementum layer, which often leads to loss of the dental root structure (85-87). Therefore, based on a well-known clinical observation, viable cementum and/or its intact molecules, are likely to have a major role in recruiting cells that differentiate later into cementoblasts to form new cementum which in turn is a critical step for the following restoration of the structure and function of the previously damage periodontium (77). In other

words, the good condition of cementum is not only an important factor that assist in the appropriate formation of new reparative cementum, but is also essential for the regeneration and maturation of periodontium.

Periodontal ligament (PDL), which is a component of periodontium, is a non-mineralized connective tissue and, at the same time, is the source for the mineralized tissue forming cells. The pool of PDL cellular population consists of fibroblasts, endothelial cells, perivascular cells and cells of epithelial rests of Malassez (ERM) as well as the progenitor cells that can differentiate into fibroblasts, osteoblasts or cementoblasts (80). On the other hand, PDL cells play an important role in the bone remodeling activities during orthodontic tooth movement by regulating the actions of osteoclasts through the OPG/RANKL/RANK system (88-90). Moreover, cells of epithelial rests of Malassez (ERM) present in PDL can react to the mechanical stress during orthodontic tooth movement by increasing their proliferation rate and cell size, and thereby could protect the root surface by acting like a cushion that maintains the space between alveolar bone and cementum (76).

2.2.6 Possible Protective Role of Cementum in OITRR

One of the major differences between the bone and the mineralized dental tissues is their susceptibility to resorption. Bone normally undergoes continuous physiological remodeling to which the dental tissues appear to be resistant under normal conditions (91). The cells covering bone surfaces (osteoblasts precursors

and stromal cells) regulate the process of bone resorption by controlling the activities of the resorbing cells (osteoclasts) through the OPG/RANKL/RANK system (92, 93). Osteoprotegerin (OPG), receptor activator for nuclear factor kappa B ligand (RANKL), and receptor activator for nuclear factor kappa B (RANK) are all members of the tumor necrosis factor (TNF) receptor/ligand superfamily. The cells covering bone surfaces express RANKL on their surfaces, which bind to RANK on the surface of osteoclastic precursor cells. This interaction is necessary for the development and the activity of osteoclasts. The same cells covering the bone surfaces produce OPG, which act as a decoy receptor that bind to RANKL and block the interaction between RANKL and RANK and thus suppress the development and the activity of osteoclasts (93). A number of hormones and inflammatory mediators control the process of osteoclastic bone resorption by adjusting the expression balance between RANKL and OPG. For example: TNF-α, IL-1, parathyroid hormone (PTH), and 1,25-dihydroxyvitamin D3 all stimulate bone resorption by stimulating the expression of RANKL and inhibiting the production of OPG. On the other hand, TGF-ß and estrogen suppress bone resorption by increasing OPG production. However, not all regulation of the bone resorption is exclusively through the OPG/RANKL/RANK system since calcitonin was found to directly suppress the activity of osteoclastic cells (93).

It is known that teeth root surfaces are more resistant to resorption than alveolar bone. Cementum covers the dental root and forms a protective barrier preventing resorbing cells from gaining access to the root surface (91). Hypothetically, this

inherent relative resistance of cementum to resorption under normal condition was linked to the presence of a non-mineralized layer (precementum) that covers the external surface of cementum (91). It has also been postulated that cementum contains proteinase inhibitors, within precementum and cementum matrices (94). These proteinase inhibitors were suggested to be associated with the resistance of cementum tissues to blood vessel invasion, which in turn is an essential step in any physiological remodeling process (94). Moreover, cementum does not respond in the same way to mediators that normally stimulate bone resorption such as parathyroid hormone (PTH) (92, 95, 96).

Breakdown of the cementum barrier is therefore required to allow odontoclasts to colonize the denuded root surface and start the resorption process (9, 24, 26, 91, 97). In orthodontically induced tooth root resorption (OITRR), the pressure applied at the root surface during tooth movement can directly damage the cementum barrier. Cementum death in the pressure regions, in addition to necrosis of the periodontal membrane, has been clearly established during tooth movement (97). Moreover, undamaged cementum layer could also be removed during the eliminating process of the necrotic tissue adjacent to the root surface following the application of orthodontic force (25, 26).

Unfavorable changes in the structure of cementum can cause destruction of the surrounding tissues by triggering inflammatory and immune responses (98). Moving teeth with preexisting nonviable cementum resulted in a markedly

increase in the vulnerability of the root surface to resorption (51). On the other hand, the pressure caused by the tooth movement can reduce the normal cementum thickness and alter its mineral content and physical properties at the compressed root surface where the resorption usually takes place (72, 99, 100).

Viable cementum is crucial not only for preserving the structure of the dental root during tooth movement, but also for the vitality of the surrounding periodontal ligament cells (77). The periodontal ligament would conceivably provide additional protection to the root structure during tooth movement- physically by acting like a cushion that diffuses the pressure against the root (76) and biologically by producing mediators that stimulate the appropriate remodeling of the surrounding alveolar bone opposing the dental root during tooth movement and thus reduce the stress concentration at the compressed root surface (88-90).

Theoretically, based on the literature, cementum layer augmentation may indeed provide additional protection to dental root during orthodontic tooth movement. Moreover, clinical observations in patients with a history of earlier orthodontic treatment showed a decrease in the degree of root resorption during the second treatment (101). This additional resistance against OITRR could be attributed to cementum remodeling in the root surface during the first treatment (24). Therefore, tooth root surface remodeling by inducing new cementum formation might be an important preventive factor that influences the onset and the progression of OITRR, and this would be a novel discovery.

2.2.7 Cementum Regeneration

Cementum regeneration has been well investigated by using a direct application of a variety of growth and differentiation factors in order to stimulate cell repopulation around a previously exposed dental root due to periodontal disease. Several studies have shown that the application of platelet-derived growth factor/insulin like growth factor-1(102, 103); bone morphogenetic protein (BMP) (104); and basic fibroblast growth factor (bFGF) (105) result in significant amounts of new bone and cementum formation. Moreover, Emdogain® (EMD), a formulation of Enamel Matrix Proteins (EMP), is used clinically for periodontal regeneration therapy. EMD is a commercially available acid extract of fetal porcine enamel matrix protein. Amelogenin is the major protein component of EMD, which proved to stimulate cementum formation when directly contacting the exposed root surfaces for enough period of time (106). EMD is used locally in the previously diseased roots to regenerate lost periodontal soft and hard tissues (107).

One of the major problems of applying bioactive molecules directly to the exposed root is that they need to bind efficiently to the target location and remain bio-available and bioactive for long periods of time (77). Moreover, these molecules should allow for a direct connection between mineralized dentin and non-mineralized fibrous periodontal ligament (77). Therefore, these therapeutic molecules not only should directly contact the target tissues, but also have to

bring together the two different environments, which are the mineralized and non-mineralized tissues (77).

Unlike periodontally involved teeth, the dental root surfaces that are susceptible to resorption during tooth movement are not exposed to the outer oral environment. Therefore, the direct application of the aforementioned bioactive molecules is not applicable to induce new cementum formation on the sound root surface prior to tooth movement in the *in vivo* setting. For this reason, we propose the systemic administration of cyclosporine A (CsA), or the surface application of low-level laser therapy (LLLT), as potential treatments to induce new cementum formation in sound tooth root surfaces.

2.3 Cyclosporine A

2.3.1 Pharmacological Properties of CsA

The first successful kidney transplant procedure was performed during the middle of the last century. Since then organ transplantation is becoming an ever-increasing treatment of choice for end-stage organ failure (108). Organ transplantation procedures necessitate the use of immunosuppressant drugs in order to prevent the rejection of the new transplanted organ by the body's immune system. Therefore, more attention was required to discover new immunosuppressive medications and more studies were focused on their biological actions as well as the side effects that are associated with their uses (109). These drugs are also prescribed in the treatment of autoimmune diseases,

such as rheumatoid arthritis and psoriasis, where the body's immune system actually attacks its own cells (108).

Cyclosporine A (CsA) is a powerful immunosuppressive agent and one of the major drugs that have a significant impact on transplant medicine and in the therapy of autoimmune diseases. CsA is a hydrophobic cyclic polypeptide consisting of 11 amino acids. It is isolated as a metabolite from the fungus Beauveria nivea. It was discovered in 1976 during the search for new antibiotic agents; however, CsA was found to exert a broad range of pharmacological effects including anti-parasitic, fungicidal, anti-inflammatory and immunosuppression effects (110).

As an immunosuppressive agent, the primary function of CsA is to suppress the activity of helper/inducer T lymphocytes (CD4+ cells). At a molecular level, the normal activation process of T lymphocytes starts by binding of a specific antigen to the lymphocyte receptor which results in the activation of a number of cell signaling pathways leading to transcriptional activation, and subsequent cellular responses such as lymphocyte proliferation and cytokine production (111). CsA directly binds to an intracellular protein within T lymphocytes and blocks the aforementioned signaling pathway that lead to a temporary suppression of the cellular immune response (110, 112).

The immunosuppressive efficiency of CsA not only depends on its ability to inhibit the activity of CD4+ T lymphocytes but also to suppress the subsequent release of associated cytokines (IL-2, IL-6 and Interferon gamma) that are produced as a result of these cells activation. Therefore, the repression effect of CsA on the other components of the immune system, rather than T-cells, is achieved as a consequence of inhibition of cytokine expression (113). On that basis, CsA indirectly inhibits the growth, differentiation, and activity of different non-T-cells that are involved in immune reaction such as B-lymphocytes, eosinophils and mast cells, even though, it was reported that CsA could directly inhibit the release of histamine and prostaglandin from human mast cells (113). On the other hand, CsA, at therapeutic dose, has no significant effect (neither directly nor indirectly) on the function of other components of immune system including neutrophils, natural killer (NK) cells and macrophages as well as the phagocytic activity associated with these cells actions (113).

The chemical characteristic of CsA results in an incomplete absorption of the drug from the small intestine, following an oral administration (114). The low water solubility of CsA causes a bioavailability of only 30% compared with an intravenous infusion. Peak absorption occurs in 4 to 5 hours, and equilibrium is reached approximately 8 to 12 hours following oral administration (115, 116). Moreover, the absorption of oral CsA dose and the subsequent bioavailability depends mainly on the biliary function and flow; therefore, the variability in the drug absorption between patients is directly related to the condition of the biliary

system. Patients with biliary diversion and cholestasis are at higher risk of sub-therapeutic levels of CsA therapy (116).

Administration of CsA by subcutaneous injection provides more consistent pharmacokinetic profile than any other administrations route in rat model (117). The subcutaneous injection route of CsA offered a constant absorption rate with a steady serum level of the drug over the 24 hours following administration in rats. Moreover, a daily dose CsA of 10 mg/kg of rats' body weight by subcutaneous injection provided plasma peak and trough levels of around 1000 and 750 ng/ml, respectively, with a bioavailability reaching about 80% (117). It was shown that a serum level over 400 ng/ml is needed for CsA to be effective as an immunosuppressive agent in animals (118). Therefore, the oral doses of CsA has to be larger than the subcutaneous injection doses in order to obtain comparable bioavailability and thus, achieve similar pharmacological effect, due to the drug absorption differences between the administration routes (117). Moreover, handling animals with the subcutaneous injection approach is easier than any other administration routes. Less complication was reported by using subcutaneous injection, which only requires needle insertion into the skin folds on the back of rat's neck (117).

In blood, CsA is mostly bound to the following: 50% erythrocytes, 5% lymphocytes and 40% lipoproteins, with approximately 5% free in the plasma (119). In the liver, CsA and its metabolites are taken up into the hepatocytes for

further metabolization by the cytochrome P450 monoxygenase system. The metabolites are mainly excreted from the hepatocytes into bile, with only a smaller portion released into blood. The terminal half-life of CsA is approximately 19 hours (range 10-27 hours). The major route of elimination of CsA is through the bile (feces). About 95% of a single dose is eliminated in feces over a sampling of 96 hours (110). Less than 1% of an administered dose of CsA is excreted in the bile as parent drug. Renal excretion is a minor pathway with only 4–6% of a CsA dose eliminated by the kidney and found in the urine as metabolites (110). CsA is metabolized to more than 30 metabolites. Cytochrome P450 monoxygenase system, located in liver and small intestine, are the site of several drug interactions and are responsible for the biotransformation of CsA and its metabolites. It is still not clear if the metabolites are involved in the immunosuppressive and/or toxic activities of CsA, even though isolated metabolites can show some of the activity of the original compound (120).

Because of the variations in the drug absorption following oral administration, monitoring the CsA dose is necessary in order to avoid overdose toxicity or to prevent possible sub-therapeutic dose that could result in organ rejection. CsA dose should be determined based on the formulation used (ie, Neoral versus Sandimmune) as well as blood levels (116). Several techniques exist for the measurement of CsA levels, including radioimmunoassay and high-pressure liquid chromatography (116). The levels can be measured in whole blood, serum, or plasma. However, the radioimmunoassay measurement of the whole blood

levels is the most currently used technique. In the first 3 to 6 months after transplant, the desire level is 150 to 200 ng/mL; then the level could be maintained at 100 to 150 ng/mL after that. However, these levels are considered guidelines and might need to be adjusted based on the subsequent side effect (116).

Several factors have been identified that can influence the pharmacokinetic profile and the clearance of CsA, such as age, hepatic function, hematocrit, and lipoprotein concentrations (121). Moreover, a number of clinically relevant drugs are well established to interact with CsA. These interactions fall under two major categories: pharmacokinetic or pharmacodynamic interactions. Pharmacokinetic interactions are characterized by either an increase or decrease in the CsA concentration followed an alteration in the function of cytochrome P-450 system caused by the co-administrated drugs. However, other drugs can affect CsA absorption, distribution, and elimination by different mechanisms. On the other hand, Pharmacodynamic interactions are manifested by an increase in the toxic effect, such as nephrotoxicity, of a certain CsA dose. Management of these interactions necessitate the awareness of the effect of each concomitant drug beforehand. Moreover, monitoring CsA blood concentration as well as the health condition of the patient is important when attempting to start or discontinue any drug that has the potential to interact with CsA treatment (122).

2.3.2 CsA Side Effects

Several side effects associated with CsA treatment have been identified. The most common side effects of CsA are nephrotoxicity, neurotoxicity, hepatotoxicity, hypertension, infections, and gingival overgrowth. The complications of these side effects could require dose adjustments or a complete discontinuation of the drug in some cases (116).

Acute or chronic nephrotoxicity are considered the most significant side effects of CsA treatment. The acute nephrotoxicity results from transient vasoconstriction of the kidney blood supply which often resolves spontaneously after therapy termination (116). The irreversible chronic nephrotoxicity is a more severe type that characterized by a permanent damage of the kidney structure and blood supply (116). Furthermore, several drugs can interact with CsA and increase the risk of nephrotoxicity including non-steroidal anti-inflammatory agents, aminoglycosides, and various antifungal agents (116). Neurotoxicity is another common side effect of CsA therapy that causes headaches, tremors, seizures, or coma in severe cases. Neurotoxicity was reported in about 50% of CsA treated patients (116). Hepatotoxicity was also reported in patients receiving CsA, which caused by mild to moderate impairment of liver enzyme functions (116).

Although CsA is considered an immunosuppressive agent, CsA treatment is not always associated with an increase prevalence of bacterial and fungal infections.

However, immunosuppressed patients are at higher risk for some opportunistic viral infections such as herpes simplex, herpes zoster and cytomegalovirus (110).

Severe gingival overgrowth (GO) is a side effect commonly found in patients treated with CsA. The pathogenesis of GO induced by CsA is still not completely known and it is associated with many different risk factors (119). The relationship between CsA administration and the severity degree of GO varies between patients, and this variability could be observed within the same patient as well. The severity of GO in patients receiving CsA is directly related to several factors including: serum and salivary drug concentrations, time since drug assumption, age, concomitant medication and oral hygiene. Different approaches for managing GO in patients treated with CsA have been proposed including the use of specific oral hygiene programs, surgical removal of the overgrowth tissues, and/or changing the pharmacological agent (119).

2.3.3 CsA Pharmacological Action in Periodontium

Several studies of the effect of CsA in periodontium have been performed in order to understand the cause and the mechanism of the gingival overgrowth (GO) associated with the drug administration. Histologically, the CsA induced GO is described by gingival epithelial hyperplasia and interstitial fibrosis associated with focal inflammatory cell infiltration (123) in addition to an accumulation of a collagen filled extracellular matrix (ECM) within the gingival connective tissue (123, 124).

A study was done to investigate the effect of CsA on collagen production in fibroblast cultures obtained from normal human gingival, indicated that CsA induced GO could be directly related to the observed increase in type I collagen synthesis. CsA stimulates fibroblasts to increase the expression of type I procollagen mRNA, which was found to be decreased by the presence of a protein synthesis inhibitor such as cycloheximide (125). Moreover, CsA effect on gingival fibroblasts is not only on increasing collagen synthesis, but also on regulating the secretion of various matrix metalloproteinases (MMPs) such as collagenase (MMP-1), and tissue inhibitor of metalloproteinase (TIMP). Overall, CsA can directly stimulate the deposition of dense collagen networks in gingival tissues and also decrease the collagenolytic activity by reducing collagenase expression and increasing TIMP production by fibroblasts (126).

CsA was found to be responsible for an increase in the concentration of transforming growth factor-β (TGF-β) in gingival crevicular fluid (127). This increase in TGF-β was suggested as the reason behind the reduction of proteolytic activity in periodontium due to CsA administration (128). TGF-β is one of the major bioactive mediators that control connective tissue development and homeostasis as well as wound repair. TGF-β is a multifunctional bioactive peptide that regulates diverse biologic activities including cell proliferation and differentiation in addition to its ability to directly activate gene expression for the synthesis of extracellular matrix protein components including collagen (127). CsA

was also found to up-regulate other growth factors in periodontium such as: vascular endothelial growth factor (VEGF) (123), platelet-derived growth factors (PDGFs) (129), and epidermal growth factor (EGF) (130).

Nitric oxide (NO), a free radical involved in regulation of various cellular activities, may also play a role in CsA induced gingival overgrowth (GO) (131). NO is generated locally from L-arginine by the enzyme nitric oxide synthase (NOS), which is produced by several cells including macrophages and vascular smooth muscle cells (131). It was reported that CsA administration increased the local NOS expression in rats' gingival tissues, which in turn increased the production of NO (131).

The anti-inflammatory effects of CsA in the periodontium, by inhibiting the production of several active inflammatory molecules, were linked to the overgrowth of gingival tissues induced by the drug administration. The inflammatory molecules such as prostaglandin E2 (PGE2) have important roles in the remodeling activities in the periodontium by facilitating the destruction and the rearrangement of its connective tissues (132). CsA was found to reduce the production of PGE2 by inhibiting the synthesis of cyclooxygenase-2 (COX-2) in both gingival tissue and cultured gingival cells (132, 133). Moreover, the down-regulation of other inflammatory molecules such as interleukin-1β and tumor necrosis factor-α were also observed in gingival tissue after CsA therapy and in cultured gingival fibroblasts (133, 134).

The effect of CsA on human bone is still not clearly defined. A number of studies in transplant patients suggested that CsA causes bone loss; however it is difficult to be certain because these patients are usually treated with a combination of drugs, other than CsA, including glucocorticoids, which also could stimulate bone resorption (135). On the other hand, the ability of CsA to inhibit the production of inflammatory cytokines associated with the T-cells activation could provide a direct protective effect against bone resorption. This protective effect was demonstrated *in vivo*, as CsA prevented bone loss that usually occurs in association with arthritis in rats. Moreover, CsA can directly inhibit *in-vitro* bone resorption induced by the application of active mediators such as interleukin-1 (IL-1), prostaglandin E2 (PGE2), 1,25-dihydroxy-vitamin D3, and parathyroid hormone (136).

The variation in the effect of CsA in the bone density could be related to the drug dose level. A study found that only a high oral dose of CsA, around 30 mg/kg, would decrease the bone volume in both growing and adult rats (137). Moreover, gender-related differences in the effect of CsA on the bone tissues were also suggested. It has been reported that CsA stimulates bone formation in female rats while it increases bone resorption in male rats, even though, neither sex hormones nor gonadectomy were found to modulate the CsA effect on osseous tissues (138). Therefore, it could be postulated that the decrease in male rats' mandibular bone mass following CsA therapy, as reported in the literature (139), is related to the

animal gender. Accordingly, the effect of CsA on alveolar bone is controversial. CsA therapy could have a suppression effect on alveolar bone mass, specifically on osteoid formation around the molar regions (140). However, others found that use of immunosuppressive levels of CsA has no effect on alveolar bone homeostasis in rats' healthy periodontium tissues(141).

CsA was reported to stimulate the healing processes of oral wounds resulting from injuries of the alveolar bone and periodontal soft tissues (142). It was shown that CsA accelerates the healing after tooth extraction in rats' dental alveolar bony socket and subsequently forms an enlarged edentulous soft tissue ridge. Histologically, this healing occurred at a faster rate in the hard tissues than in the soft tissues (142). Moreover, in the presence of periodontal disease, CsA treatment was found to influence the alveolar bone remodeling by decreasing resorption and stimulating osseous tissues formation around rats' dental roots (141).

2.3.4 CsA Induce New Cementum Formation

The effect of CsA treatment in the formation of dental hard tissues has been investigated. Many studies have demonstrated that administration of CsA induces the formation of a significant amount of new cementum tissues that accumulated over all rats' dental root surfaces (143-147).

Daily administration of an oral dose of 30 mg/kg of CsA in young and adult male Sprague-Dawley rats resulted in the formation of new cementum regardless

animals age (143). A thicker new acellular cementum layers and spurs were found close to the enlarged gingival connective tissues. The deposition rate of the new cementum after one month of daily oral dose of CsA was more evident in the cervical third of the root. The new cementum layer was firmly attached to the root surface. Moreover, the orientation of the periodontal collagen fibers insertion would indicate that new cementum layer formed by the CsA administration is functionally intact (143).

Comparable results were also obtained by using subcutaneous injection to deliver a daily dose 10 mg/kg body weight of CsA in male Wistar rats (147, 148). However, the cementum thickness was significantly more over the root apical third in all the groups that received daily injection of CsA, in comparison to a control group (147). Furthermore, the induced new cementum layer by CsA administration through subcutaneous injection route was mostly cellular cementum type over the root apical part, which is different from the results obtained by the pervious study which found that oral doses of CsA stimulate the formation of a distinctive, acellular, type of cementum mainly on the root cervical third (143, 147). No explanation was provided regarding these differences in the cementum type and location that was induced by each drug administration route, even though, both techniques caused gingival overgrowth which is a common side effect of CsA treatment (143, 147).

In order to evaluate the rate of new cementum deposition following daily CsA treatment for 7 weeks, fluorescent markers, calcein and alizarin red, were used on alternate weeks in order to label the rate of cementum formation, at one-week interval (146). It has been shown that the highest apposition rate of new cementum was found in the first week of CsA daily administration, which was then decreased gradually afterward in the following observation intervals (146).

Contrary to the other side effects of CsA treatment, the accumulated new cementum layers induced by CsA administrations persist, structurally and functionally, for a long period of time after the termination of the treatment regardless the type of the drug administration route (144, 147). This finding could be directly related to the fact that dental root cementum resists resorption and does not undergo physiological remodeling (92).

Several suggestions have been made in order to illustrate the mechanism behind the ability of CsA to induce new cementum formation. The method that CsA stimulates the cementum formation could be similar to the process that is responsible for the overgrowth of gingival tissues induced by the drug administration (143). CsA can directly stimulate the deposition of dense collagen by the fibroblasts in the gingival tissues and also decrease the collagenolytic activity by reducing collagenase expression and increasing the production of tissue inhibitor of metalloproteinase by fibroblasts (125, 126). Moreover, as discussed earlier, the cells activities during cementum development, maturation

and regeneration have been linked to the expression of specific growth factors including transforming growth factor-β and platelet-derived growth factor (73). CsA is therefore capable in stimulating the production of these growth factors in the periodontium around the dental root (128, 129). On the other hand, it has been suggested that the increase in cementum deposition could be a compensatory response for the possible decrease in the alveolar bone mass around the dental root as a result of CsA treatment (146).

2.3.5 CsA Effect in Orthodontic Treatment

The increasing number of patients who undergo organ transplant made it inevitable to find patients receiving a CsA medication in orthodontic clinics. Certain points should be considered during orthodontic tooth movement in patients receiving CsA treatment. Gingival overgrowth (GO) induced by CsA could complicate the placement of appropriate orthodontic appliance. During orthodontic treatment, GO may cover brackets, occlude buccal tubes, delay teeth eruption, and prevent space closure (149, 150). As well, the orthodontic appliance itself can complicate the use of conventional oral hygiene measures. This usually results in more plaque accumulation that can increase the potential and the severity of CsA induced GO during the presence of the appliance. Management of such complications would require a combined periodontal and surgical approach in order to improve oral hygiene and re-contour the gingival tissues (149, 150).

It is recommended to postpone any orthodontic treatment for at least 6 months after starting the CsA course, since the peak of gingival overgrowth usually takes place during the first months of the CsA therapy (149). Using small size brackets and avoiding cemented bands around teeth would help reduce the irritation of gingival tissue caused by any contact with the orthodontic appliances (149). Moreover, modification of orthodontic treatment plan might be required in CsA treated patients. The overgrowth of gingival tissues caused by CsA could prevent the total space closure between teeth. Therefore, a non-extraction treatment plan is preferred in order to minimize the potential of residual spaces that resist closing at the end of treatment (150). Bonded fixed retainer is also recommended in order to prevent space opening after treatment. Nevertheless, the retainer should be properly designed in order to avoid gingival impingement and plaque accumulation as possible. On the other hand, the continual change in gingival tissues architecture requires the arrangement of retainer-check appointments more frequently to ensure full seating of the removable retainers (149, 150).

2.4 Low-Level Laser Therapy

2.4.1 Laser

Laser is a general term used to describe a distinctive kind of electromagnetic radiation that is produced by special devices in a form of light. Electromagnetic radiation is a form of energy, which travel at speed of light and propagates through free space or material medium by exhibiting the properties of both waves and particles at the same time. This means that electromagnetic radiation has two

unique characteristics: travels at speed of light in a form of "waves" with all the essential properties of a wave (e.g. wavelength, polarization, interference); and also consists of "particles" that display the major properties of a particle (e.g. reflection, refraction, influenced by gravity) (151). To illustrate the relation between these two seemingly different behaviors, it is easier to understand the basic unit of all electromagnetic radiation, which called photon. A photon exhibits the properties of both a wave and a particle. Moreover, a photon carries a certain amount of energy called photon energy. The longer the wavelength, the lower the photon energy, and *vice versa* (151).

The wavelength is determined by measuring the distance between consecutive points of the repeated waves such as the distance from the one wave peak to the peak of the next one (152). Electromagnetic radiation is also measured in frequency, which represents the number of occurrence of successive peaks per unit time (e.g. second), or the number of wave passes per second. Frequency is calculated in unit hertz, which is the number of successive waves per second. Therefore, the wavelength is inversely related to frequency. The longer the wavelength, the lower the frequency, and the vice versa (152).

The range of wavelengths of electromagnetic radiation is plotted on the electromagnetic spectrum. This range extends from the highest frequency gamma rays, which have the shortest wavelength of less than 0.1 nanometer (nm), to the lowest frequency radio waves with wavelength longer than hundreds meters (152).

In physics, the term “light” describes a form of electromagnetic radiation with a wavelength range measured in nanometers. Light range extends in a very narrow region within the electromagnetic spectrum, whereas the visible light, which we see with our eyes, extends in an even narrower region (152).

We perceive visible light as the colors that the human eye can detect. Visible light consists of the seven rainbow colors: red, orange, yellow, green, blue, indigo, and violet. Each color has a different wavelength, ranging from dark red (750 nm), which has the longest wavelength, to violet (400 nm), which has the shortest wavelength (152). Other wavelengths such as infrared (longer than 750 nm) and ultraviolet (shorter than 400 nm) are also considered light even though they are not visible by human eyes. The range of laser light includes all the infrared, visible, and ultraviolet wavelengths. (152).

The term "laser" is an acronym stands for “*Light Amplification by Stimulated Emission of Radiation”*. Albert Einstein theorized the concept of stimulated emission of electromagnetic radiation based on his quantum theory of light (153). He stated that when the atoms are exposed to an outside source of energy, a photon would be released from an excited atom and interacted with a second excited atom. This process would result in the release of two identical photons that travel in the same direction. These identical photons would interact with additional excited atoms and continue to multiply through the process of stimulated emission. Therefore, the outcome of this process would be transmitted

as light energy that is composed of identical wavelengths (152). Landberg verified the laser theory and laser was practically produced thereafter (151). Maiman introduced the first commercially available laser device, forty years after the publication of Einstein's first theory (154).

Laser light demonstrates the major properties of light. However, the light emitted by laser devices acts differently than other ordinary forms of light, such as light produced by a light bulb. The unique characteristics of laser light come from the behavior of its waves and energy, which are considered collimated, coherent, and monochromatic (151, 152). Laser light beam is collimated because its waves are travelling in a nearly parallel manner to one another with less amount of divergence, which maintain the beam intensity over long distances. Laser light is coherent because its photons are organized in phase with one another and travel in the same direction at the same time in a consistent relationship. Two laser waves are considered coherent as the peak of one wave aligns with the other wave peak, and thus improves the amplitude or the power of the resultant laser beam. Monochromatic nature of laser light means that its beam is made up of a single wavelength (single color) or a narrow range of wavelengths or colors. Therefore, laser is an extremely efficient way to deliver energy because it uniquely combines the three aforementioned properties (collimated, coherent, and monochromatic). On the other hand, laser also shares other properties with regular light. For example, laser light is polarized when all its waves oscillate in the same plane (151, 152).

Regardless of the variations in the wavelength, output power, and size, every laser device consists of three major components including: an energy source, a lasing medium, and a resonance cavity. The energy source could be a high intensity strobe light or an electrical current. The energy from the source activates the lasing medium, which is composed of one of the following state: a solid medium consists of electrically non-conducting crystal (solid laser); a solid medium with a semiconducting crystal constituent (semiconducting or diode laser); a medium with mixture of gases in a closed vessel (gas laser); or a liquid state medium (liquid laser). The chemical elements of the lasing medium determine the wavelength of the produced laser beam. The resonance cavity (resonator) contains the lasing medium between two parallel mirrors on both ends of the cavity. One of the mirrors is 100% reflective; the other is 95% reflective. The 95% reflective mirror allows the laser light to exit the resonance cavity (151, 153).

Laser application in medical field falls under two main categories: surgical and therapeutic laser treatments (155). The surgical lasers, also called hard lasers or high level lasers, provide high thermal energy that can be used for surgical purposes. On the other hand, therapeutic lasers, also called soft lasers, cold lasers or low level lasers, operate in low non-thermal energy at wavelengths assumed to stimulate various cellular activities which can be used clinically to promote tissue healing and reduce inflammatory reactions, edema and pain (155).

Lasers have been studied for use in dentistry since their development. However,

in the past two decades, the clinical applications of lasers in dental practice have been a subject of substantial amount of research (156). In dentistry, several types of lasers have been defined and denominated according to: the physical state of the lasing medium (e.g., gas, liquid, solid state, or semiconductor diode) or the chemical composition of the lasing medium (e.g., Erbium: Yttrium Aluminium Garnet (Er:YAG)) (Table 1) (156). Moreover, for safety purposes, lasers have been classified according to the potential hazard to eyes and skin, from class I (the safest) to class IV (harmful) (156).

Lasing medium	Composition	Wavelength(s)
Argon	Gas Laser	488, 515 nm
KTP	Solid Laser	532 nm
Helium-neon	Gas Laser	633 nm
Diode	Semiconductor	635, 670, 810, 830, 980 nm
Nd:YAG	Solid Laser	1064 nm
Er.Cr:YSGG	Solid Laser	2780 nm
Er:YAG	Solid Laser	2940 nm
CO_2	Gas Laser	9600, 10600 nm

Table 1: common laser types used in dentistry (156).

At the present time, several laser technologies are being used in dental practice. For example, Laser fluorescence systems have been developed for dental caries detection (157). Several laser devices with wavelengths in the middle-infrared range are used currently for preparing dental cavity and removing caries (156). Lasers also can be used as a curing source for dental restorative resins (158). Low-

level laser energy is useful for photochemical activation of some oxygen-releasing dyes that are capable of eradicating some of the antibiotic resistance microorganisms, which exist in subgingival plaque (156). Laser energy is also used to initiate certain photochemical reactions used for photodynamic therapy, which has been employed in the treatment of malignancies of the oral mucosa, such as multi-focal squamous cell carcinoma (159). Surgical lasers are widely used in dental practice for various soft tissue procedures such as gingival contouring. The major advantage of surgical lasers lies in its ability to reduce operative bleeding and to decrease post-operative pain and complication (156). Surgical lasers were promoted for periodontal pocket curettage as a potential method to eradicate the pathogenic bacteria over the diseased dental root (160). However, no evidence was found to support the advantage of using Er:YAG surgical laser over the traditional scaling and root planning (SRP) in treating periodontal diseases (161). Moreover, surgical lasers, such as Nd:YAG, were found to cause more damage to the root surface when compared with the traditional SRP in periodontal pocket curettage (162).

2.4.2 Laser/Tissue Interaction

When applying laser light on tissue surface it can be reflected, scattered, absorbed or transmitted (163). Reflected light bounces off the tissue surface, which therefore limits the amount of energy that enters the tissue. However, when laser enters the tissue, its energy scatters by bouncing between the tissue's particles, which results in the distribution of this energy over a large volume within the tissue. However,

when tissue components absorb laser light, they reduce its energy scattering. In general, energy absorption occurs after a certain amount of scattering of the laser beam and is responsible for the tissue reaction. Finally, transmission occurs when laser light irradiates and pass through a given tissue boundary (163).

The concept behind using laser energy in the medical field is that different types of tissue reactions are identified following the energy absorption of different lasers' wavelengths. First of all, absorption of laser energy by tissue is the first and the most important step to achieve any reaction. The first law of photobiology states: "there must be absorption before any reaction occurs". Therefore, the mechanism of absorption is very important for the laser user to understand (164). For example, the fact that dark colored clothing becomes warmer in sunshine than lighter colored ones illustrates how different thermal reactions occur that are the consequence of the ability of different mediums to absorb light energy (164).

Several laser exposure parameters affect the absorption of laser energy by the tissue and subsequently the reaction of this tissue to laser therapy; and thus should be considered beforehand when exposing a patient to a laser treatment (163). Laser parameters fall under two major categories: "inherent parameters" and "user-controlled parameters". Inherent parameters are fixed to each laser device, but could vary from a device to another, which include: wavelength of the laser light, waveform (beam type), beam mode, and the possible output power range. On the other hand, user-controlled parameters are the range of output variables that each

device is providing, which are selected by the user including: the output power of the laser beam, the size of the irradiated area, and the length of irradiation time. Selecting the appropriate laser device should be based on its inherent parameters according to the treatment goals and the expected treatment outcomes, whereas user-controlled parameters affect the treatment techniques and the range of the final biological responses (164).

The wavelength of the laser light is the most important parameter that determines the degree to which the laser energy is absorbed by the target tissue (165). The distance that the laser beam travels within the tissue before losing its energy depends on how much tissue's components absorb the light energy of that laser wavelength. Therefore, for a certain tissue type, every laser wavelength has a specific penetration depth (166). On the other hand, the output power of the laser light influences the energy of the penetrated beam, which in turn affects the absorption mechanism. However, the penetration depth of a particular wavelength is limited by the optical properties of the target tissue regardless how much is the output power of that wavelength (166).

Tissue's components are made up of a mixture of different substances that usually vary between tissue types. Each tissue type has a specific optical property, which allows some laser wavelengths to penetrate deeply, but prevents other wavelengths from getting through, limiting their absorption to only the external tissue's layers (160). The optical properties of a tissue are not only identified by

the properties of their components, but also by the concentration and the distribution of theses components within the target tissue (i.e. tissue's structure) (167). Water molecules, or macromolecules such as proteins, hemoglobin, and melanin are the principal absorbing components in biological tissues that influence the penetration depth of each particular laser wavelength (168).

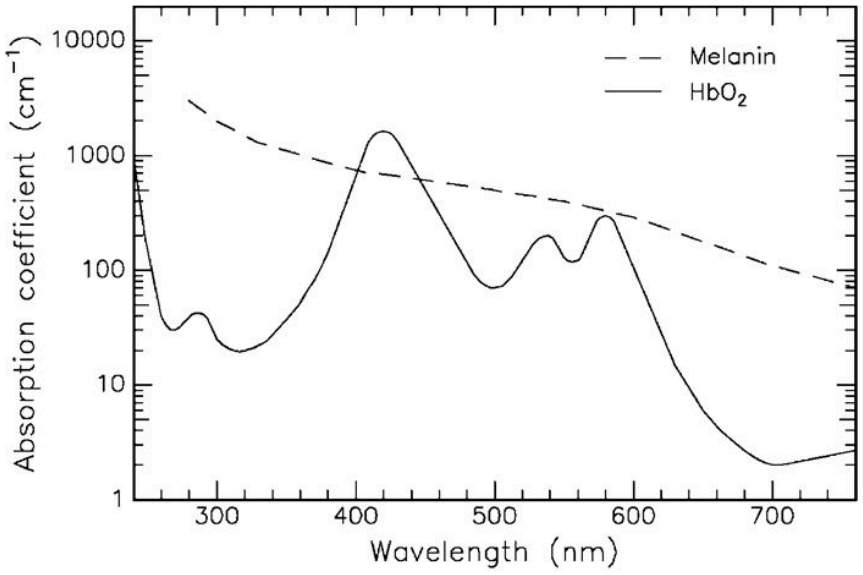

Figure 3: laser light absorption spectra by both melanin in skin and hemoglobin (HbO_2) in blood (168).

In general, water molecules are considered the main absorbing tissue's components of laser light in infrared wavelengths spectrum, whereas proteins, melanin, and hemoglobin, are the major absorbers of the wavelengths in the ultraviolet and visible range of the spectrum (168). The absorption coefficients of both melanin and hemoglobin are illustrated in relation to a range of different laser wavelengths in Figure 3 (168). The larger the coefficient value indicates the

more absorption of the wavelength by the substance, and thus less penetration of this wavelength is expected through this substance.

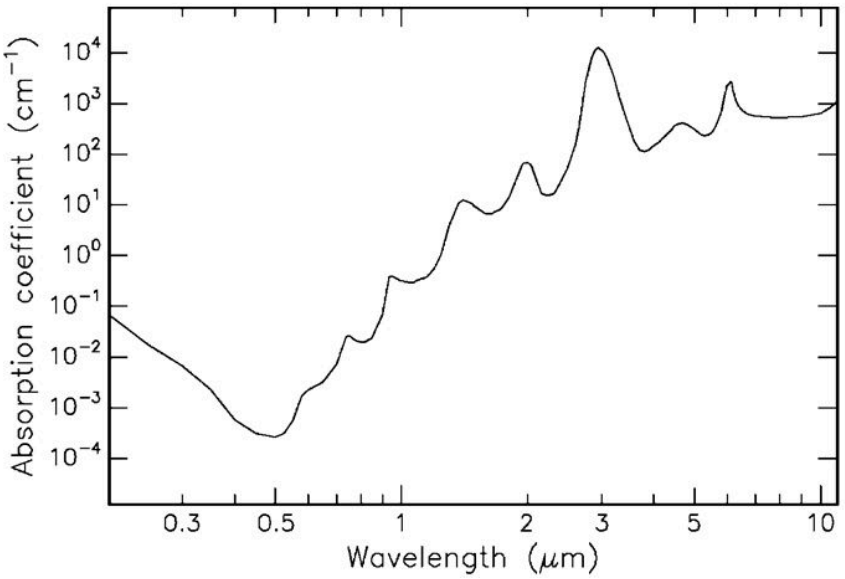

Figure 4: laser light absorption spectrum by water (168).

Melanin is a natural pigment substance of skin that influences the tissue's color and provides protection against the harmful ultraviolet radiation. The absorption coefficient of melanin shows a relatively constant increase across the laser visible wavelengths spectrum (from deep red wavelength at 750 nm to violet at 400 nm) toward the ultraviolet end (less than 400 nm) (168). Hemoglobin shows several increasing absorption peaks for laser wavelengths around 280 nm, 420 nm, 540 nm, and 580 nm, which then exhibits a sudden decrease in the absorption of wavelengths starting at 600 nm toward infrared spectrum (more than 750 nm) (168). On the other hand, the absorption coefficient of tissue's protein components increases in the ultraviolet range of laser light with an absorption peak of wavelength at 280 nm (168). The absorption coefficient of water (Figure 4), which

is an important component of most tissues, is small for laser wavelengths in the ultraviolet range and even smaller for those in visible light region. However, water absorption of laser light shows a gradual (non-linear) increase toward the far end of infrared wavelengths spectrum (168).

The absorption of laser light at wavelength in the range of ultraviolet, less than 400 nm, and visible light, between 400 nm violet and 750 nm deep red, depends mainly on the tissue relative content of melanin, and hemoglobin (168). In contrast, laser at far-infrared wavelengths, such as CO_2 laser at 10600 nm, are almost completely absorbed by water, which limits the penetration of these lasers to the first few, water rich, tissue's layers (164). However, laser wavelengths in the near-infrared spectrum are not strongly absorbed either by the tissue's macromolecules or by water (168). Therefore, a "therapeutic window" of laser light is outlined in the wavelengths range between 600 nm and 1200 nm. In this spectral range, laser light penetrates deeply at a lower loss, and thus distributes the energy of the laser beam over a large volume within the target tissue (168).

As discussed before, the relative depth of tissue penetration depends mainly on the laser light wavelength. However, as laser light pass through a given tissue, an attenuation of laser energy happens as an exponential decrease produced by the scattering and absorption by the tissue components (169). Table 2 approximates the tissue depth, which reduces the incident energy of various laser light

wavelengths to 37% of their original value before hitting tissue surface (163, 164, 166, 167, 169-175).

Wavelength (nm) of laser light	**Penetration depth (mm) before losing 37% of its energy**
300	0.06
400	0.09
500	0.23
600	0.5 – 1.0
700	1.0
800	2.0 – 3.0
1000	3.0
10600	0.03

Table 2: tissue depth that reduces the energy of various wavelengths of laser light to 37%

Laser energy can be delivered in varying waveforms that include continuous and pulsed, which describes the way in which the output power from the laser beam is distributed over time (160). Continuous wave lasers deliver a relatively large amount of energy to the tissue in a fixed and uninterrupted flow, usually at low to moderate power intensities. Continuous waveform is produced by emitting the laser beam at the same amount of power that has been set on the device, which is sustained for as long as the laser is emitted (160). Moreover, continuous waveform can be interrupted or gated by delivering repeatedly short laser streams at low to moderate power intensities with a precisely timed resting period in between each stream (160). However, it is important to understand that interrupting the continuous wave is substantially different from pulsed laser waveform. The latter

generates and repetitively delivers an ultra-short blast of laser energy at very high power peak, or intensity, compared to those with continuous or interrupted wave lasers. Pulsing the beam is performed by building up the energy for a certain period of time and then releasing it over a very short duration, which creating a pulse with a peak power, or intensity, much greater than what has been set on the device (160).

The spatial distribution of the power in the beam is known as beam mode, which affects both the beam profile and the imprint pattern of the beam on the target tissue (164). A common beam mode for medical application is Gaussian mode, where the power of the beam is mostly focused in the center. The imprint pattern associated with Gaussian mode is characterized by a 'hot spot' at the center of the irradiated area and the incident power is decreasing as approaching the beam circumference (164). However, delivering the beam through fiber optic scrambles the pattern of the beam mode resulting in a homogeneous beam profile and imprint pattern (164). Moreover, the coherence of the laser light is reduced when delivering the beam through a fiber optic or other waveguide, resulting in about 25% to 40% loss in the final output power of the delivered beam (151). Therefore, it is important to measure the final output power of the beam before each application when conducting the laser light through a fiber optic guidance in order to adjust the delivered power for any expected loss of energy.

Power is the instantaneous amount of energy that produced by the laser device, which can be precisely set and controlled by the user in association with other output parameters such as exposure duration and waveform. Mathematically, the total amount of the delivered energy (joules) is equal to the product of laser light power (watts) multiplied by the exposure duration (second) (e.g. 100 mW × 10 seconds = 1000 mJ = 1 J) (163). The dose of laser irradiation is the amount of energy, which conducted into a given tissue. The application of a reasonable dose within an appropriate therapeutic window is required in laser therapy. However, the size of the irradiated area (spot size) is an important variable that should be considered when calculating the dose of the laser therapy, since the laser energy could be conducted through a small point (e.g. 1 mm^2) or through an area of several square centimeters (151). Therefore, the dose can be expressed as power density. Mathematically, the power density (W/cm^2) of laser beam is the product of power (watts) divided by the irradiated area (cm^2). An appropriate power density (W/cm^2) is necessary to trigger biologic effects, and therefore longer laser exposure may not compensate for low power output (176). However, it is useful to also express the dose of laser therapy as an energy density (J/cm^2) when treating tissue surfaces for specific time. The energy density is calculated as the energy (joules) divided by the irradiated area (cm^2). Power density is also referred to as the irradiance or intensity, whereas energy density may be called the dose or fluence (167).

The irradiated area (cm^2) is calculated by using the formula related to the shape of the emitted spot. For example, for the circle shape spot, the irradiated area (cm^2) is equal to π times r^2, where π = 3.142 and r = the radius or half the diameter of the laser spot in centimeters (164). Therefore, the value of the energy density is inversely related to the square value of the diameter of the irradiated area. For example, halving the diameter of the tissue surface spot size, with a fixed exposure time and output power, will increase the energy density by four; whereas doubling the spot size diameter will reduce the energy density by one quarter (164). In other words, if the irradiated area is 1 cm^2, and the energy density is 1/1 = 1 J/cm^2, decreasing the area (e.g. 0.25 cm^2), while fixing all other parameters, will increase the energy density (i.e. 1/0.25 = 4 J/cm^2) (151).

The dose calculation for pulsed laser waveform is different from what was previously discussed. For example, power density for pulsed lasers (W/cm2) is equal to (peak power of the pulse x pulse duration x pulses frequency) / irradiated area (cm^2) (171). Therefore, the parameters of the laser device, such as wavelength, waveform and output power, should be clearly specified before planning any dose recommendation. Moreover, treatment prescription should clarify the following: the irradiated area, the exposure duration, the dose per irradiated area, the dose per treatment session, when different doses are given to different areas, intervals between treatment sessions, as well as the total dose for the whole series of treatment sessions for each patient (171).

As discussed earlier, absorption of laser energy by the tissue is required for the subsequent local and systemic tissue reactions to take place. In general, the optical properties of the target tissue determine the penetration depth of the laser energy at a certain wavelength (168). Moreover, the wavelength itself in addition to other parameters such as waveform, output power, exposure time, size of irradiated area, power density, and energy density are all very important factors that influence the energy amount of the penetrated laser beam, which in turn affects the absorption mechanism and the subsequent biological reactions, either thermal or non-thermal type of reactions that take place at tissue, cellular or even microcellular level (168).

The second law of photobiology states: "for every photon absorbed: an activated particle such as atom, molecule or free radical is formed" (164). In other words, when a tissue particle absorbs laser photon, the photon energy is therefore transferred to this particle, which in turn raising the particle condition to an excited state. The way in which this excitation is dissipated will create a biological reaction (164). The useful applications of laser in medical field utilize several types of biological reactions include: photothermal reaction; photoablative reaction; photodisruptive reaction (photomechanical or plasma induced); photochemical reaction; or photobioactivation reaction (photobiostimulation) (167).

Photothermal reaction occurs when the absorbed photon energy generates heat and elevates tissue temperature. Most surgical laser systems (high level laser) utilize tissue photothermal reactions that range according to the generated temperatures within the target tissues. When the laser energy raises tissue temperature above 40º C, the mildest photothermal reaction occurs in the form of protein denaturation, which is then changed as the temperature increases from coagulation (above 68º C) through vaporization (above 100º C) to carbonization in the higher temperature range (above 150º C). The mild forms of protein denaturation can be reversible while the remaining photothermal reactions are irreversible and destructive in nature (164).

Photoablation reaction occurs when the absorbed photon energy results in a process of tissue decomposition due to the breakdown of the bonds between tissue's substances, without a thermal involvement. This mechanism utilizes ultraviolet wavelength laser and is usually used for laser eye surgeries (167). However, photoablation term should be distinguished and not confused with the widely used term ablation, which is commonly used to describe any process of tissue removal by laser energy regardless of the mechanism behind it (167). Photodisruptive reaction, also utilized for laser eye surgeries, occurs when tissue absorbs high photon energy resulting in either the generation of shock waves, cavitation, or jet formation within the tissue (called photomechanical disruption). Photodisruptive reaction also happens in the form of plasma formation, which occurs when the absorption of the high photon energy results in the ionization of

tissue's molecules and atoms, and thus increases the strength of the tissue local electrical field (167). In photochemical reaction, the energy of laser photon can activate a photosensitive compound that has been administered earlier in a target tissue. The activation of this photosensitive compound can be used for tissue diagnosis or even for releasing of therapeutic agent within a target tissue (164).

When the absorbed photon energy alters the normal tissue behavior and metabolic rate, either of stimulative or repressive nature, without a significant thermal effect, the result is called photobioactivation reactions or photobiostimulation reactions. These reactions described the phenomena that occur following low-level laser therapy (LLLT), which is one of the more interesting and fastest growing applications of lasers in medicine (164).

All the laser-tissues interaction mechanisms that are used in the medical field utilize energy density ranging from approximately 1 J/cm^2 to 1000 J/cm^2. However, power density of medical laser systems varies much greater from around 0.01 W/cm^2 to 10^{16} W/cm^2 according to the range of the required final biological responses (168). Therefore, the exposure duration of the proper power density is a very important parameter when selecting a specific type of laser-tissue interaction mechanism, since the correlation between the power density and exposure duration resulted in approximately similar energy density for the different types of biological interactions (168). Accordingly, the time scale can be divided into four sections as following: continuous wave or exposure time more

than 1 second for photochemical or photobioactivation reactions; 1 minute down to 1 microsecond for photothermal reactions; 1 microsecond down to 1 nanosecond for photoablation; and less than 1 nanosecond for photodisruptive reactions (168).

2.4.3 Low-Level Laser Therapy

The basic concept of low-level laser therapy (LLLT) is that laser radiation has a wavelength-dependent capability to either stimulate or repress certain cellular behavior and metabolic rate in the absence of significant thermal effect (164, 169, 176). Pioneer researchers assumed that low-level laser radiation only stimulates biological behaviors because of the initial reports indicated that LLLT was able to accelerate wound healing and hair growth. For this reason, the phenomenon was initially termed "biostimulation or photobiostimulation" (169). However, the following accumulated evidence found that LLLT not only able to stimulate, but also suppress some physiological functions in order to reach normalization and tissue homeostasis (176). Therefore, it could be more appropriate to identify such phenomenon as "laser photobiomodulation" or "laser photobioactivation" reactions in order to describe the possible stimulatory or suppressive alteration in normal tissue function and metabolic rate following irradiation of the tissue with low-level laser (176). On the other hand, the term "therapeutic laser" describes the purposes of using this approach in medical field. The terms such as "soft", "cold", "low intensity", "low level", and "low power", all describe the low energy feature of the laser beam used in this method and the lack of significant increase in tissue

temperature following absorption of such energy (164, 169, 176). Since their development, several clinical applications of LLLT have been reported. LLLT dramatically promotes tissue healing, reduces edema and inflammation, attenuates pain, stimulates bone remodeling and repair, restores immune system imbalance, brings back the normal neural function following injury, equilibrates the abnormal hormonal level, and activates the process of endorphin release (176, 177).

Proponents of low-level lasers point to the non-invasive nature of this kind of therapy (177). Lasers that have been used in LLLT are considered safe and classified as class III according to the safety classifications of medical devices, whereas surgical lasers are more harmful and classified as class IV (176). There is no report in the literature stating any harmful side effect of applying LLLT in medical field (176). However, the risk of eye injury during LLLT is possible, especially for high output power in the non-visible light range. Therefore, as a safety precaution according to the American National Standard for safe use of lasers in health care, the patient, the therapist, and everybody present in the room must wear protective goggles, specific for the used wavelength, during the LLLT procedure (176, 178).

During the 1960s in Budapest, Mester was the pioneer in exploring and investigating the effect of LLLT. His first animal studies were done in order to clarify what he had thought a possible carcinogenic effect of LLLT(179). However, he found an increase in the epithelial growth during a wound healing

following the twice-a-week application of 1 J/cm² laser radiation (ruby lasers at 694.3 nm wavelength) for three weeks (179). He also found that application of higher doses did not improve this effect, but in contrary, if the dose was increased too much, the result was opposite and the wound healing was inhibited (151, 179, 180). This work established the concept of LLLT and over time it became more accepted due to the non-invasive nature of this laser and the lack of harmful side effect. Since then, it was obvious that low level laser irradiation can alter tissue behavior at the level of cells and subcellular organelles and thus offering a wide range of possible applications in medical field (151, 180).

This work was followed by others who used HeNe (Helium-Neon) laser, a gas laser emitting continuous waves; at 632.8 nm wavelength with output power ranging between 1 to 5 mW. The HeNe laser was the most commonly used LLLT in the mid to late 1970s. The main disadvantages of the medically effective HeNe laser device are its size and also the relatively high price. In order to get a therapeutically applicable HeNe laser device with output power up to 100 mW, the size of the device then has to be much bigger which became difficult to handle for medical applications (151, 176).

The recent advance in technology made it possible to construct laser devices with parameters that more suitable for therapeutic applications. Nowadays, both gallium-arsenide (GaAs) and gallium-aluminum-arsenide (GaAlAs), near-infrared wavelengths semiconductor diodes lasers, are considered ideal devices for

applying LLLT. There is a growing belief that these two devices not only are able to exert a wider range of biological effects, but also are more effective (151, 169). Most of the contemporary LLLT research and medical applications are done with GaAs and GaAlAs diodes with wavelengths ranging between 820 nm and 904 nm, even though HeNe devices are still used (169).

The GaAs (gallium-arsenide; 904 nm) diode laser was introduced for biostimulation in the early 1980s. The emitted light of GaAs is non-visible in the infrared range. The energy of GaAs laser system can be delivered only in pulsed waveform due to the tendency of the device to overheat when run for long periods in continuous waveform. The typical GaAs system used in LLLT works with a pulse peak power up to 100 W and each pulse length ranging between 100 and 200 nanoseconds (151).

The GaAlAs (gallium-aluminum-arsenide) diode laser for biostimulation was developed in the late 1980s. The energy of GaAlAs laser system can be delivered in both continuous and pulsed waveform. The percentage of each substance used in the lasing medium indicates the wavelength of GaAlAs system, which could range from 660 to 890 nm (151). However, tissue peak penetrations were observed with GaAlAs laser system at 830 nm wavelength (164). In general, GaAlAs system proved to be more effective than the previous GaAs system; and also gives better biostimulation results than Nd:YAG (1064 nm) system even for the more deeply located tissue targets, without the heat related side effect that are usually observed

with the YAG system used for LLLT application (166). Early GaAlAs systems were only able to provide an output powers range from 10 to 30 mW, however since the late 1990s they have been improved to reach up to 500 mW. Studies of the effect of different output powers on the therapeutic outcomes of GaAlAs found that, any output powers below 60 mW result in a delayed biological effect; however output powers above 100 mW were sometime associated with the development of quasi-photothermal effect, which was characterized by episodes of pain exacerbation following involuntary muscular spasm and nerve syncope (166). Therefore, the recommended output power of the GaAlAs continuous waveform systems was set between 60 and 100 mW with power densities in the range between 1.5 W/cm² to 3 W/cm² (166). These power densities are too low to generate any significant thermal side effect (± 1º C) on the target molecules (166). The maximum increase of the tissue local temperature up to 1º C following the application of the aforementioned power doses was linked to the increase of the cells metabolic activities rather that the amount of energy associated with output power delivered by the laser beam (181).

Not all lasers are appropriate for biostimulation. Wavelength of the laser light should be longer than 600 nm in order to trigger the required biological response (151). The majority of the published reports about the application of low-level laser in medical field were done by HeNe, GaAs, and GaAlAs laser systems (151), however biostimulatory effect have been also reported with other laser types such as Nd:YAG laser at 1064 nm (182) and CO_2 laser at 10600 nm (183). As discussed

earlier, the penetration of laser beam in the range of far-infrared wavelength (i.e. CO_2 at 10600 nm) is limited to the tissue's outermost layers (164). Therefore, CO_2 laser at 10600 nm is not useful for stimulating the deeply located tissues as its entire energy is absorbed by the surface. On the other hand, even though lasers in the range of red visible light (e.g. HeNe at 632.8 nm) are able to penetrate deep, the peak penetration depth is observed with the near-infrared wavelength range (e.g. GaAs at 904 nm; GaAlAs at 820 to 840 nm; Nd:YAG 1064 nm) (164, 184). Contrary to the HeNe, GaAs, and GaAlAs laser systems, the main drawback with the use of Nd:YAG for biostimulation purpose is the potential significant thermal side effect, which could result in heat-induced tissue necrosis (185).

As discussed earlier, wavelength of laser light is the most important determinant in how light affect tissue. The wavelength indicates the distance to which emitted laser beam is able to cross within a specific tissue. However, the energy of the laser light decreases at an exponential rate as the laser light pass through a given tissue, as a result of the scattering and absorption of laser energy by the tissue components (169). The light of HeNe laser with 632.8 nm wavelength at red visible range penetrates about 0.5 to 1 mm inside a tissue before losing 37% of its incident energy; however lasers light with longer wavelengths at near-infrared range (e.g. GaAlAs at 820 to 840 nm; GaAs at 904 nm) penetrate nearly to 3 mm within the same tissue before losing the same fraction of its energy (164, 166, 169-174).

Early investigators have suggested the appropriate energy density dose for LLLT around 4 J/cm² (169, 179, 180). More recent reports indicate that the energy density between 4 and 6 J/cm² may be more appropriate (181). The ideal threshold of the cellular response to laser stimulation (optical window) was observed with energy density doses between 4 and 6 J/cm². Nevertheless, the energy of the laser light required the minimum time to reach the cellular response threshold if therapeutic dose was between 4 and 6 J/cm² (181). On the other hand, applications of LLLT using excessively high output power not only delivered laser energy too quickly, but also lead to low energy absorption by the tissue's components and thus unsatisfactory response (181). Therefore, application of repeated low doses, at a given intervals sessions (e.g. once a day for two weeks) induces much greater effects than the same total dose given in one treatment session (151).

Laboratory research showed that LLLT with energy density around 0.01 J/cm² could stimulate a cellular response (169). Therefore, the therapeutic penetration depth was defined as the possible distance that laser beam, with energy density around 4 J/cm², can pass through the tissue before attenuating its incident energy to the 0.01 J/cm² level (169). It was postulated that therapeutic penetration depth, of 4-6 J/cm² LLLT dose, is approximately equivalent to 8-10 mm for wavelength of 632.8 nm (HeNe lasers); 30-40 mm for wavelengths of 830 nm (GaAlAs laser); and up to 50 mm for wavelength of 904 nm (GaAs lasers) (172, 175). In conclusion, along with using the established energy density dose, the wavelengths of GaAlAs and GaAs lasers have been proved to have the required penetration depth to

deliver the appropriate amounts of their therapeutic energy, which in turn insure the optimum energy absorption by the tooth root surfaces and therefore trigger the intended biological response.

There are two established techniques in LLLT that have been used to deliver the laser beam to the target tissue surface. This means that application of the laser light on the tissue surface has two ways: the contact technique when the delivery device directly touches the tissue surface; or the non-contact technique by holding the delivery device at a distance away from the tissue (164). The non-contacting technique itself can be used in two different ways: either by holding the delivery device steadily on one spot; or by scanning the beam across the target tissue. There are certain cases where non-contacting LLLT technique is preferred especially when treating open wound and burn tissue. On the other hand, contact LLLT technique can increase the purity of the laser beam received by the tissue and thus increase its penetration depth. Therefore, it has been suggested that the most effective application of the LLLT should be the contact technique whenever possible (164). The irradiated surface area in the contact technique is equal to the aperture size. Moreover, applying pressure in contact LLLT technique may assures deeper penetration by thinning the overlying tissue and providing a degree of blanching of the superficial blood vessels (164).

Anyway, whatever the technique used to deliver the low-level laser beam, the incident angle of the beam when touching the tissue surface should be as perpendicular as possible to improve the beam penetration by minimizing the

reflection or refraction of the laser light (181). For all these reasons, when planning for intraoral application of LLLT over dental roots, it is recommended to use the contact technique at a right angle when possible in order to improve the penetration capability of the laser beam and therefore maximizing the expected therapeutic effect (Figure 5) (176).

Figure 5: intraoral application of LLLT (176).

2.4.4 Some Biological Actions of LLLT

Several laboratory studies and clinical investigations have found that LLLT can influence the behavior of many cell types simultaneously, resulting in favorable tissue response that can be used clinically to treat, stimulate, or normalize several medical conditions (177). The effects of low-level lasers on the oral tissues have been investigated. LLLT can stimulate and accelerate the healing processes of oral wounds in tissues such as the soft tissues and the dental alveolar bone (186).

Several studies have been done to illustrate the mechanism behind the ability of LLLT to accelerate oral wounds healing (186). It was found that LLLT (pulsed wave GaAs at 904 nm wavelength) is capable of activating the production of the

latent transforming growth factor-β (TGF-β) complex (187). Moreover, an increase in expression of TGF-β was reported even under hypoxic condition in vitro following the LLLT (continuous wave GaAlAs at 808 nm wavelength) (188). TGF-β exerts a wide range of biological responses that are considered important in the process of wound healing (187). Another study investigated the stimulatory effects of LLLT on fibroblast proliferation. It was shown that LLLT (660 nm) is able to stimulate the production of basic fibroblast growth factor (b-FGF), which is a multifunctional polypeptide that is able to stimulate the proliferation and differentiation of fibroblasts during wound healing (189).

LLLT was suggested to have anti-inflammatory effects in the periodontium. Application of LLLT (continuous wave GaAlAs at 830 nm wavelength) significantly reduces the production of prostaglandin E2 (PGE2) in human gingival fibroblast cells by inhibiting the expression of cyclooxygenase-2 (COX-2) gene (190). Moreover, it was found that LLLT can stimulate the remodeling of periodontal tissue by inducing collagen synthesis, equilibrating the secretion of various remodeling matrix metalloproteinases enzymes, and inhibiting gene expression of pro-inflammatory cytokines such as interleukin-1 (IL-1) (191).

Several studies have reported that LLLT (GaAlAs) can stimulate bone formation, enhance bone repair, and improve the quality of bone structure by influencing the appropriate cellular functions that provide the favorable environment to accelerate the primary bone regenerative process (192-194). It was shown that, a daily

application of LLLT for one week using a GaAlAs laser significantly accelerates bone repair during the wound healing process after tooth extraction in a rat model. This acceleration was due to both increased fibroblast proliferation and accelerated formation of bone matrix by osteoblasts cells (195). Speeding up the process of bone formation following LLLT application was not only linked to the increase in osteoblastic activity but also explained by the ability of LLLT to enhance bone vascularization (196) and increase ATP levels within target tissue (197); which in turn creating a favorable environment to stimulate bone formation that characterized by organized collagen fibers (198). On that basis, the efficiency of LLLT application to increase tissue vascularity was more evident by using GaAlAs system with wavelength around 830 nm (164, 199). Application of continuous wave GaAlAs (830 nm, 35 mW power, 1.4 J energy and 178 J/cm2 fluency) at a single dose directly to surgically created bone defects, in rats, accelerated the bone repair process dramatically by optimizing the proper cascade of inflammatory response followed by an increase in the healing capacity of the target tissue that characterized by an enhanced tissue vascularity and increased in the production of ATP level (200). Moreover, application of continuous wave GaAlAs LLLT (around 830 nm wavelength) accelerated the process of bone healing and increased the amount of bone formation significantly during the consolidation phase after mandibular distraction osteogenesis in rabbits (201, 202).

Besides the ability of LLLT to optimize the local conditions that accelerate the process of bone formation, the energy of the low-level laser is capable of

increasing the production of potent mediators that have a direct effect in stimulation the activity of calcified tissue's forming cells. It was reported that LLLT (GaAlAs at 830 nm) could directly induce osteoblasts proliferation and differentiation *in-vitro* by increasing the activity of alkaline phosphatase, and stimulating the expression of osteocalcin that lead to an increase in the calcium level accumulation (203). It was also found that LLLT (GaAlAs at 830 nm) is able to stimulate the local production of insulin-like growth factor-1 (IGF-1) and bone morphogenetic protein (BMP) that are known as effective mediators in stimulating the formation of calcified tissue (204, 205). Moreover, the stimulatory bone formation effect of LLLT (GaAlAs at 830 nm) was linked to the increase in the expression of the osteoglycin gene, which is a small leucine-rich proteoglycan (SLRP), located in bone extracellular matrix, that is thought to play a role in bone tissue formation and mineralization (206).

2.4.5 LLLT Effects in Orthodontic Treatment

The special effect of low-level lasers in stimulating bone formation, either by providing the appropriate environment or by influencing the related cellular activity, offers an interesting treatment modality that is able to enhance the remodeling and regenerative capability of the periodontal connective tissues. Positive results have been reported in studies of the effect of LLLT on tooth movement during orthodontic treatment (207, 208).

Many studies confirmed that LLLT is able to reduce the level of pain during orthodontic treatment (209-212). A double blind clinical study found that only one or two applications of LLLT (continuous wave GaAlAs at 830 nm) were able to attenuate the pain intensity that usually happens during orthodontic tooth movement (213). Another single blind clinical study concluded that one time application of LLLT (continuous wave GaAlAs at 830 nm for 20 seconds per each of 6 different points per tooth with a dose of 5 J/cm² at 100 mW) was enough to significantly reduce the pain intensity in orthodontic patients after the placement of elastic separators (214). A recent randomized controlled clinical trial on a sample of 60 patients reported that LLLT (continuous wave GaAlAs at 830 nm for 22 seconds irradiation over each buccal and palatal root aspect with a dose of 80 J/cm² at 100 mW) caused a significant reduction of the pain level up to 7 days following the activation of orthodontic final archwire (215). This decrease in pain level could be attributed to the ability of LLLT (continuous wave GaAlAs at 830 nm) in inhibiting the local production of prostaglandin (PGE2) and interleukin-1 (IL-1); since high levels of PGE2 and IL-1 trigger the process of pain induction, and both molecules are produced abundantly in the periodontal ligament (PDL) during orthodontic tooth movement (216).

The effects of LLLT in accelerating tooth movement rate during orthodontic treatment have attracted attention (217-219). A study on rats concluded that the daily application of LLLT GaAlAs at 830 nm (continuous wave for 3 minutes at three different 0.6 mm diameter points with 100 mW and total 35.3W/cm² for

each tooth) significantly accelerates the rate of orthodontic tooth movement, 1.3 fold greater than control, during 12 days treatment (220). This biostimulatory effect was explained by the ability of LLLT to enhance the alveolar bone remodeling capability that is characterized by a significant increase in the amount of bone formation and rate of cellular proliferation in the tension side of the dental root as well as the number of osteoclasts in the pressure side (220). Another animal study found that nine days of LLLT application (continuous wave GaAlAs at 830 nm for 2.15 minutes at four different 0.6 mm diameter points with total 54 J/cm² for each tooth per day) significantly increased the amount of tooth movement in rats (221). This significant difference in the amount of tooth movement was noticeable starting from the day 3 after initiation of the orthodontic treatment in the LLLT group. The acceleration of tooth movement was linked to the stimulatory effect on the process of alveolar bone remodeling in LLLT group, indicated by the significant increases in the amount of bone formation, blood vessels dilatation, and periodontal cell proliferation in the tension side of the dental root as well as the increase in the number and activity of osteoclasts in the opposite pressure side (221-224).

These findings were also supported by other clinical observations. A significant clinical acceleration of the tooth movement during canines' retraction was reported in patients treated with only 4 days application of LLLT GaAlAs at 780 nm wavelength (continuous wave for 10 seconds per each of the ten different 0.04 cm^2 spot area per tooth, at 20 mW; 5 J/cm²) during each month of canine

movement following the extraction of maxillary first premolar (225). Similar results were concluded by another clinical study using 4 days application of LLLT GaAlAs at 809 nm (continuous wave for 10 or 20 seconds per each of 6 different points per tooth, at 100 mW; with total 8J). LLLT causes a significant acceleration of the teeth movement and patients experience a significantly lower degree of pain level in teeth that received LLLT during the orthodontic treatment (226). A recent clinical study on a sample of 20 patients showed that 6 times of LLLT application (continuous wave GaAlAs at 808 nm for 10 seconds per each of 10 different points per tooth with a dose of 0.71 J/cm² at 20 mW) significantly accelerated the retraction of the maxillary lateral incisors (208).

The mechanism that LLLT accelerates the rate of tooth movement lies in its ability to stimulate the remodeling activity of the alveolar bone surrounding the dental root. Histologically, it was shown that 7 days of LLLT daily application (continuous wave GaAlAs at 808 nm for 10 seconds at 96 mW: 4.98 J/cm²) significantly increases the remodeling and the turnover rate of the connective tissues surrounding the root during tooth movement in rats (227). This study showed that LLLT significantly increases the expression of periodontal fibronectin and collagen type I, associated with dense connective tissue and an increase number of fibroblasts, osteoblasts, and undifferentiated mesenchymal cells (227). LLLT (continuous wave GaAlAs at 810 nm) is effective in stimulating alveolar bone resorption at the pressure side of the dental root during orthodontic treatment by regulating the activities of osteoclasts through the

OPG/RANKL/RANK system (228, 229). In the same way, LLLT (continuous wave GaAlAs at 830 nm) is also capable of stimulating bone formation and activating the cellular proliferation and differentiation of osteoblasts in the tension side during tooth movement (220, 221, 230). Moreover, it was reported that 7 days of LLLT daily application (continuous wave GaAlAs at 830 nm) significantly stimulated bone formation in the midpalatal suture during rapid palatal expansion (RPE) in rats (231). These results indicate that LLLT application at the range of 830 nm wavelength is an effective modality in stimulating the remodeling activity and the regenerative capability of the connective tissues around the dental root.

Finally, the use of justifiable parameters is essential to insure laser energy absorption by the target tissue and subsequently to produce the required biological response. Therefore, the application of too low output power laser could not trigger the required biological effects and could result in a delayed treatment response; and this could not be fully compensated by longer exposure duration (176). Reportedly, application of 5 mW output power, of two continuous wave LLLT at 850 and 630 nm wavelengths for 5 minutes, was too low to express the required stimulatory effect on the rate of orthodontic tooth movements in rabbits (232). Moreover, delivering the laser beam with an aperture size smaller than the target tissue size could limit the appropriate tissue irradiation and the energy absorption. It is also important to consider the relation between the aperture size and the treatment dose. For example, halving the diameter of the tissue surface spot size will increase the energy density by four. Accordingly, no significant

effect was found from the daily LLLT (continuous wave GaAlAs at 860 nm; 100 mW; aperture size 0.09 cm^2) on the rate of patients' tooth movement (233). This could be explained either by the relatively small aperture size that failed to irradiate the whole periodontium surrounding the human dental root, or because the resulted energy density was very high (each point 25 J/cm^2) to produce the stimulatory effect on the rate of tooth movement, since the application of far higher doses could give an opposite, inhibitory, response (151, 179, 180, 219).

3 STATEMENT OF THE PROBLEM

Orthodontically induced tooth root resorption (OITRR) is a common deleterious consequence of orthodontic tooth movement resulting in the loss of the dental root structure. OITRR is a type of external root resorption, which originates from the pressure applied to the root during orthodontic tooth movement. This pressure produces an ischemic injury adjacent to the compressed root surface and subsequently initiates complex inflammatory interactions that are related to biological repairing and remodeling activities (1, 24). The frequency of teeth showing some grades of OITRR is quite high. However, only two to five percent of orthodontic patients experienced severe OITRR beyond one third of the root length (6, 7). The major effects of severe OITRR are related to an impaired tooth crown/root ratio that can go from mild tooth mobility to tooth loss (8). If OITRR could be prevented, it would be an important contribution toward reducing one of the most potentially negative side effects in an orthodontic treatment.

Many possible factors that may cause or facilitate OITRR have been studied. These factors include: the amount to which dental root is displaced, treatment duration (10), magnitude of the applied force (11), direction of applied force (12, 13), method of force application (continuous or intermittent) (13, 14), age (15), root morphology (16-18) and/or genetic factors (19). However, no claim can be made that OITRR is caused directly or exclusively by only one of these factors. For this reason, it is believed that other key causative and/or preventive factors have yet to be identified (5, 24).

The precise pathological events and trigger factors that are responsible for the initiation and the progression of the OITRR are still uncertain. However, breakdown of the cementum layer caused by orthodontic pressure is required to allow the process of root resorption to take place (9, 26, 97). Dental root surfaces are more resistant to resorption than alveolar bone because of the fact that the presence of an intact cementum tissue forms a protective barrier preventing resorbing cells from gaining access to the root surface (77, 91). This inherent relative resistance of cementum to resorption has been explained by the presence of the precementum, which is a thin non-mineralized layer covering the external surface of cementum (91). Moreover, viable cementum is essential for the vitality of the periodontal ligament cells around the dental root (77). Accordingly, healthy periodontal ligament can provide additional protection to the root structure during tooth movement either by acting like a cushion that diffuse the pressure against the root or by reducing the stress concentration at the compressed root surface by producing mediators that stimulate the appropriate remodeling of the opposing alveolar bone (76, 88-91). On the other hand, it is well documented that application of orthodontic force to move teeth with unfavorable cementum condition can increase the susceptibility of the dental root surface to resorption during orthodontic tooth movement (51).

Based on the aforementioned reports from the literature, cementum layer augmentation may provide additional protection to dental root against resorption.

Clinical observations in patients with a history of earlier orthodontic treatment showed a decrease in the degree of root resorption during the second treatment (101). Moreover, less root resorption was found in children treated in two phases than in children treated in one phase orthodontic treatment (234). Hypothetically, this additional resistance against OITRR could be attributed to cementum remodeling during the first treatment (24). Therefore, tooth root surface remodeling by inducing new cementum formation might be an important preventive factor that influences the onset and the progression of orthodontically induced tooth root resorption (OITRR), and according to our best knowledge, this would be a novel discovery.

Many studies have investigated the effect of a direct topical application of different growth and differentiation factors in order to induce cementum formation around a previously exposed dental root surface due to periodontal disease (102-106). However, unlike periodontally involved teeth, the dental root surfaces susceptible to resorption during tooth movement are usually not exposed to the outer oral environment and this makes these surfaces inaccessible to any therapeutic topical application (77). On the other hand, it was reported that the systemic administration of cyclosporine A (CsA) (127, 129), or the surface application of low-level laser therapy (LLLT) (187, 189, 204), can increase the local production of some growth factors around dental roots, such as transforming growth factor-β (TGF-β), platelet-derived growth factors (PDGFs), insulin-like growth factor-1 (IGF-1) and basic fibroblast growth factor (b-FGF). These factors

have been recognized as having a role in the cementum formation and development (73). For this reason, we proposed the systemic administration of CsA or the surface application of LLLT, as potential treatments to induce new cementum formation in sound dental root surfaces prior to tooth movement.

Several studies have demonstrated that systemic administration of Cyclosporine A (CsA) induces the formation of significant amounts of new cementum over all dental root surfaces in rats (143-148). The amounts of the new cementum formed in all these studies were reported after one month of daily treatment of CsA, however, one study (146) reported that the highest apposition rates of new cementum were found in the first two weeks of the daily administration of a similar CsA dose. Moreover, the doses were well tolerated by the animals and the new cementum layer persists, structurally and functionally, for a long period of time after the termination of the treatment regardless the type of the drug administration route (144, 147). Administration of CsA by subcutaneous injection provides more consistent pharmacokinetic profile than any other administration route in rat model (117). A constant absorption rate with a steady serum level of the drug over the 24 hours was observed following CsA subcutaneous administration in rats. It was shown that daily dose CsA of 10 mg/kg of rats' body weight by subcutaneous injection provided plasma peak and trough levels of around 1000 and 750 ng/ml, respectively, with a bioavailability reached about 80% (117). CsA, a polypeptide produced by a fungus, is a potent immunosuppressive drug currently used to prevent rejection in transplant

medicine and in the therapy of autoimmune diseases (110). CsA was discovered during a search for new antibiotics. This drug exerts a broad range of pharmacological effects as well as a number of potentially significant side effects and adverse drug interactions (110).

The non-invasive nature of low level laser therapy (LLLT), in combination with its ability to enhance tissue remodeling and repair, would theoretically make it a potential preferable method to stimulate new cementum formation in dental root surfaces. Therapeutic approach of LLLT is safe and completely different from surgical lasers. The mechanism behind LLLT is that laser radiation has a wavelength-dependent capability to either stimulate or repress certain cellular behavior and metabolic rate by absorbing laser light energy in the absence of significant thermal effect (164, 169, 176, 177). Several studies have reported that LLLT (GaAlAs) can influence the appropriate cellular activities, stimulate tissue vascularity, and increase the tissue ATP level that provide the favorable environment to accelerate the process of mineralized tissue formation (192, 193, 200). Moreover, it was reported that LLLT (GaAlAs at 830 nm) is capable of increasing the production of potent mediators that have a direct effect in stimulation the activity of calcified tissue's forming cells (203). On the other hand, it was shown that LLLT (GaAlAs) significantly accelerates the orthodontic tooth movement by stimulating alveolar bone remodeling, as indicated by the cellular proliferation and the enhanced mineralized tissue formation around dental roots (217, 220, 227). Moreover, several clinical trials found that LLLT application at 830

nm wavelength can reduce the intensity of orthodontic pain (213-215). This decrease in pain level was linked to the ability of the same wavelength LLLT in inhibiting the production of some inflammatory molecules such as prostaglandin (PGE2) and interleukin-1 (IL-1) (216). Therefore, it could be said that 830 nm wavelength LLLT can also enhance the cementum growth by providing more protection from any physiological process that lead to cementum resorption, since the high levels of both PGE2 and IL-1 are not only involved in pain induction, but also increase the susceptibility of mineralized tissue toward resorption (29, 30, 64, 65). Theoretically, in order to stimulate cementum cells which are located deeply in the periodontal space, the near-infrared continuous wave gallium-aluminum-arsenide (GaAlAs) low level laser at 830 nm (nanometer) wavelengths with 100 mW (milliWatt) output power and exposures dose of 4 to 6 J/cm² per-treatment, would provide justifiable parameters to insure the appropriate energy absorption by the cells and thus stimulate the required tissue remodeling (164, 166, 169-174).

There are several advantages that make rats a suitable model for this study. Obviously, the relationship between the pathological sequences of OITRR and the cementum biology cannot be attained in tissue culture. Several studies in literature about the effects of different biological and pharmacological agents on OITRR utilized convenient designs of orthodontic appliances in rats (40, 42, 46, 52, 58, 61, 66, 67, 235-240). The rat model will offer the advantage of comparing our outcome results to studies using this same model and this can provide insights as to possible mechanisms that may have relevance in humans. Our major research goal

is to test the effect of cementum remodeling on root resorption due to orthodontic tooth movement. In light of this, only the rat model's cementum has been tested and verified to respond to the systemic administration of Cyclosporine (CsA) (143-147). Moreover, low level laser therapy (LLLT) application in rats has been tested and shows a significant remodeling activity in the connective tissues around dental roots (220, 227). Furthermore, the small physical size of the rat will enable the use of micro-computed tomography (micro-CT) as a potential non-invasive modality to investigate the cementum growth in an *in vivo* setting. Larger animals will not fit into the high-resolution micro-CT imager that is located at University of Alberta. However, the difference in "cementogenesis and cementum biology" such as "attachment mode of cementum to dentin and the rate of cementum apposition" between rodents and larger mammal species, including humans should be taken in consideration before suggesting a clinical application of any treatment modality (77).

4 RESEARCH OBJECTIVES

- Evaluate and compare the amount of new cementum formed independently either by cyclosporine A, or by low-level laser therapy, in rats dental roots surfaces.

- Investigate the role of the remodeled new cementum, induced either by cyclosporine A or by low-level laser therapy, on orthodontically induced tooth root resorption in rats.

5 HYPOTHESES

1- The pharmacological action of cyclosporine A will induce the formation of a significant amount of new cementum on rat's dental root surfaces.

2- The photobiomodulation action of low-level laser therapy will induce the formation of a significant amount of new cementum on rat's dental root surfaces.

3- Remodeling the rat's dental root surfaces by inducing new cementum formation either by cyclosporine A, or by low-level laser therapy, would provide a significant protective effect against orthodontically induced tooth root resorption.

6 METHODOLOGY

In order to accomplish the study objectives, a pilot study and two different animal experiments were performed. All the experiments procedures were done by the student (MA), except for the preparation of the histological sections.

Female Sprague-Dawley (SD) rats (Biosciences Animal Service, Edmonton, Alberta), aged six weeks old (180 ± 10 grams) were used in all the experiments as will be discussed later. The animal experiments protocol was approved by Animal Care and Use Committee for Health Sciences at University of Alberta (animal use protocol number: 601).

The animals were randomly distributed into labeled cages, two rats per cage, and housed at the University of Alberta Health Sciences Laboratory Animal Services (HSLAS) Facility. Ear notching identified each rat. All the animals in all the following experiments were given 7 days to adapt to the new environment and exposed to the standard 12-hour light/dark cycles. The animals were given water *ad libitum* and fed ground rat chow in powder form to create a soft diet that would help prevent orthodontic appliance breakage. The weight and general condition of all the animals were assessed daily throughout the study period.

6.1 Pilot Study

A small preliminary study was conducted to assess the feasibility of the planned *in vivo* analytical procedure for evaluating the cementum growth in response to

the proposed treatment in our main study. Four female, 6-week-old, Sprague-Dawley (SD) rats were used and randomly divided into two experimental groups. Two rats received a daily dose of 10 mg/kg of cyclosporine A (CsA; Sandimmune Injection, Novartis) by subcutaneous injection for two weeks. The other two rats served as the control group and received no treatment.

Initially, all of the pilot study animals were to undergo a high-resolution *in vivo* micro-CT scanning immediately before treatment start (Time 0) and at the end of the two-week treatment (Time 1). Each rat was exposed to radiation for approximately 50 minutes during the Time 0 micro-CT session. The images were obtained at a 9 μm resolution with a 0.025 mm thick titanium filter. However, severe tissue degeneration was observed in the right-side eyes of all the animals 10 days after of the baseline micro-CT scanning session. We informed the University of Alberta Health Sciences Laboratory Animal Services (HSLAS) about the incident and decided to discontinue the pilot experiment by euthanizing all animals by CO_2 asphyxiation.

We found that increasing the duration of the radiation exposure during the micro-CT scanning session, to acquire high-resolution *in vivo* images, affected the animals' health and the study results. Therefore, we selected the low-resolution, non-invasive, scanning parameters for all *in vivo* micro-CT procedures in the main study, which will be discussed later in the first animal experiment (see below, section 6.2.3).

6.2 First Animal Experiment

6.2.1 Experimental Procedures

To investigate the effect of cyclosporine A, or low-level laser therapy, in dental root cementum formation and the root volume change, a total sample of 18 female Sprague-Dawley (SD) rats, aged six weeks old were used and randomly divided into three treatment groups of 6 animals (n=6) per each group as following:

CsA Group: 6 rats received a daily dose of 10 mg/kg of body weight cyclosporine A (CsA) (Sandimmune Injection, Novartis) by subcutaneous injection for 2 weeks to induce new cementum formation and dental root volumetric change in both right and left maxillary first molars' mesial roots. Sandimmune Injection is supplied in 1ml or 5ml sterile ampoules containing 50 mg of CsA per ml in polyoxyethylated castor oil and ethanol. This solution was diluted to 1:10 with normal saline immediately prior to use as indicated by the supplier. The rats were weighed twice a week in order to adjust the CsA dose.

LLLT Group: 6 rats received a daily dose of low-level laser therapy (LLLT) for 2 weeks to induce new cementum formation and root volumetric change in both right and left maxillary first molars' mesial roots. An 830 nm wavelength gallium-aluminum-arsenide (GaAlAs) laser system (MediCom Maestro) was used. The roots were irradiated by continuous wave at 100 mW output power using 0.05 cm^2 beam spot area and power density dose of 2 W/cm^2. The output power was measured before each application by a gauge connected to the system (Figure 6).

Figure 6: measuring the output power prior to each LLLT application.

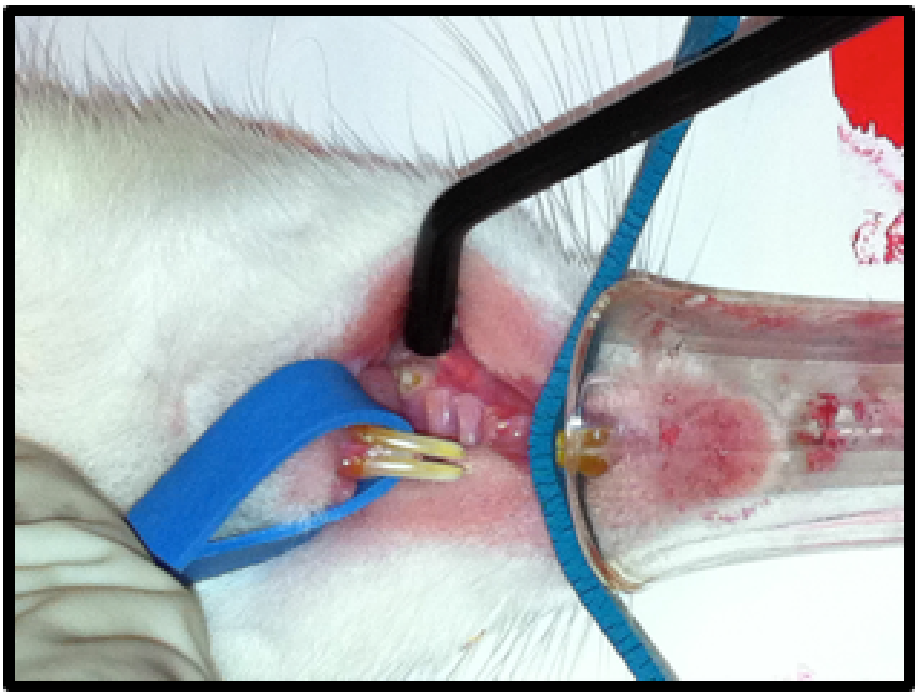

Figure 7: surface application of low-level laser therapy.

A rigid light guide delivered the laser beam (Figure 7) by placing the end of this guide tip in contact with the gingiva over the roots of both right and left maxillary first molars at four different points, the mesial, buccal, distal and lingual sides, for each molar. Irradiation was performed for 3 seconds at each point, with total energy density dose of 6 joules/cm^2 for each point once a day for 2 weeks. Animals of this group were anesthetized by Isoflurane inhalation daily prior to laser treatment to prevent device biting by the animal during the treatment.

Control Group: 6 rats received no treatment for 2 weeks. The dental root volumetric changes, due to normal growth, and the cementum thickness of this group were used in order to evaluate and compare the effect of the other treatment groups in this experiment.

6.2.2 Procedures Timeline

All animals in the first experiment (CsA, LLLT and control groups) were subjected to *in vivo* micro-CT imaging at 18 μm resolution immediately before treatment start (Time 0) and at the end of the two-week treatment (Time 1). Animals were anesthetized by Isoflurane inhalation during the entire imaging session. The root volumes, of all maxillary first molars' mesial roots, were obtained from the micro-CT analyses at each observation time point. Moreover, changes in dental root volume between the different observational time points, was calculated in response to each treatment.

At the end of the experimental time period, all animals were euthanized by CO_2 asphyxiation. All maxillary right and left first molars were then dissected and processed for histological evaluations. The mesial roots of all maxillary first molars of all the groups were subjected to histological analyses to compare the amount of new cementum induced by CsA and LLLT. The best treatment in inducing cementum formation was selected at the end of this experiment and used thereafter in the second animal experiment as will be discussed later.

6.2.3 Micro-CT Imaging

The micro-CT imager (Skyscan 1076) is located at University of Alberta, Pharmaceutical Orthopaedic Research Lab, at 2nd floor of the Katz Group Centre (room 2-108). At the time of each *in vivo* micro-CT imaging session, animals were transported directly from the HSLAS housing facility and then anesthetized using Isoflurane inhalation. Whilst under general anesthesia, rats were placed supine in an imaging bed and secured with masking tape to avoid movement during the imaging procedure. The imaging bed slides into the micro-CT imager, where the rat remains stationary under general anesthesia until the X-ray source-detector pair has completed 180 degrees of rotation around the animal, in approximately 30 minutes. After each non-invasive imaging session, the animal was removed from anesthesia, permitted to recover, and then returned to the animal housing facility.

For the first animal experiment, two *in vivo* micro-CT imaging sessions were performed for all the animals immediately before treatment start (Time 0) and at the end of the two-week treatment (Time 1). The images were obtained at 18 μm resolution with 1 mm thick aluminum filter. After that, raw images data set was reconstructed (from tif files to bmps) by using NRecon software (version 1.4.4). Data analyses were performed on the reconstructed images by using CTAn software (version 1.6.1.0). The same micro-CT imager company (Skyscan N.V., Kontich, Belgium) provided the previously indicated software.

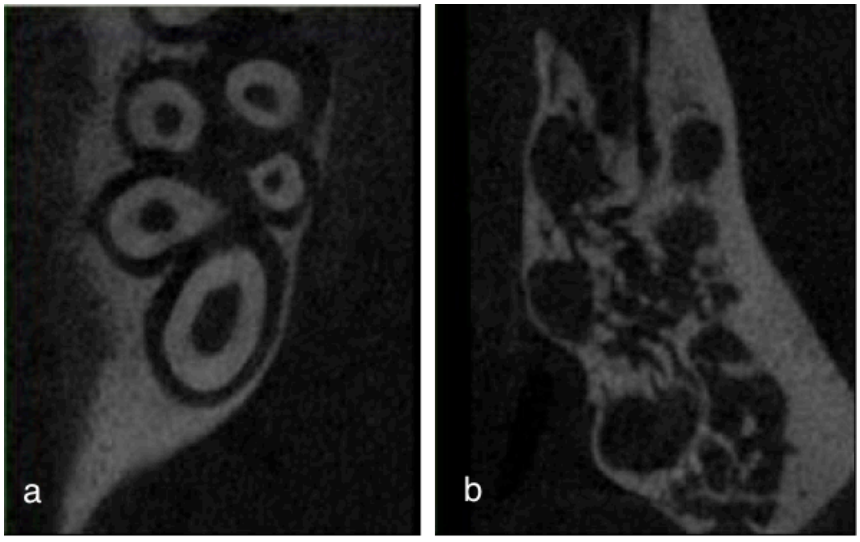

Figure 8: micro-CT volume of interest consists of all the cross-section root slices below the furcation area. Starting from this slice (a) where the roots completely separated and proceed toward the root apex until the end of the root (b).

Root volume was estimated by using micro-CT analyses from the first experiment. The mesial roots of all animals' maxillary right and left first molars were projected and sliced in cross sections. Root volume was analyzed at each time point by including all the cross-sectional slices below the furcation area,

starting from the slice where the roots completely separated (Figure 8a) and proceed toward the root apex until the end of the root (Figure 8b). After that, a region of interest was selected and drawn by including the area of each root (Figure 9a) through all the root slices that have been previously produced. Furthermore, a contrast threshold value was adjusted, fixed and applied to all slices in order to precisely include the root area and exclude the non-root area (Figure 9b). The threshold value was set to distinguish and include the area of root hard tissues from the surrounding periodontal soft tissues. Moreover, the area representing the soft tissues inside the radicular pulp was excluded because its density degree was similar to that displaying the periodontal soft tissues on the images. As a final step, the computer aggregated the included root area of all indicated slices and end up with a volume of interest that represents the dental root hard tissue volume.

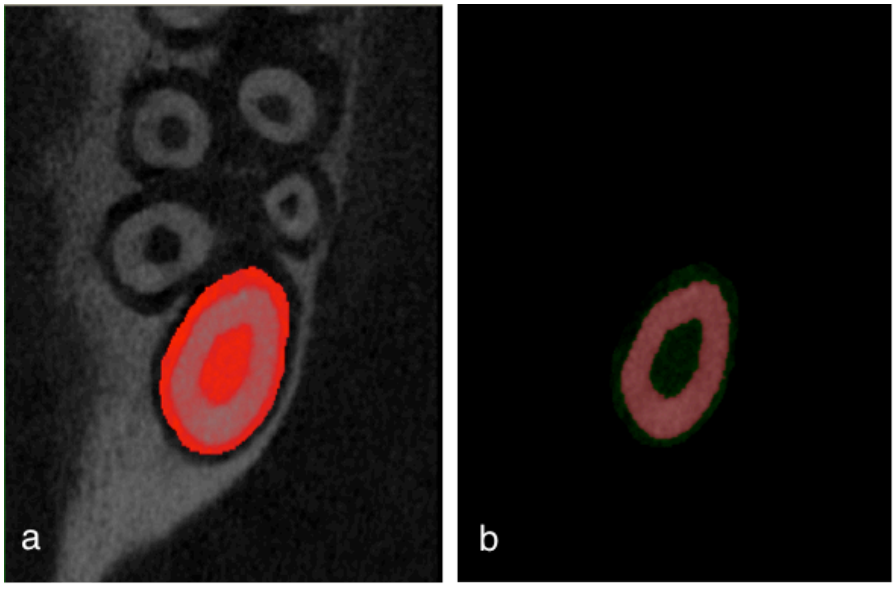

Figure 9: micro-CT region of interest. As shown in (a), select and draw the root area. (b), applying a threshold value to outline the root area; r*ed area* in (b) represent the area of root hard tissues.

6.2.4 Histomorphometric Analysis

At the end of the first experiment time period, the animals were euthanized by CO_2 asphyxiation. Each maxilla was immediately dissected. Specimens maxillary right and left first molar of each animal were cut and fixed in neutral-buffered 10% formalin solution for 48 hours. After that all specimens were decalcified using 10% ethylene diamine tetra-acetic acid (EDTA) solution for 4 weeks and then embedded in paraffin.

Once the decalcification was completed, all specimens were prepared for histological processing. The molars' crowns were removed and the mesial roots of all maxillary right and left first molars were dissected and processed for histological evaluations. Ten cross-section slices, 5 μm thick, were taken at 50 μm intervals through the whole length of each mesial root, starting where the roots completely separated, below the furcation area, and proceeding toward the root apex until the end of the root. The sections were mounted on glass slides, stained with hematoxylin and eosin (H&E) and examined under a light microscope using ZEISS AXIO microscope (Carl Zeiss, Germany).

The slides were prepared to be viewed in cross-section plane in order to show the cementum thickness in all the different aspects of the root surface. All slides pictures were taken by Optronics MacroFire digital microscope camera (Optronics®, California, USA). Using PictureFrame™ analysis software (version

2.3; Optronics®, California, USA), the extent of the cementum layer was calculated by multiple linear measurements that estimated the cementum width at each root aspects, the mesial, buccal, lingual and distal (Figure 10). The cementum thickness of each slide was calculated by averaging the extent of the cementum layer of all the root aspects in the slide. The total cementum thickness of each root is the average of cementum thickness of all its slides.

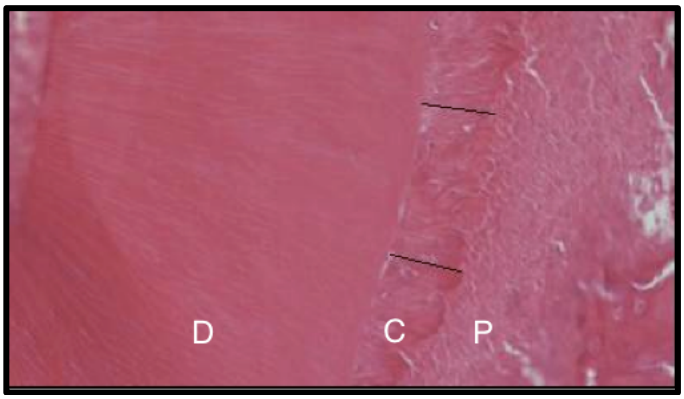

Figure 10: measuring cementum thickness (10X scale). The black line represents the extent of cementum layer. The layers are (D) dentin, (C) cementum, and (P) periodontal ligaments.

6.2.5 Statistical Analyses

When comparing between unrelated animals that each has received just one treatment (between-subjects comparisons), ignoring the correlation between the right and left side measurements of each animal will lead to an underestimation of P value, which in turn result in an incorrect rejection of a true null hypothesis (type I error) (241). Therefore, measurements from the right and left molars of the same rat were averaged and used as a single variable per each animal in all the statistical analyses of the first animal experiment. For this reason, the final total

sample size of the first experiment was 18 roots (Total: n = 18). Each group sample size was 6 roots (n = 6 for each group).

Due to the small sample size, non-parametric tests were considered the appropriate statistical models to use in the first animal experiment. The statistical tests were performed by using the software SPSS (IBM Corp, version21).

The Root-Volume-Difference-Proportion (RVDP) variables were created mathematically from the data of the micro-CT analyses in order to perform the non-parametric tests. The Kruskal-Wallis non-parametric test was performed on the RVDP to compare the root volume change between all the treatment groups.

Regarding the data obtained from the histomorphometric analyses, the following non-parametric tests analyzed and compared the amount of cementum thickness formed in response to each treatment. A Kruskal-Wallis test was performed to evaluate the cementum thickness between the three treatment groups. Three different Mann-Whitney tests were done to compare the mean cementum thickness between every two different treatment group. Moreover, four different Kruskal-Wallis tests were performed to compare the cementum thickness in all the four different root aspects (mesial, buccal, lingual and distal root surfaces) between the treatment groups. Furthermore, three different Friedman's non-parametric tests were performed to compare the cementum thicknesses between the different aspects of the root surfaces within each treatment group.

6.3 Second Animal Experiment

6.3.1 Experimental Procedures

Based on the results of the first animal experiment, where only LLLT exposure increased cementum thickness as will be discussed later in the results section, a follow-up animal experiment with split-mouth design was done in order to investigate the role of the LLLT-induced cementum overgrowth on the amount of root resorption caused by orthodontic tooth movement in rats. A sample of 10 female Sprague-Dawley (SD) rats aged six weeks old were used in this experiment. However, whilst anesthetized by Isoflurane inhalation, one rat died at the beginning of the experiment, which resulted in a final total sample of 9 female SD rats for the second experiment.

The right and left maxillary first molars of each rat were divided into treatment and control groups. All right side maxillary first molars served as treatment group, while all contralateral left side maxillary first molars were considered as control. The decision of which molars were allocated to treatment was made before starting the experiment. Because the operator is right-handed, the treatment was assigned to the right side in order to make the experiment easier to conduct in an animal model. There were 9 molars per each group (n=9), as following:

Remodeled Cementum group: all right side maxillary first molars (n=9) of all the animals in this experiment, received a daily dose of low-level laser therapy (LLLT) for 2 weeks, using the same technique and dose that was used in the first

experiment (see above; section 6.2.1, LLLT Group), in order to induce cementum formation in the mesial roots. An 830 nm wavelength gallium-aluminum-arsenide (GaAlAs) continuous wave laser system (MediCom Maestro) was used at 100 mW output power; with 0.05 cm^2 beam spot area; and power density dose of 2 W/cm^2. The output power was measured daily, before each application, by a gauge connected to the same laser system (Figure 6). A rigid light guide delivered the laser beam (Figure 7) by placing the end of this guide tip in contact with the gingiva over the roots of right maxillary first molars at four different points, the mesial, buccal, distal and lingual sides. Irradiation was performed for 3 seconds at each point, with total energy density dose of 6 $joules/cm^2$ for each point once a day for 2 weeks. Animals were anesthetized by Isoflurane inhalation daily prior to laser treatment to prevent device biting by the animal during the treatment.

Control group: at the same time, all left side maxillary first molars of all animals in this experiment (n=9) received no treatment for the two-week period. All mesial roots of all the left maxillary first molar of the second animal experiment were considered the control to comply with a split-mouth design that was applied to this experiment.

After two weeks, the LLLT treatments were stopped and orthodontic appliances were immediately placed in order to apply mesial orthodontic tooth movement of all the right and left maxillary first molars of all the animals for the next 4 weeks. The orthodontic appliance design was similar to the one described by Leiker *et al*

(66). For each animal, two nickel-titanium closed-coil springs (GAC Orthodontics Corporation, product number: 10-000-05) were placed between the maxillary incisors and both maxillary right and left first molars to produce 100-gram force (1 Newton). The exact force produced by spring's activation was measured by dynamometer (Correx Gram Force Gauges, Haag-Streit) once at the initial activation (Figure 11). The springs were attached to the above-indicated teeth by 0.010-inch ligature wires and were not reactivated during the experiment (Figure 12).

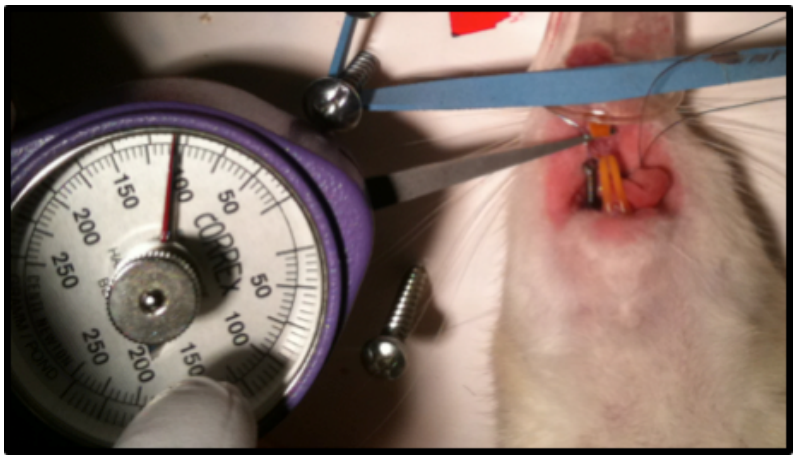

Figure 11: measuring the force applied by the closed coil spring.

Rats were operated under Isoflurane inhalation general anesthesia in order to place the orthodontic appliances. The ligature wires were securely placed and tightened around the maxillary molars below the crowns height of contour. Moreover, grooves were prepared on the mesial, and distal surfaces of both maxillary incisors to assist placement of the ligature wires firmly around the maxillary incisors. Finally, in order to prevent breakage of the ligature wires, the

lower incisors were trimmed and a layer of composite resin was placed over the wires. The composite layer would also help preventing possible pulpal irritation due to grooves preparation. This orthodontic (Figure 12) model has been established and used by several studies in the literature and was effective in inducing root resorption (46, 66, 67).

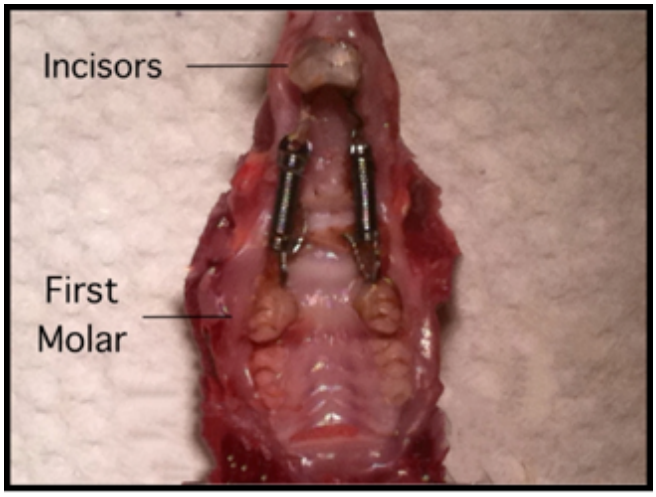

Figure 12: the orthodontic appliance design.

6.3.2 Procedures Timeline

The second animal experiment extended for six weeks. The daily LLLT treatment for all right side maxillary first molars lasted two weeks immediately before placing the orthodontic appliances bilaterally to move the right and left molars mesially over the next four weeks.

At the end of the experimental time period, all animals were euthanized by CO_2 asphyxiation. The maxillae were then dissected and fixed in neutral-buffered 10%

formalin solution for 48 hours. After that, all maxillae were subjected to high-resolution *ex vivo* micro-CT imaging. The mesial root resorption volumes of all maxillary right and left first molars caused by the orthodontic tooth movement were obtained from the micro-CT analyses to evaluate the effect of the initial root surfaces remodeling caused by LLLT treatment on the amount of OITRR.

After that, all maxillary right and left first molars were then dissected and processed for histological evaluations. The mesial roots were subjected to histological analyses for further evaluation of the of root surfaces remodeling by inducing new cementum formation as well as the location and extent of root resorption caused by orthodontic tooth movement.

6.3.3 Micro-CT Imaging

The micro-CT imager (Skyscan 1076) is located at University of Alberta, Pharmaceutical Orthopaedic Research Lab, at 2nd floor of the Katz Group Centre (room 2-108). Each maxilla was exposed to radiation for approximately 50 minutes during the micro-CT scanning. The images were obtained at 9 μm resolution with 1 mm thick aluminum filter. After that, raw images data set was reconstructed (from tif files to bmps) by using NRecon software (version 1.4.4). Data analyses were performed on the reconstructed images by using CTAn software (version 1.6.1.0). The same micro-CT imager company (Skyscan N.V., Kontich, Belgium) provided the software for images reconstruction and analyses.

The resorption volume of the external dental root surfaces was estimated in the second experiment by using micro-CT analyses. The mesial roots of all the right and left maxillary first molars were projected and sliced in cross sections through the whole length of each root below the furcation area, starting where the roots completely separated (Figure 8a) and proceed toward the root apex until the end of the root (Figure 8b).

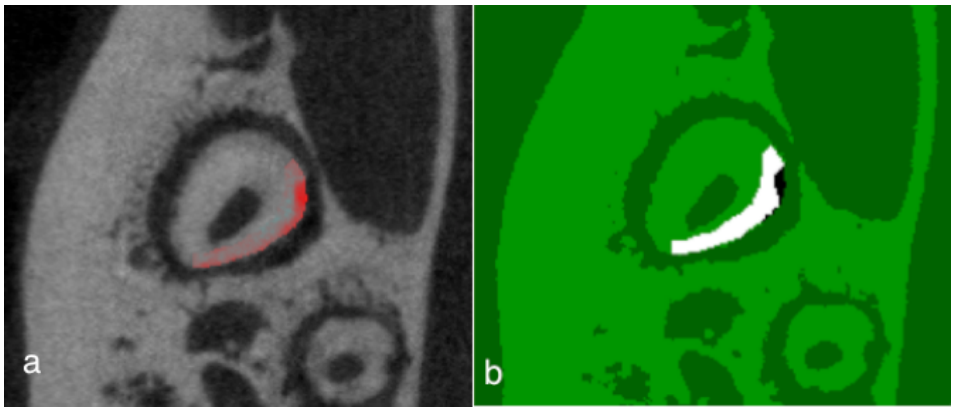

Figure 13: measuring resorption area. As shown in (a), select and draw the external root surface area. Then (b), applying a threshold value to outline the root resorption area; *black area* in (b) represents resorption area.

For each root slice, different regions of interest were used in order to represent the area of all the different aspects of external root surface, the mesial, buccal, lingual, and distal. At each aspect, the region of interest was selected and drawn by tracing the estimated external root surface periphery, including the resorption area, whenever resorption was evident at the indicated aspect (Figure 13a) through all the root's cross-sectional slices. After that, a contrast threshold value was adjusted, fixed and applied to all slices in order to precisely distinguish and include the root resorption area from that displaying the sound root hard tissue

(Figure 13b). As a final step, the computer aggregated the included resorption area from each region of interest of all the root's slices and end up with a volume of interest that represents the volume of root resorption at each aspect of the external root surface. The total resorption volume of each root is the sum of those volumes in all its aspects.

6.3.4 Histological Evaluation

Once all the micro-CT analyses were completed, specimens include maxillary right and left first molar of each animal were cut and stored in neutral-buffered 10% formalin solution for 48 hours. After that all specimens were decalcified using 10% ethylene diamine tetra-acetic acid (EDTA) solution for 4 weeks and then embedded in paraffin to be ready for histological processing.

The mesial roots of all maxillary right and left first molars were processed for histological evaluations. Ten sagittal slices, 5 μm thick, were taken at 20 μm intervals through the whole bucco-lingual width of each mesial root. The sections were mounted on glass slides, stained with hematoxylin and eosin (H&E) and examined under a light microscope using ZEISS AXIO microscope (Carl Zeiss, Germany).

The extent, location and severity of external root surfaces resorption in relation to cementum types in the second experiment were evaluated descriptively. The slides were prepared to be viewed in sagittal plane in order to show the overall

pattern of root resorption along the mesial and distal surfaces, which were supposed to receive the highest amount of pressure resulting from the tipping orthodontic tooth movement. At the same time, the sagittal view can be used to display any root shortening which is considered a severe form of root resorption caused by orthodontic tooth movement. All slides pictures were taken by Optronics MacroFire digital microscope camera (Optronics®, California, USA).

6.3.5 Statistical Analysis

The split-mouth design of the second animal experiment has made it possible to use of the Paired Samples t-test on the data obtained from the micro-CT analyses. Therefore, once the statistical test assumptions were validated, the Paired Samples t-test was used to measure the effect of the initial LLLT remodeling treatment on the resorption volumes of the dental root surfaces caused by the orthodontic tooth movement. The hypothesis of interest was whether the mean resorption volume of the root surfaces was the same in both groups. The statistical tests were performed by using the software SPSS (IBM Corp, version21).

7 RESULTS

7.1 Evaluating the Amount of New Cementum Induced by CsA and LLLT from the First Animal Experiment

All animals in the first experiment gained weight during treatment period. When performing a Kruskal-Wallis test, there was no significant difference between all groups regarding animals' weights at each observational point, immediately before treatment start (Time 0) and at the end of the two-week treatment (Time 1). However, the weight difference between Time 1 and Time 0 was significantly more in the control group in comparison to the other treatment groups (Table 3). The control group received no treatment and that could explain the increase in body weight difference in this group. The stress of the daily LLLT application and CsA treatments might affect the normal body weight growth in both treatment groups.

Body weights (g)			
Treatment	Body Weight		Weight Difference
	Time 0	Time 1	
Control	202 ± 11	248 ± 15	45 ± 7 [a]
CsA	197 ± 7	231 ± 7	34 ± 6
LLLT	197 ± 9	230 ± 9	33 ± 4

Data are presented as mean ± standard deviation, when n=6
CSA: Cyclosporine A; LLLT: low-level laser therapy
Time 0: immediately before treatment start; Time 1: at the end of two weeks treatment
[a] statistically significant compared with both other treatment groups, P-value < 0.05

Table 3: body weights of animals in the first experiment.

7.1.1 Results Obtained from Micro-CT Analyses of the First Experiment

7.1.1.1 Assumptions for the Statistical Tests

The following box-plot (Figure 14) compares the root volume (mm^3) of the three treatment groups (CSA, LLLT and control) at each observational point, immediately before treatment start (Time 0) and at the end of the two-week treatment (Time 1).

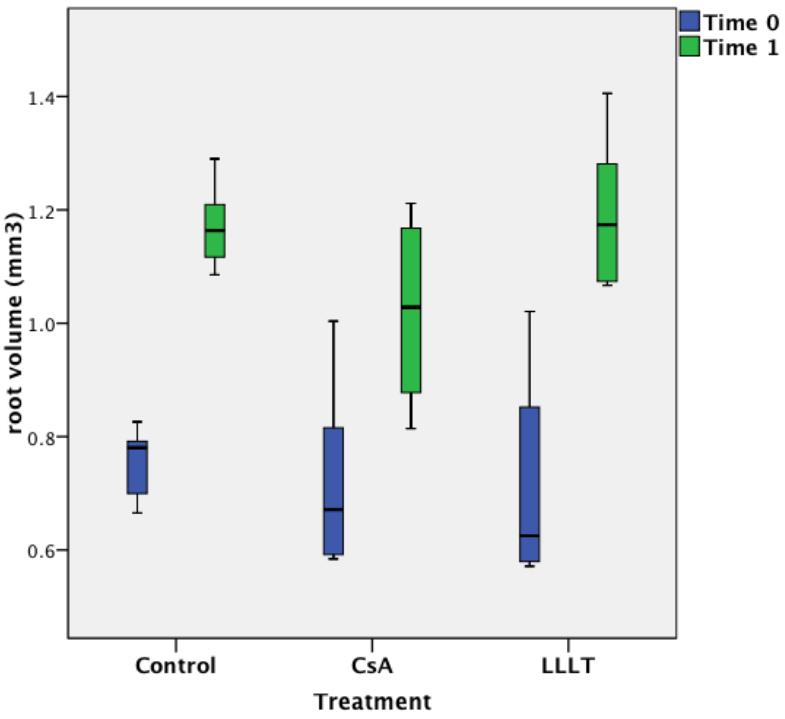

Figure 14: root volumes before and after each treatment.

As seen from the following Table 4, normality is not violated in the data obtained from micro-CT analyses for all treatment groups at each observation time point according to both Kolmogorov-Smirnov and Shapiro-Wilk values (non-significant p-values)

	Treatment	Kolmogorov-Smirnov			Shapiro-Wilk		
		Statistic	df	Sig.	Statistic	df	Sig.
Time0	Control	.289	6	.128	.898	6	.365
	CSA	.247	6	.200	.869	6	.221
	LLLT	.272	6	.186	.813	6	.077
Time1	Control	.216	6	.200	.941	6	.665
	CSA	.166	6	.200	.942	6	.677
	LLLT	.185	6	.200	.920	6	.508

Table 4: test of normality of data from first experiment micro-CT.

Moreover, equal variance assumption is not violated between the treatment groups at each time points, as Levene's test in the following Table 5 shows that the variance between the groups is not significant

	Levene Statistic	df1	df2	Sig.
Time0	3.128	2	15	.073
Time1	1.162	2	15	.339

Table 5: test of homogeneity of variances of data from first experiment micro-CT.

Based on the valid statistical assumptions, both parametric (see Appendices) and non-parametric tests are applicable to perform on the data obtained from the first experiment micro-CT analyses. However, the sample size for the first experiment was too small to accurately conclude the results based on parametric statistical analyses. For that reason, the non-parametric analyses were considered the most appropriate statistical models.

7.1.1.2 Statistical Tests

Comparing the proportion of root volume difference

Each root volume value was measured by micro-CT scanning at two different time points. In order to subject this type of data to non-parametric tests, Root-Volume-Difference-Proportion (RVDP) variables were calculated by mathematic subtracting of the root volume value at the end of the two-week treatment (Time 1), from the volume value of the same root immediately before treatment start (Time 0); then divide this emerging value by the root volume at Time 0.

The following box-plot (Figure 15) compares Root-Volume-Difference-Proportion (RVDP) of the three treatment groups (CsA, LLLT and control).

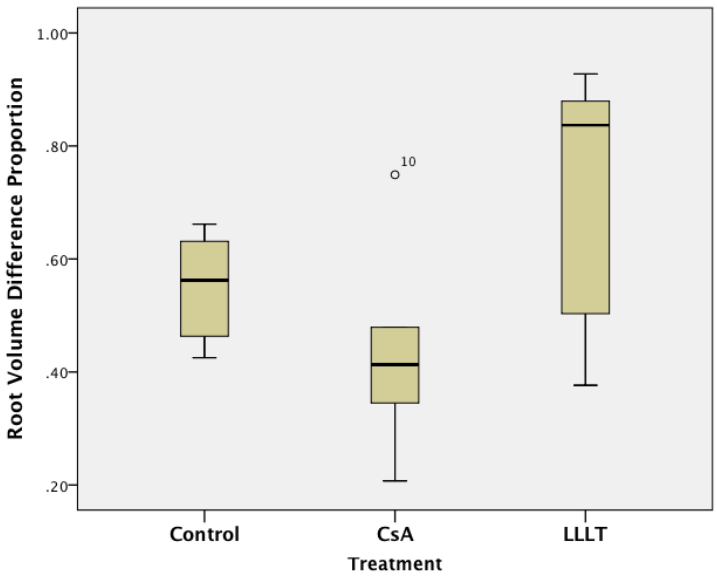

Figure 15: Root-Volume-Difference-Proportion of each treatment group.

Kruskal-Wallis test (Table 6) shows that the mean Root-Volume-Difference-Proportion (RVDP) is non-significantly different (p=0.067) between treatment groups, meaning that Root-Volume-Difference-Proportion is the same in all the three treatment groups.

Null Hypothesis	Test	Sig.	Decision
The distribution of **root volume difference proportion** is the same across categories of all treatment groups	Independent-Samples Kruskal-Wallis Test	0.067	**Retain** the null hypothesis
The significant level is 0.05			

Table 6: Kruskal-Wallis test of RVDP between all groups.

7.1.1.3 Summary of Micro-CT Analyses from First Experiment

Parametric (see Appendices) and non-parametric analyses gave slightly different results, even though they both pointed to the same pattern of the differences between the treatment groups in this study. However, due to the small sample size, it is safer to lean toward non-parametric results on this data set.

On the other hand, since each root volume was measured at two time points (Time 0 and Time 1), new different sets of variables were created mathematically in order to subject those kinds of data to non-parametric analyses. Moreover, rather than merely considering the difference of root volume between the two time points (see Appendices), calculating the proportion of root volume difference to the root volume at the baseline, added some strength to the test and ruled out the effect of the inter-subject roots volumes variability between treatment groups at the baseline.

Therefore, the non-parametric tests on the Root-Volume-Difference-Proportion values were found to be the most appropriate statistical model for the data obtained from the *in vivo* micro-CT analyses of the first animal experiment. In conclusion, for two weeks treatment, neither LLLT nor CsA treatments have any significant effect (p=0.067) in changing the rat's dental root volume when compared radiographically with the normally growing rats (control), even though LLLT group in average shows some stimulatory growth effect of root volume.

Root volume (mm^3) from micro-CT analyses			
Treatment	Root Volume		Root Volume Difference Proportion
	Time 0	Time 1	
Control	0.76 ± 0.06	1.17 ± 0.08	0.55 ± 0.09
CsA	0.72 ± 0.16	1.02 ± 0.16	0.43 ± 0.18
LLLT	0.71 ± 0.18	1.20 ± 0.13	0.73 ± 0.23
Data are presented as mean ± standard deviation, when n=6 CsA: Cyclosporine A; LLLT: low-level laser therapy Time 0: immediately before treatment start; Time 1: at the end of two weeks treatment Root-Volume-Difference-Proportion = (Time 1 – Time 0)/Time 0			

Table 7: summary of root volume analyses from micro-CT of the first experiment.

The means and standard deviations of the root volume obtained from the micro-CT analyses at each observation time are summarized in Table 7. Inference to population cannot be applied in an animal experiment, however, causal inference can be drawn from the results of this experiment because the random assignment of animals to each treatment group.

7.1.2 Results Obtained from Histomorphometric Analyses of the First Experiment

7.1.2.1 Assumptions for the Statistical Tests

The following box-plot (Figure 16) compares the total cementum thickness (μm) of the three treatment groups (CSA, LLLT and control) at the end of two weeks treatment.

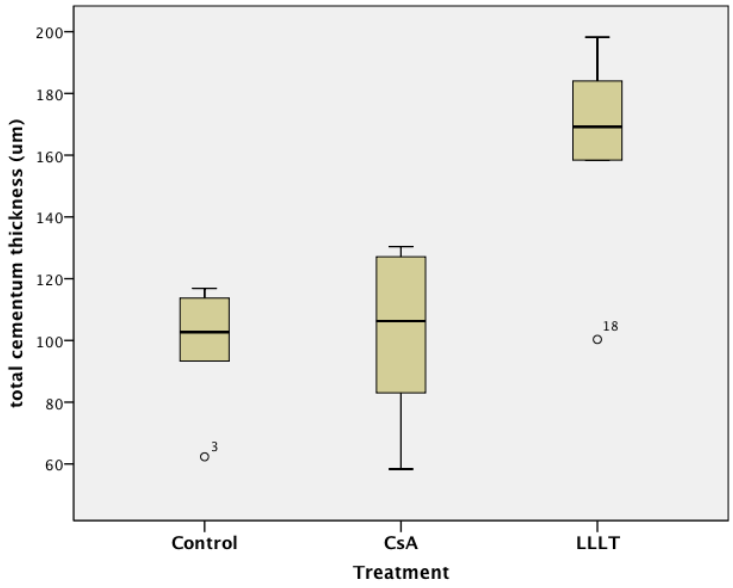

Figure 16: total cementum thickness of each treatment group.

As seen from the following Table 8, normality is not violated in the data obtained from histomorphometric analyses for all treatment groups at the end of two weeks treatment according to both Kolmogorov-Smirnov and Shapiro-Wilk values (non-significant p-values).

	Treatment	Kolmogorov-Smirnov			Shapiro-Wilk		
		Statistic	df	Sig.	Statistic	df	Sig.
Total Cementum thickness	Control	.230	6	.200	.865	6	.206
	CSA	.229	6	.200	.912	6	.450
	LLLT	.277	6	.166	.877	6	.257

Table 8: tests of normality of histomorphometric data.

Moreover, equal variance assumption is not violated between the treatment groups, as Levene's test in the following Table 9 shows that the variance between the groups is not significant.

Total cementum thickness

Levene Statistic	df1	df2	Sig.
.538	2	15	.595

Table 9: test of homogeneity of variances of histomorphometric data.

The statistical assumptions were valid to apply the one-way ANOVA parametric test on the data obtained from the histomorphometric analyses (see Appendices). However, the sample size of the first experiment was too small to accurately conclude the results based on the parametric statistical analyses. Therefore, the following non-parametric analyses were considered the appropriate statistical tests to examine and compare cementum thickness in response to each treatment in the first animal experiment.

7.1.2.2 Statistical Tests

Comparing the total cementum thickness between treatment groups

Kruskal-Wallis test (Table 10) shows that the total amount of cementum thickness is not the same (p=0.019) between the three treatment groups (CSA, LLLT and control) after two weeks treatment. Therefore, at least one of the treatments has a significant effect on the mean amount of total cementum thickness on rat's dental root surfaces.

Null Hypothesis	Test	Sig.	Decision
The distribution of **total cementum thickness** is the same across categories of all treatment groups	Independent-Samples Kruskal-Wallis Test	0.019	**Reject** the null hypothesis
The significant level is 0.05			

Table 10: Kruskal-Wallis test of total cementum thickness between all groups.

Another three different Mann-Whitney tests (the following tables) were done to compare the cementum thickness between every two different treatment groups.

Two Mann-Whitney tests (Table 11) were done to compare the cementum thickness in LLLT group to both CsA and control groups. It was found that, two weeks of LLLT treatment increased the cementum thickness significantly on rat's dental root surfaces in comparison to both CsA treatment (p=0.015) and control (p=0.015), as shown respectively in the following table (Table 11).

Null Hypothesis	Test	Sig.	Decision
The distribution of **total cementum thickness** is the same across categories of LLLT and CsA treatment groups	Independent-Samples Mann-Whitney U Test	0.015	**Reject** the null hypothesis
The distribution of **total cementum thickness** is the same across categories of LLLT treatment and Control groups	Independent-Samples Mann-Whitney U Test	0.015	**Reject** the null hypothesis
The significant level is 0.05			

Table 11: Mann-Whitney test of total cementum thickness between LLLT and CSA treatments; and between LLLT and control.

On the other hand, there was no difference between the CsA and control group regarding the cementum thickness as shown from Mann-Whitney test (Table 12). Therefore, two weeks of CsA treatment had no significant effect on the amount of cementum thickness on rat's dental root surfaces in comparison to control group.

Null Hypothesis	Test	Sig.	Decision
The distribution of **total cementum thickness** is the same across categories of CsA treatment and Control groups	Independent-Samples Mann-Whitney U Test	0.818	**Retain** the null hypothesis
The significant level is 0.05			

Table 12: Mann-Whitney test of total cementum thickness between CsA and control.

Comparing the cementum thickness over the different aspects of the root surface between treatment groups.

The following box-plot (Figure 17) compares the average cementum thickness (µm) at the different aspects of root surface of each treatment group.

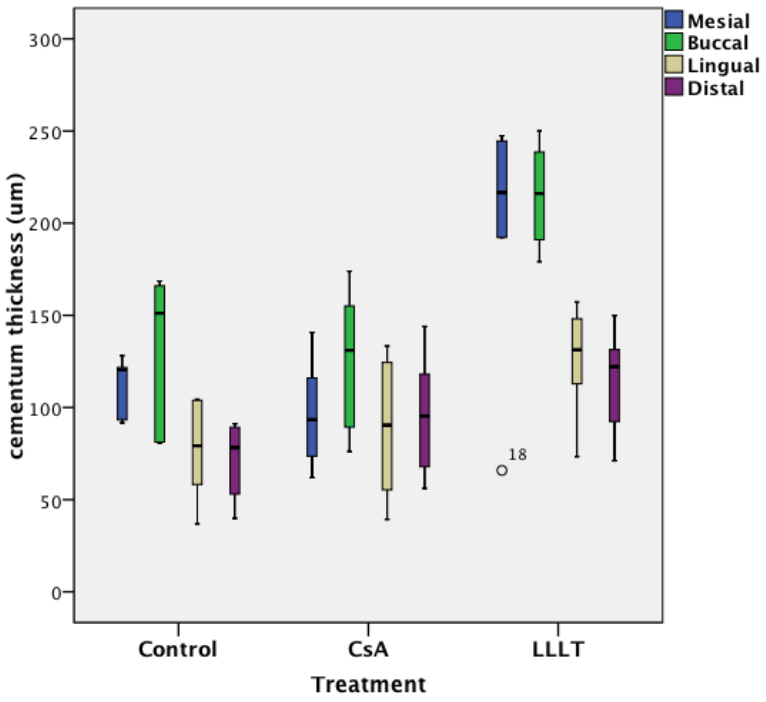

Figure 17: cementum thickness at each root surface of each treatment group.

Four different Kruskal-Wallis tests (Table 13) were performed to compare all groups regarding the cementum thickness formed over the different aspects of rats' dental root surface. The cementum thickness was significantly different between treatment groups at mesial (p=0.042), buccal (p=0.003) and lingual (p=0.042) surfaces. However, there was no significant difference (p=0.076) in the cementum thicknesses at the distal surfaces between all groups.

Null Hypothesis	Test	Sig.	Decision
The distribution of **Mesial** surface cementum thickness is the same across categories of all treatment groups	Independent-Samples Kruskal-Wallis Test	0.042	**Reject** the null hypothesis
The distribution of **Buccal** surface cementum thickness is the same across categories of all treatment groups	Independent-Samples Kruskal-Wallis Test	0.003	**Reject** the null hypothesis
The distribution of **Lingual** surface cementum thickness is the same across categories of all treatment groups	Independent-Samples Kruskal-Wallis Test	0.042	**Reject** the null hypothesis
The distribution of **Distal** surface cementum thickness is the same across categories of all treatment groups	Independent-Samples Kruskal-Wallis Test	0.076	**Retain** the null hypothesis
The significant level is 0.05			

Table 13: Kruskal-Wallis tests of cementum thickness at each root surface between all groups.

On the other hand, another four different Mann-Whitney tests (Table 14) found no difference regarding cementum thickness in all the different aspects of root surfaces when compared between CsA group and control.

Null Hypothesis	Test	Sig.	Decision
The distribution of **Mesial** surface cementum thickness is the same across categories of CsA treatment and Control groups	Independent-Samples Mann-Whitney U Test	0.240	**Retain** the null hypothesis
The distribution of **Buccal** surface cementum thickness is the same across categories of CsA treatment and Control groups	Independent-Samples Mann-Whitney U Test	0.699	**Retain** the null hypothesis
The distribution of **Lingual** surface cementum thickness is the same across categories of CsA treatment and Control groups	Independent-Samples Mann-Whitney U Test	0.589	**Retain** the null hypothesis
The distribution of **Distal** surface cementum thickness is the same across categories of CsA treatment and Control groups	Independent-Samples Mann-Whitney U Test	0.310	**Retain** the null hypothesis
The significant level is 0.05			

Table 14: Mann-Whitney tests of cementum thickness at each root surface between CsA and control.

Comparing the cementum thickness over the different aspects of the root surface within each treatment group.

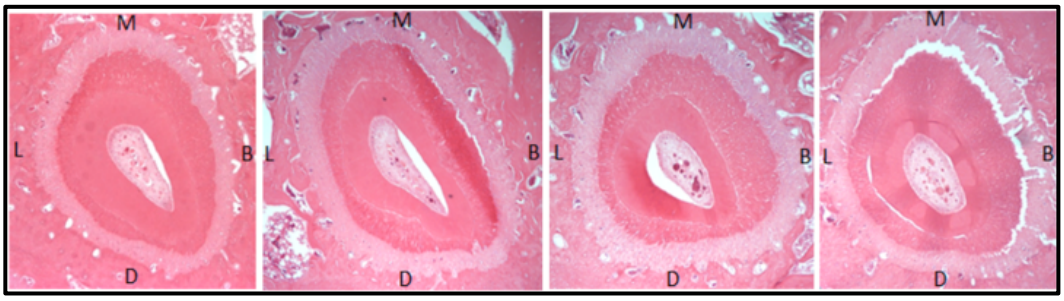

Figure 18: cross-section histological slides from different animals in LLLT treatment group. It is noticeable that the mesial (M) and buccal (B) surfaces show larger cementum thickness than both the distal (D) and lingual (L) surfaces.

The previous cross-section-slide pictures (Figure 18) are samples of different mesial roots (from different animals) from LLLT treatment group at the same (5X scale) magnification values. It is noticeable that the mesial and buccal surfaces show larger cementum thickness than both the distal and lingual surfaces.

Null Hypothesis	Test	Sig.	Decision
The distributions of **Mesial**, **Buccal**, **Lingual** and **Distal** cementum are the same within **LLLT** group	Related-Samples Friedman's Two-Way Analysis of Variance by Ranks	0.013	**Reject** the null hypothesis

Ranks	
Surfaces of LLLT group	Mean Rank
Cementum thickness at **Mesial** surfaces	3.33
Cementum thickness at **Bucca**l surfaces	3.33
Cementum thickness at **Lingual** surfaces	2.0
Cementum thickness at **Distal** surfaces	1.33

Table 15: Friedman's test of cementum thickness between root surfaces within LLLT group.

This finding was confirmed by Friedman's non-parametric test (Table 15), which compared the cementum thickness between the different aspects of the mesial roots after two weeks LLLT treatment. It could be concluded that, the cementum thickness was not the same between the different aspects of the mesial roots of the LLLT treatment group.

On the other hand, the following cross-section-slide pictures (Figure 19) are samples of different mesial roots (from different animals) form CSA treatment group at the same (5X scale) magnification values. No noticeable difference can be found in cementum thickness between the different root surfaces

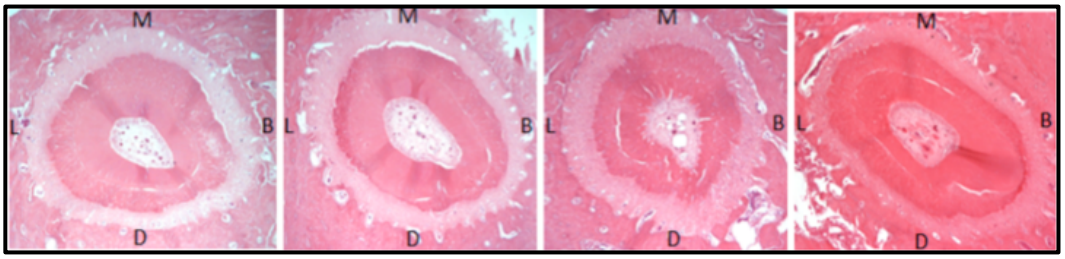

Figure 19: cross-section histological slides from different animals in CsA treatment group. No difference in cementum thickness between the different root surfaces.

This finding was confirmed by another Friedman's non-parametric test (Table 16), which compared the cementum thickness between the different aspects of the mesial roots after two weeks CsA treatment. It could be concluded that, the cementum thickness was the same between the different aspects of the mesial roots of the CsA treatment group.

Null Hypothesis	Test	Sig.	Decision
The distributions of **Mesial**, **Buccal**, **Lingual** and **Distal** cementum are the same within **CsA** group	Related-Samples Friedman's Two-Way Analysis of Variance by Ranks	0.050	**Retain** the null hypothesis

Ranks	
Surfaces of CsA group	Mean Rank
Cementum thickness at **Mesial** surfaces	2.17
Cementum thickness at **Buccal** surfaces	3.67
Cementum thickness at **Lingual** surfaces	1.67
Cementum thickness at **Distal** surfaces	2.5

Table 16 Friedman's test of cementum thickness between root surfaces within CsA group.

The following cross-section-slide pictures (Figure 20) are samples of different mesial roots (form different animals) from control group at the same (5X scale) magnification values. The mesial and buccal surfaces show larger cementum thickness when compared with the distal and lingual surfaces.

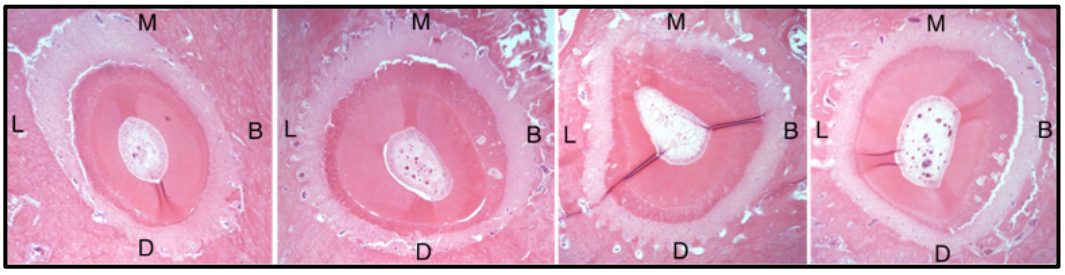

Figure 20: cross-section histological slides from different animals in control group. Notice the cementum thickness at the mesial (M), buccal (B), distal (D) and lingual (L) surfaces.

This finding was confirmed by another Friedman's non-parametric test (Table 17), which compared the cementum thickness between the different aspects of the mesial roots of the control group. It could be said that, the cementum thickness was the not the same between the different aspects of the mesial roots of the control group.

Null Hypothesis	Test	Sig.	Decision
The distributions of **Mesial**, **Buccal**, **Lingual** and **Distal** cementum are the same within **Control** group	Related-Samples Friedman's Two-Way Analysis of Variance by Ranks	0.019	**Reject** the null hypothesis

Ranks	
Surfaces of Control group	Mean Rank
Cementum thickness at **Mesial** surfaces	3.33
Cementum thickness at **Buccal** surfaces	3.33
Cementum thickness at **Lingual** surfaces	1.67
Cementum thickness at **Distal** surfaces	1.67

Table 17 Friedman's test of cementum thickness between root surfaces within control group.

7.1.2.3 Summary of Histomorphometric Analyses from First Experiment

The same conclusion could be drawn from both parametric (see Appendices) and non-parametric results. Although the p-values were different, both parametric and non-parametric analyses showed the same pattern of the differences between the treatment groups regarding cementum thickness in this study. However, as mentioned before, it is safer to lean toward non-parametric results due to the small sample size. Therefore, the non-parametric tests on the cementum thickness values were considered the most appropriate statistical model for the data obtained from the histomorphometric analyses of the first animal experiment.

LLLT group showed a significant increase in the cementum thicknesses (p=0.019) compared with both control and CsA groups. On the other hand, there was no difference (p=0.818) when comparing cementum thickness between control and CsA. Therefore, it could be concluded that, on average, two weeks of LLLT treatment has a significant effect on the formation of more new cementum on rat's

dental root surfaces in comparison to both CsA treatment and control. The means and standard deviations of cementum thickness obtained from the histomorphometric analyses for each group are summarized in Table 18. Inference to population cannot be applied in an animal experiment, however, causal inference can be drawn from the results of this experiment because the random assignment of animals to each treatment group.

Cementum thickness (μm) from histological analyses					
Treatment	Averages of Root Cementum Thickness				
	Mesial Surface	Buccal Surface	Distal Surface	Lingual Surface	Total Surfaces
Control	113 ± 16	133 ± 41	72 ± 21	77 ± 27	99 ± 20
CsA	97 ± 29	126 ± 38	96 ± 35	89 ± 39	102 ± 29
LLLT	197 ± 68 [a]	215 ± 30 [b]	115 ± 28	126 ± 30 [a]	163 ± 34 [a]
Data are presented as mean ± standard deviation, when n=6 CSA: Cyclosporine A; LLLT: low-level laser therapy [a] statistically significant compared with both other groups, P-value < 0.05 [b] statistically significant compared with both other groups, P-value < 0.01					

Table 18: summary of cementum thickness evaluation from the histomorphometric analyses of the first experiment.

When comparing the cementum thicknesses between different aspects of the root surfaces within each treatment group, the mesial and buccal surfaces of the roots that received low-level laser therapy showed significantly more cementum thickness compared with the distal and lingual surfaces of the roots in the same group. Moreover, when compared with both other groups, the cementum thickness was significantly more in LLLT group was significantly more in all the root aspects except the distal surface.

On the other hand, there was no difference in the cementum thicknesses between the different aspects of the root surfaces within CsA group itself. In the same time, no difference was found in cementum thickness in all the different root surfaces in CsA group when compared with the control; even though, there was a significant difference in the cementum thicknesses between the different aspects of the root surfaces within the control group.

7.2 Evaluating the Effect of the LLLT-Induced Root Surfaces Remodeling on OITRR from the Second Animal Experiment

All animals in the second experiment gained weight during the six-week study period. The following Error-Bar diagram (Figure 21) represents the body-weight growth curve of all animals during the six weeks experiment period, at two weeks interval.

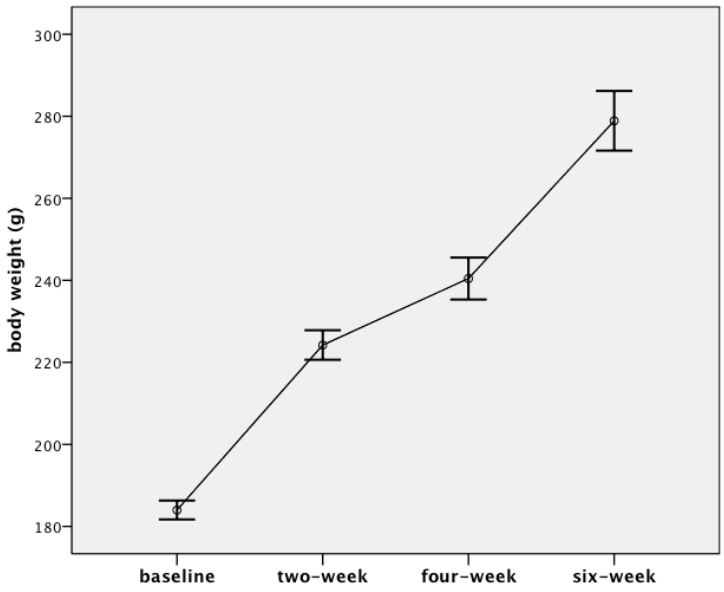

Figure 21: animals body-weight growth curve in the second experiment.

The increasing rate of body weight growth had been affected slightly after implanting the orthodontic appliances. However, two weeks after appliances insertion, the rate of growth returned to normal. It seems that the appliances had an effect on the normal feeding process, which then return to normal once the animals had got used to their presence. Nevertheless, both treatment and teeth movements were well tolerated by all the animals in the second experiment, as observed by the increases in body weights and the well-being general conditions of all the animals.

7.2.1 Results Obtained from Micro-CT Analyses of the second Experiment

7.2.1.1 Assumptions for the Statistical Tests

The following box-plot (Figure 22) compares the total resorption volumes (mm^3) of the external surfaces of the mesial root due to orthodontic movement between the Remodeled-Cementum group and control.

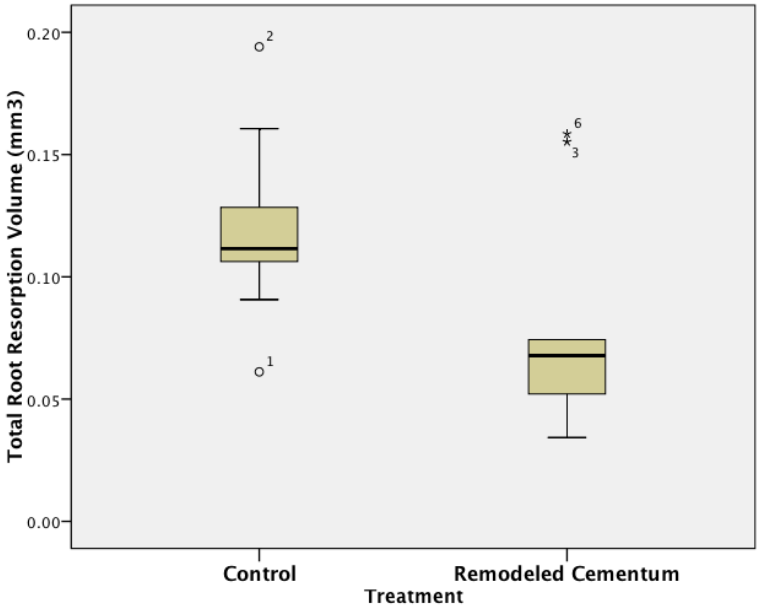

Figure 22: total root resorption volume in both treatment groups.

Both data are close to normal distribution. The control group is normally distributed according to the non-significant p-values form Kolmogorov-Smirnov and Shapiro-Wilk tests. However, the data from Remodeled-Cementum group showed more positive skewness with a presence of multiple outliers. The Kolmogorov-Smirnov and Shapiro-Wilk tests showed significant p-values for the Remodeled-Cementum group (Table 19).

	Kolmogorov-Smirnov			Shapiro-Wilk		
	Statistic	df	Sig.	Statistic	df	Sig.
Control	.200	9	.200	.958	9	.773
Remodeled Cementum	.339	9	.004	.791	9	.016

Table 19: tests of normality of total resorption volume data

The statistical tests for data obtained from the split-mouth design study should consider the relation between groups and the matched-paired nature of the data. Therefore, a Paired Samples t-test was considered the appropriate model to perform on the matched-paired data obtained from micro-CT analyses of the second experiment. However, due to the apparent violation of normality assumption, two additional statistical tests were performed (see Appendices) in order to validate the results of the Paired Samples t-test. Therefore, the Paired Samples t-test was found robust enough to stand the apparent considerable violations of normality in the data of the present study.

7.2.1.2 Paired Samples t-test of Micro-CT Data

In order to test the hypothesis of this study, the following Paired Samples t-test was performed to analyze the effect of the initial LLLT-induced cementum remodeling on the amount of external root resorption caused the subsequent orthodontic tooth movement, with the following null hypothesis:

Ho: the mean total amount of resorption volumes caused by orthodontic tooth movement is the same in the remodeled-cementum group and control.

	Mean	N	Std. Deviation	Std. Error Mean
Total Control	.1208	9	.0387	.0129
Total Remodeled-Cementum	.0813	9	.0448	.0149

Table 20 Paired Samples statistics of total root resorption volume.

Pair 1	Paired Differences					t	df	Sig.
	Mean	Std. Deviation	Std. Error Mean	95% Confidence Interval of the Difference				
				Lower	Upper			
Total Control – Total Remodeled-Cementum	.0395	.0444	.0148	.0054	.0737	2.674	8	.028

Table 21: Paired Samples t-test of total root resorption volume.

From the previous two tables (Tables 20 and 21), there is a significant difference ($p=0.028$) in the total amount of root resorption volume caused by orthodontic tooth movement between the LLLT treated roots and control. Therefore, roots that received LLLT treatment for two weeks showed significantly less root resorption caused by the subsequent tooth movement when compared with the control. In other words, the preexisting root surfaces remodeling caused by two weeks of LLLT treatment had a significant protective effect against root resorption during the four-week orthodontic tooth movement.

Additional analyses were done in order to correlate the second experiment findings with those from the first experiment that showed more cementum formation on the mesial and buccal surfaces in comparison to the distal and lingual surfaces within the LLLT group. Two more Paired Samples t-tests were

performed on the micro-CT data of the second experiment to compare the resorption volumes (mm^3) of mesial roots' two halves (the mesial-buccal and the distal-lingual aspects) due to orthodontic movement between the Remodeled-Cementum group and control. The following box-plot (Figure 23) compares the orthodontically induced root resorption volumes (mm^3) of the mesial roots' two halves, the mesial-buccal and the distal-lingual aspects, between the Remodeled-Cementum group and control.

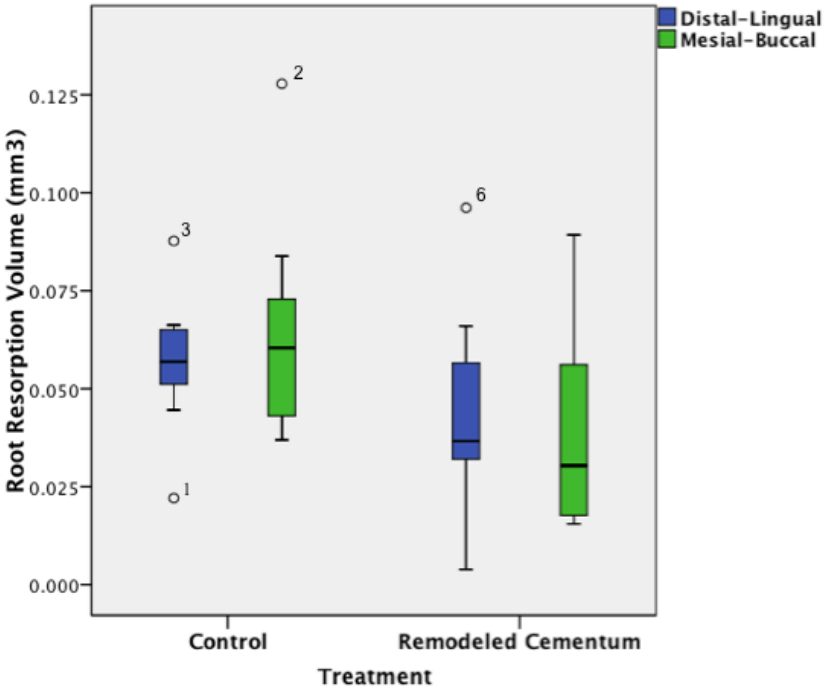

Figure 23: root resorption volume at mesial-buccal and distal-lingual surfaces in both treatment groups.

Two different Paired Samples t-tests (Table 22) showed no significant difference on the amount the orthodontically induced resorption volumes when comparing both roots' two halves: the mesial-buccal (p=0.058) and the distal-lingual (p=0.158) aspects, between the Remodeled-Cementum group and control.

However, the difference in mean root resorption was more when comparing the mesial-buccal aspects, meaning that the protective effect, against root resorption of the preexisting root surfaces remodeling caused by two weeks LLLT, was greater on average on the mesial and buccal aspects of the dental root surfaces.

		Paired Differences					t	df	Sig.
		Mean	Std. Deviation	Std. Error Mean	95% Confidence Interval of the Difference				
					Lower	Upper			
Pair 1	MesialBuccal Control – MesialBuccal Remodeled Cemetum	.025	.0350	.0117	-.0011	.0526	2.2	8	.058
Pair 2	DistalLingual Control - DistalLingual Remodeled Cementum	.013	.0266	.0089	-.0066	.0342	1.5	8	.158

Table 22: Paired Samples t-tests of resorption volume at mesial-buccal and distal-lingual surfaces.

7.2.1.3 Summary of Micro-CT Analyses from Second Experiment

When comparing the root resorption volume caused by orthodontic tooth movement between the formerly LLLT treated roots and the control, similar results were found from the parametric Paired Samples t-tests on the raw and log-transformed data (see Appendices). Moreover, the exact same conclusion can be drawn from the non-parametric Wilcoxon Signed Rank tests on the raw data obtain from the micro-CT analyses of the second animal experiment (see Appendices). Therefore, the Paired Samples t-test was found to be robust enough to stand the considerable violations of the raw data normality assumption, meaning that the normality assumption was violated to some degree but the test still provided valid results when performed directly on the raw data. For these

reasons, the parametric Paired Samples t-tests on the raw values of root resorption volumes were found to be the most appropriate statistical model for the data obtained from the *ex vivo* micro-CT analyses of the second animal experiment.

Orthodontically induced root resorption volume (mm^3) from the micro-CT analyses			
Treatment	Volume of Root Resorption		
	Mesial and Buccal Root Surfaces	Distal and Lingual Root Surfaces	Total Root Surfaces
Control	0.064 ± 0.029	0.057 ± 0.018	0.121 ± 0.039
Remodeled Cementum	0.038 ± 0.025	0.043 ± 0.027	0.081 ± 0.045 [a]
Data are presented as mean ± standard deviation, when n=9 [a] statistically significant compared with the control, P-value < 0.05			

Table 23: summary of orthodontically induced root resorption volume from the micro-CT analyses in the second experiment.

The means and standard deviations of the volume of orthodontically induced tooth root resorption obtained from the micro-CT analyses of the second experiment are summarized in the Table 23. In conclusion, the total volumes of root resorption due to orthodontic tooth movement were found to be significantly less (p=0.028) in the teeth exposed to LLLT compared with the control teeth that received no treatment. In other words, the preexisting root surfaces remodeling caused by two weeks LLLT treatment had a protective effects against root resorption caused by the following four weeks orthodontic tooth movement. Moreover, resorption volumes in the mesial and buccal root surfaces were less on average than in the distal and lingual root surfaces in the teeth that received LLLT compared with the same surfaces in the control group.

7.2.2 Results Discerned from Histological Evaluation of the second Experiment

After completing the evaluation of the external root resorption volume from the micro-CT analyses, the extent and severity degree of roots surfaces resorption were evaluated histologically in the second experiment.

Preparing the histological slides to be viewed in sagittal plane facilitates the description of the type and severity of the external root surface resorption along the mesial and distal sides, which were supposed to receive the highest amount of pressure resulting from the force applied by the tipping orthodontic tooth movement. Moreover, root shortening, which is a severe type of OITRR; can be displayed well in a sagittal view.

On the other hand, only resorptions that happen in the mesial and distal plane can be displayed in the sagittal view, which make it less accurate to assess the amount of OITRR from the histological analyses compared with the micro-CT analyses. Moreover, due to an inappropriate preparation of the histological sections, it was difficult to get true mid-sagittal sections in the middle of the mesial roots along their entire vertical height for all the samples during the histological processing. This made it difficult to properly calculate the average of cementum thickness for some slides. For these reasons, the histological analysis of the second animal experiment was kept descriptive.

The following sagittal-sectioned slide images (Figures 24 and 25) are samples of different mesial roots (from different animals) from both Remodeled-Cementum and control group at the same (5X scale) magnification values.

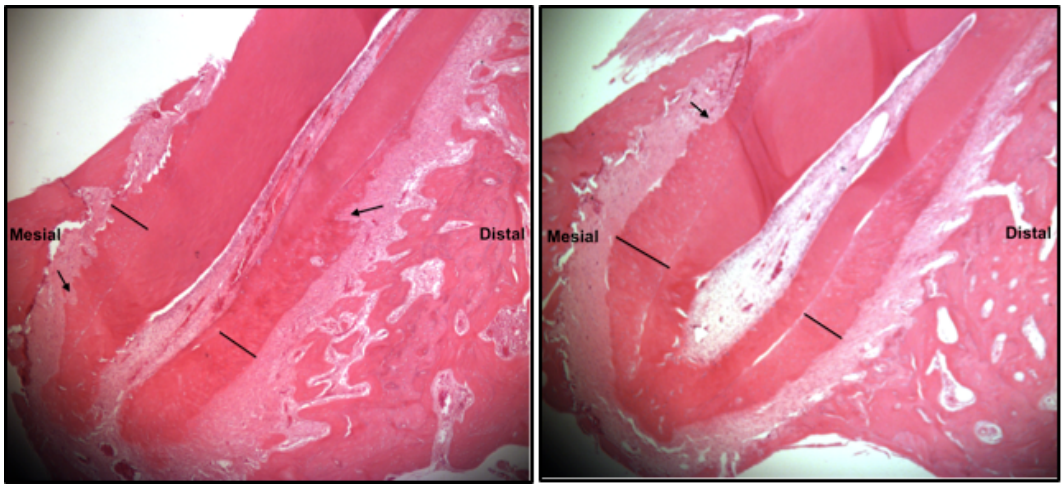

Figure 24: sagittal histological slides from **Remodeled Cementum** group. Black lines represent the highest cementum thickness; solid-line arrows point to external root surface resorption lacunae.

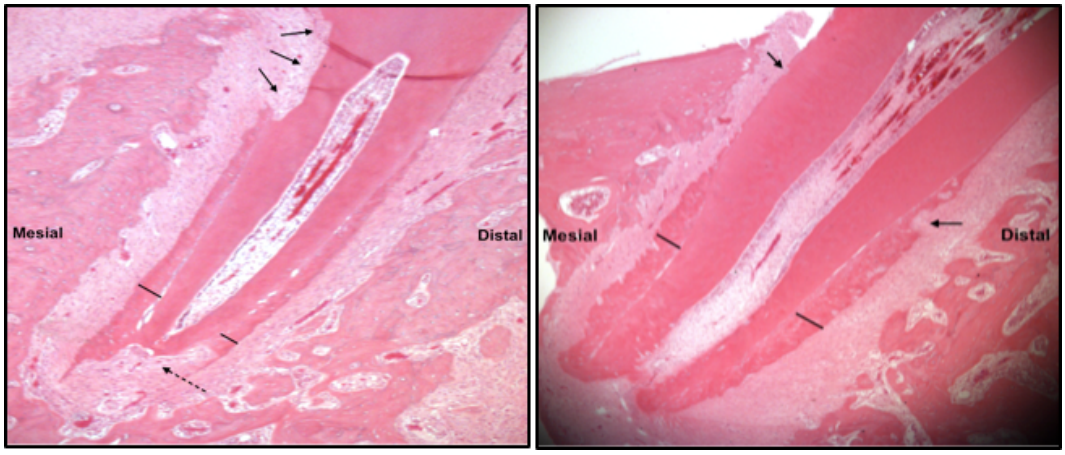

Figure 25: sagittal histological slides from **control** group. Black lines represent the highest cementum thickness; solid-line arrows pointed to external root surface resorption lacunae; dashed-line arrow shows the root shortening.

It was visually noticeable that more cementum was formed over the roots surfaces that received LLLT treatment, before starting teeth movement, in comparison to control. Uneven increases in the cementum thickness were noticed over the apical portions of the LLLT treated root surfaces. Moreover, it was clear that external root surfaces of both groups showed a considerable amount of resorption due to the force applied by the orthodontic treatment. Histologically, there were no clear general trends to indicate which surface was more affected by resorption in both groups. However, in the roots surfaces that were exposed to the initial LLLT treatment, the resorption lacunae were mostly confined to the outer cementum layer with some extended even deeper to involve the outer layer of radicular dentin. On the other hand, roots surfaces of the control group showed more incidents of deep resorption lacunae that involves both cementum and the outer layers of dentin. Moreover, one mesial root sample from the control group (Figure 25) clearly exhibited a sign of an irreversible root shortening process, which is considered a more severe type of OITRR.

In conclusion, the histological evaluation of the second animal experiment was used to describe the type and the severity degree of the OITRR. An equal number of slides from each group were considered appropriately prepared and were used for the histological evaluation. The amount of root resorption caused by orthodontic treatment was evaluated and analyzed more properly from the micro-CT analyses, however, the histological evaluation shows that the initial LLLT

treatment appears to not only decrease the volume of external root surface resorption, but also to decrease the degree of OITRR severity. Moreover, the apparent increase in cementum thickness covering the root apical portion may be related to the remodeling activities that had happened over the root surfaces that were exposed to LLLT immediately before starting the orthodontic tooth movement.

8 DISCUSSION

8.1 Amount of New Cementum Induced by LLLT and CsA in the First Animal Experiment

The first animal study evaluated the two-week treatment effect of either low-level laser therapy (LLLT) or cyclosporine A (CsA) on the formation of dental root cementum in rats. Histologically, we found that LLLT stimulated the remodeling of the dental root surfaces by significantly increasing the cementum layer thickness. More cementum was observed in the mesial, buccal and lingual surfaces in the LLLT group. In contrast, we did not observe any difference in cementum formation among rat molars treated with CsA. However, by performing *in vivo* micro-CT scans over the two-week timeframe on the same samples, we did not detect any significant change in the root hard tissue volume between the groups.

The histological analyses in the present experiment showed a significant increase in the cementum thickness in the LLLT group compared with both the control and CsA groups. The primary mechanism underlying LLLT is that laser radiation, at a wavelength longer than 600 nm, has a capability to stimulate favorable cellular activities and metabolic rates by absorbing light energy (151, 164, 169, 176). However, laser wavelengths in the near-infrared spectrum have relatively greater penetration due to the fact that the energy of those wavelengths is not strongly absorbed by water or macromolecules within the tissues such as hemoglobin and

melanin (168). Therefore, many studies have reported that laser light in this spectral range, including the light emitted by our low-level laser system, is useful and more effective in biostimulating deep tissue (164, 166, 168, 184). According to the literature, the gallium-aluminum-arsenide (GaAlAs) LLLT system which emits laser at 830 nm wavelength is able to reach and stimulate tissue remodeling around the dental roots in rats by influencing the appropriate cellular behaviors, enhancing tissue vascularity, increasing alkaline phosphatase activity, reducing the production inflammatory molecules, and promoting the expressions of several growth factors and cytokines (203-206, 216, 220, 221, 230).

The wavelength of laser light is the most important determinant of the biological tissue response following the LLLT application (165, 168). Each laser device has certain inherent parameters including the wavelength and waveform that cannot be changed by the operator (163). Therefore, before purchasing the LLLT system for this thesis project, laser wavelength and waveform were chosen based on the best available evidence in order to achieve the treatment goals (164, 168, 216, 220). On the other hand, the LLLT system provides several user-controlled parameters that can be precisely set by the user in order to control the treatment dosage (163). The use of a justifiable treatment dosage is essential to insure that the target tissue absorbs the low-level laser energy and subsequently produces the required biological response (163, 164, 166). A reasonably low dose of laser energy within an appropriate therapeutic window is necessary to trigger biologic effects, as delivering the same wavelength at far higher doses can cause an opposite,

inhibitory, response (151, 179, 180, 219). The application of too low output power laser can result in a delayed treatment response; and this cannot be fully compensated by longer exposure duration (176). In contrast, applications of LLLT using excessively high output power not only delivers laser energy too quickly, but may also limit the appropriate energy absorption by the tissue's components, generating an unsatisfactory response (181).

Based on the present study results, the utilized LLLT treatment dosage and duration have proved useful in stimulating cementum tissue growth. Reportedly, the output power, waveform, power density, and energy density of our LLLT treatment are considered within the optimum LLLT dose needed to stimulate any target tissue at an ideal cellular response threshold (166, 181, 219). Moreover, by delivering laser energy repeatedly at low doses in intervals (i.e., once a day for two weeks), this LLLT treatment protocol is assumed to induce much greater effects than the same total dose given in fewer treatment sessions (151).

As it will be discussed in more detail in the next section, the major goal of this research project was to test the effect of increased root cementum thickness on the root resorption caused by orthodontic movements. Based on the current findings, it was decided that the outcome of this LLLT treatment dosage and duration was sufficient to accomplish the study objectives. However, further investigations are required in order to evaluate the exact dose-response or duration-response involved in LLLT-induced cementogenesis.

The biological responses following LLLT application require the absorption of laser energy by the target tissue through endogenous absorptive chromophores primarily residing at the microcellular level (242). Currently, it is widely accepted that the mitochondria is the main target organelle of low-level laser radiation (243, 244). Photosensitivity is a well-known mitochondrial property in eukaryotic cells (245). The near-infrared low-level laser radiation is believed to be primarily absorbed by the photoacceptor cytochrome c oxidase, which is the terminal enzyme in the respiratory chain within the mitochondrial membrane (242, 243).

Several intracellular signaling pathways, which originate from the functionally changed mitochondria, have been suggested in order to explain how the primary reactions of photons with photoacceptors in the mitochondrial respiratory chain are connected with genes upregulation and DNA and RNA synthesis within the cell nucleus (246). When the photoacceptor absorbs laser photons, the photon energy is transferred to this photoacceptor within the mitochondrial respiratory chain, and the photoacceptor is then raised to an electronically excited state. The excitation can activate other respiratory chain components and triggers electron transfer from electron donors to electron acceptors, via redox reactions, which is coupled with proton transfer (H^+ ions) across the mitochondrial membrane (246). This process generates an electrochemical proton gradient called mitochondrial membrane potential ($\Delta\Psi_m$), which creates chemical energy compounds in the form of adenosine triphosphate (ATP) through oxidative phosphorylation (246,

247). It is known that even a small increase in the ATP level can significantly enhance cellular activity and metabolism (244, 246, 248). Moreover, altering $\Delta\Psi_m$ can also release calcium ions (Ca^{2+}) from the mitochondria into the cytoplasm, which in turn can trigger mitosis and cell proliferation by affecting gene expression in the nucleus via transcription factors such as nuclear factor kappa B (NF-kB) (244, 246, 248, 249).

The generation of reactive oxygen species (ROS), such as hydrogen peroxide (H_2O_2), as by-products of the respiratory chain activation is also considered an important intracellular signaling factor that can modulate cellular functions (244, 246, 248, 249). However, excessive production or inadequate removal of ROS, especially superoxide anions (O_2^-), generates an imbalanced state of oxidative stress that can damage cellular components and disturb the proper intra- and inter-cellular signaling (249, 250).

A recent proteomic analysis found that unlike alveolar bone and periodontal ligaments, cementum matrix contains a unique antioxidant protein called superoxide dismutase 3 (SOD3) that provides additional protection against the effects of oxidative stress during cementum formation (250). SOD3 is one of a group of enzymes known to catalyze the dismutation reaction of O_2^- into oxygen and H_2O_2 (250). Cementum cells are thought to express and secrete SOD3, which is then anchored to the extracellular cementum matrix; therefore, SOD3 is considered a biomarker for cementum tissues (250). Based on that, it could be

suggested that the unique composition of the cementum matrix could have the potential to balance the effect of LLLT on the mitochondrial respiratory chain activation by maximizing ATP synthesis and limiting ROS production to only the amounts required for the proper stimulatory cell signaling (249).

The exact cellular processes and regulatory factors involved in LLLT-induced cementogenesis cannot be determined based on the present study results. However, the stimulatory effects of our LLLT treatment on cementum tissue growth could be explained by the aforementioned mechanisms. Therefore, under the conditions used in this study, energy absorption from our low-level laser treatment by cementum forming cells may promote their proliferation and enhance their ability to produce more cementum tissue.

Controversies still exist regarding cementogenesis, including the exact origin of the associated cells, as well as the natures of regulatory factors involved in the elaboration of the two different cementum varieties, acellular and cellular (76, 80, 251). The cementoblasts that are responsible for the formation of each cementum type behave differently in terms of the timing and speed of tissue formation as well as the manner of mineral apposition (252). The cellular cementum was thought to be a secondary type of the acellular cementum originating from the same cell lineage (252). However, numerous evidence suggests that the different cementum types represent distinct tissues formed by cells with different phenotypes and developmental origins (80, 251).

In rat molars, the acellular cementum is a thin mineralized layer covering the coronal half of the root and containing only extrinsic (Sharpey's) fibers, which are the embedded ends of the principal periodontal ligament fibers (252). The formation of acellular cementum begins during the early stages of rat's root development by cementoblasts that differentiate in close proximity to the margins of the developing root (252). The acellular cementum is formed before tooth eruption as a slow accumulation of mineral on the developing root dentin surface (252). By contrast, the cellular cementum formation begins during the later stages of root development when the rat molar has reached occlusion approximately 25 days after birth (253). Since then, the cellular cementum continues to grow rapidly on the apical portions of the root surfaces as cementoblasts deposit collagenous matrix (intrinsic fibers) around the Sharpey's fibers and become entrapped within this newly formed matrix in which mineralization occurs (252).

In the present study, the increased cementum thickness in the LLLT group followed the normal cementum growth pattern. The growth of cellular cementum covering the apical portions of the root surfaces was more evident than the growth of acellular cementum, which is normally confined to the coronal half of the root. Interestingly, our findings are in agreement with those of another recent study that confirmed the ability of LLLT (continuous wave GaAlAs at 808 nm for 20 seconds per each molar with a dose of 2 J/cm^2 at 100 mW) to significantly stimulate cellular cementum overgrowth without affecting the normal growth of

the acellular type during root development of rat molars (254). Therefore, it seems that the stimulatory effect of LLLT mainly targets the cellular type of cementum regardless of the root developmental stage.

In the course of normal development, acellular cementum is maintained as a thin and uniform layer while the cellular cementum is characterized by ongoing, progressive apposition on the root surfaces. Several studies have reported that the energy of the low-level laser is able to increase the production of local potent mediators such as transforming growth factor-β (TGF-β) that have a direct effect in stimulating the activity of calcified tissue's forming cells (187, 188). A recent immunohistochemical investigation suggested that the effect of TGF-β may be cell-type specific in the cementum since a strong immunostaining of connective tissue growth factor (CTGF), which is a down stream mediator of TGF-β, was detected in the cementocytes and cementoblasts associated with cellular cementum, but not in cementoblasts associated with acellular cementum (251). Moreover, cementum growth requires mineralization. Inorganic pyrophosphate (PP_i) was recently identified as a potent inhibitor of hydroxyapatite crystal precipitation in acellular cementum, whereas cellular cementum was much less sensitive to fluctuations in the local PP_i concentration (255). Therefore, PP_i homeostasis could be employed by cementoblasts to curb cementum apposition in order to maintain the acellular cementum as a thin tissue on the root surface (255). Consistent with this, it is known that LLLT not only able to stimulate, but also to stabilize some physiological functions in order to reach normalization and tissue

homeostasis (176). Therefore, it could be the case that our LLLT treatment is able to optimize the local biological conditions surrounding the dental root, leading to a considerable increase in cellular cementum growth of the while maintaining the stability of the acellular cementum as a thin and uniform layer.

Cementum thickness in both the mesial and buccal surfaces of the roots in the LLLT group was significantly greater than the thickness in the distal and lingual roots surfaces within the same group (Figure 18). The angle at which the laser beam hits the root surfaces could explain this variation in cementum thickness between the different root's aspects within the LLLT group. In our experiment, the contact mode of the low-level laser guide tip was chosen to allow greater light permeability by thinning the overlying tissue and partially blanching the superficial blood vessels (164). However, due to the tissue architecture surrounding the rat's maxillary first molar, only the mesial and buccal surfaces of the mesial root were exposed by a perpendicular laser beam when the tip of our laser light guide was placed in contact with the gingiva over the different root aspects. It has been suggested that the incident angle of the laser beam should be as perpendicular as possible when exposing the tissue surface in order to minimize the reflection of the laser light and thus maximize the energy available for tissues absorption to produce the expected therapeutic effect (181). Moreover, compared with both CsA and control groups, the cementum thickness in the LLLT group was significantly more in all the root aspects except the distal surface. This difference in the response to treatment between different root surfaces could be

attributed to the proximity of the root surface to the laser source. The absorption of an appropriate amount of laser energy by the target tissue is essential to subsequently induce the required biological reaction (176). However, the energy of the laser beam decreases as the laser light passes through the tissue, and therefore, the tissue response to the laser light decreases in deeper layers (165). The distal surface of the mesial root in the rats' maxillary first molar is located deeper than the other surfaces, which may explain the different tissue response between the root surfaces in the LLLT group.

Our histological analyses also showed no difference in the cementum thicknesses between the different aspects of the root surfaces within the CsA group (Figure 19). Moreover, the daily CsA treatment over the two-week period had little, if any, effect on the cementum thickness on all the different root aspects when compared with the control group. Our findings regarding the CsA group appear to contradict the outcomes in the previous studies (143-148) after one month of daily CsA treatment. Therefore, it could be suggested that the stimulatory effects of daily CsA treatment on cementum formation may require longer than two weeks to take place. CsA treatment causes a temporary depression of mineralized tissue formation in bone during the first two weeks of daily treatment, which is followed by an increased mineralized tissue formation during later weeks according to one report (256). By contrast, another study (146) observed an increased cementum apposition rate during the first two weeks of daily CsA administration in growing rats. In that particular study, CsA was administered daily to 5-week-old rats for 7

weeks, and the cementum apposition rates subsequently decreased during later weeks (146). These observations may be explained by the effect of aging on the cementum apposition rate. Reportedly, the speed of cementum deposition is much faster before the completion of root formation in rats at 6 weeks of age (257, 258). In our study, the two-week period of daily CsA treatment was started when the rats were 7-week-old. Therefore, more than two weeks may be required for daily CsA treatment to influence the process of cementum formation in the dental roots of mature rats. Consistent with this conclusion, a recent study (148) reported an increased cementum thickness after 45 days of daily CsA treatment in 7-week-old rats at the same dose and administration route that was used in our study. Therefore, CsA-induced cementum overgrowth appears to primarily depend on the treatment duration in rats older than 6 weeks of age.

A potential limitation of this study, regarding the effect of CsA on cementum growth, is that the systemic availability of the active drug substances after drug administration was not measured. Detecting the systemic availability of CsA could have been done directly by measuring the drug level in the blood, or indirectly by monitoring for the drug side effect such as gingival overgrowth (116, 117, 119, 143). Moreover, it is recognized that the provided CsA treatment dosage and/or duration could require further adjustment. However, at that point, it was decided not to continue evaluating the effect of CsA on cementum growth for two main reasons. First, unlike CsA, the LLLT experiment provided positive results that enabled to further explore the main thesis research purpose. The second

reason is that CsA exerts a broad range of pharmacological effects as well as a number of potentially harmful side effects and adverse drug interactions (110). The main purpose of this research was to verify the effect of increased cementum thickness for the prevention of root resorption caused by orthodontic treatment. In light of this, it is questionable to suggest any future clinical application of CsA treatment for orthodontic patients just for the sake of preventing root resorption. By contrast, the non-invasive nature of LLLT would make it a preferable method to consider for any potential future clinical application that is related to our research.

In order to identify the cementum thickness, the histological slides provided adequate information on the extent of the cementum layer because H&E staining allowed sufficient contrast between the cementum and the underlying dentin tissues (Figure 10). However, the three-dimensional structure of cementum thickness could not be precisely quantified based on the two-dimensional linear measurements of a few serially sectioned histological slides (259-261). Because of the possible loss of root material during the sample physical sectioning, cutting several thin slices from the root sample and mounting them on slides for microscopic evaluation may not accurately reflect the true three-dimensional volume of the cementum tissue. Moreover, different orientation of a sample sectioning during slides preparation can cause an apparent change of cementum thickness between slides (259-261). In general, the histological studies are inherently technique sensitive and their slides preparations can be difficult to

repeat or reproduce (22, 260).

Recent advances in micro-CT imaging technology facilitate the three-dimensional quantitative evaluation of small specimens such as rat's dental roots with high spatial resolution. This allowed an easy orientation within the specimen and permits an interactive viewing of the root from the desirable direction (259, 262, 263). Micro-CT imaging has overcome the limitations associated with physical sectioning as it uses x-rays to create serial cross-section slices of the whole root sample without destroying the original sample. Thereafter, a software program enables a reproducible, three-dimensional reconstruction of the root microstructures by assembling all the individual slices. This virtual three-dimensional model permits a non-invasive analysis of the root morphology and enables the calculation of particular morphometric parameters over the whole sample's volume (263, 264). Therefore the key advantage offered by micro-CT analyses in the first experiment was the ability to quantify the volumetric change in the root structure before and after each treatment.

Our longitudinal *in vivo* micro-CT analyses showed that, over a two-week period, the mean root volume growth was greater in the LLLT group when compared with the corresponding mean in normally growing animals in the control group. However, this difference in the root volume change was not statistically significant between all groups. The root volume in this study refers to the hard tissue of the dental root comprising both radicular dentin and cementum. Root

formation in rat molars is complete before 6 weeks of age; thereafter, the root hard tissues continue to grow slowly by secondary dentin apposition at the root internal surface by specialized cells located inside the dental pulp (258). Simultaneously, new cementum is continuously formed over the root external surface throughout life by cementoblasts, which are continuously recruited from specialized progenitor cells located in the periodontal ligament (76).

Proper segmentation of the root microstructures from the surrounding tissue is required to ensure accuracy of the micro-CT measurement data (262, 264-266). The software program used in our micro-CT imaging analyses offered a manual or pre-set procedure that can outline the region of interest and remove the unwanted structures from the images (Figure 9a). For an accurate morphometric analyses within each region of interest, a threshold method was used to segment the micro-CT gray-scale images into binary (e.g., red and black in Figure 9b) in order to differentiate the root hard tissues from the surrounding soft tissues. The threshold value was obtained by identifying the middle point between the peak in the gray-scale relative to root structure and the peak relative to soft tissues. Reportedly, an accurate representation of the mineralized tissue's boundary can be obtained by selecting the threshold value in the middle point between the peaks (264, 266). Moreover, it was shown that any variation in the threshold value could result in a difference in root volume estimation (265). Therefore, the same threshold value was fixed and used for all the micro CT images of all the experiment's samples.

One of the problems of using micro-CT analyses in the first experiment was that the samples were evaluated based on images with gray-scale values that displayed the degree of mineralization. Although the segmentation of the root from the non-root soft tissues was possible, it was found difficult to distinguish between root cementum and the underlying dentin tissue by using the threshold method in the micro-CT images as both tissues displayed similar value on the images' gray-scale components. This technical difficulty in segmenting an accurate three-dimensional representation of cementum tissue has limited the advantage of using micro-CT analyses as a true alternative compared to our histological evaluation in the first experiment.

It is possible that the micro-CT images in the first experiment failed to identify certain fine details that would have been detected in higher resolution images. When analyzing small structures such as rat's dental root sample, it is highly recommended to obtain micro-CT images with the highest resolution possible in order to avoid an underestimation of the sample's mineralization density that could affect the accuracy of the related volumetric analyses (263, 267). However, as seen in our pilot study, acquiring higher resolution *in vivo* images using this particular micro-CT imager require a longer period of radiation exposure at each observational point, which affects the animals' health and the study results (268). Therefore, the utilization of micro-CT as a non-invasive modality to obtain *in vivo* longitudinal imaging at 18 μm resolution may not be precise enough to directly assess the growth in the cementum layer volume.

In conclusion, our findings suggest that the non-invasive nature of LLLT, combined with its ability to enhance tissue remodeling and repair, make it a potentially useful method to stimulate new cementum formation on dental root surfaces. This concept could be clinically useful in regenerative periodontal therapy or in reducing root resorption caused by orthodontic tooth movement. By contrast, daily CsA treatment over a two-week period had little, if any, effect on the cementum thickness on all root aspects when compared with the control group, which may define the threshold at which CsA treatment duration is able to induce new cementum formation on the dental root surfaces of mature rats. Furthermore, our *in vivo* micro-CT analysis was unable to distinctly evaluate the cementum overgrowth in the LLLT group that was otherwise verified histologically in the same tissue sample. A word of caution is advised, as extrapolation from animal studies to humans is not always straightforward. How the above-discussed mechanisms would work in humans should be explored in future research.

8.2 Effect of LLLT-Induced Root Surface Remodeling on OITRR in the Second Animal Experiment

In the second animal experiment, we found that remodeling of the dental root surfaces by stimulating more cementum formation using low-level laser therapy (LLLT), before starting orthodontic treatment, provided significant protection against orthodontically induced tooth root resorption (OITRR) in rats. This protective effect against OITRR was greater, on average, on the root surfaces that showed more cementum growth in response to LLLT immediately before applying the orthodontic force.

The basic principle of orthodontic treatment is that prolonged force application to the tooth will cause tooth movement as a result of bone remodeling around the root (269). Obviously, successful tooth movement through bone does not rely solely on bone resorption, but also on the roots remaining intact. The pressure produced by orthodontic force alters the blood flow in the compressed periodontal ligament, which in turn triggers production of local biochemical mediators that generate a favorable environment for bone resorption (269). However, factors such as continuous heavy orthodontic force can cause undesirable tissue reactions such as an ischemic necrosis in the compressed periodontal ligament, which in turn can facilitate resorption of the adjacent root surface (10, 24, 26, 91).

Our micro-CT analyses in the second experiment showed that the preexisting external root surfaces remodeling caused by two weeks of daily LLLT application had a significant protective effect against resorption of these surfaces during the following four weeks of orthodontic tooth movement in rats. The magnitude and duration of the orthodontic force used in our experiment have been shown to cause external root resorption. However, in the present split-mouth experiment design, the total volume of root resorption was significantly less in the teeth exposed to two weeks of LLLT compared with the control teeth that received no treatment immediately before starting the orthodontic tooth movement.

Using a split-mouth design increases the study efficiency by reducing the inter-subject variability, and thus increasing the study power and increasing the precision of the estimated treatment effect (270). Moreover, each animal in the split-mouth design acts as its own control and therefore a smaller sample size is enough to satisfy the study objectives compared with a parallel-group design (270). Furthermore, the split-mouth design was suitable to be performed in the second experiment as no carry-across treatment effects are expected (270). In a split-mouth design, it is assumed that each of the two treatments should be randomly assigned to either the right or left halves of the dentition. However, it is more important for the operator to avoid committing the mistake of delivering the wrong treatment to the wrong side (270). Therefore, the decision of which molars were allocated to treatment was made before starting the experiment. Because the operator is right-handed, the LLLT treatment was assigned to all the right side

molars in order to make the experiment easier to conduct in an animal model and thus help to prevent such mistake of treatment contamination of control molars.

This increased resistance of the roots surfaces against OITRR can be attributed to the ability of LLLT to stimulate more cementum formation on those surfaces. Based on our findings in the first experiment, the same daily dose for two weeks of the same LLLT system (830 nm wavelength GaAlAs), with the same technique used in the current experiment, had proved to significantly increase the cementum thickness in the mesial roots of rat maxillary first molar. The suggested mechanism behind the increased cementum thickness was that low-level laser light energy, which is within the wavelength range of our low-level laser system, is able to reach and stimulate cementum formation by providing the appropriate environment required to influence the related cellular activity (220, 221, 230). Our treatment dosage was designed based on a review of the available evidence in order to ensure the appropriate laser energy absorption by the cementum forming cells (166, 181, 219). Presuming that low-level laser energy is primarily absorbed by a photoacceptor within the mitochondrial membrane (242, 243), several intracellular signaling pathways were suggested to explain the secondary cellular response in the cementum tissue following primary activation of the photoacceptor (244, 246, 248). Therefore, we surmised that absorption of low-level laser energy from our laser system by cementum forming cells could lead to the activation of mitochondrial respiratory chain components and the initiation of subsequent cellular signaling cascades. This ultimately increases the expression of

growth factors and cytokines that stimulate cementum tissue growth by promoting cellular proliferation and function.

When comparing the different aspects of the root surface between the groups, our micro-CT analyses also found that resorption volumes in both the mesial and buccal root surfaces were less on average than the volumes in the distal and lingual root surfaces of those teeth that received LLLT compared with the same surfaces in the control group. This suggests that the protective effect against root resorption in the preexisting remodeled root surfaces, caused by two weeks of LLLT, was greater in the mesial and buccal root surfaces. The relatively increased resistance against resorption in the mesial and buccal roots surfaces that exposed to LLLT in the second experiment may reflect the increased cementum thickness that was observed on the same surfaces within the LLLT group in our first experiment. These findings imply a positive relationship between the initial increase in root surface cementum thickness and the increased resistance of that surface against OITRR. The difference in cementum thickness between the different root surfaces within the LLLT group in our first experiment was attributed to the change in tissue absorption of the laser energy caused by the angle at which the laser beam struck the root surfaces. Decreased reflection of laser light and subsequently increased available energy for tissue absorption are expected when the root surface is exposed to a perpendicular laser beam (181). Moreover, the possible diminution of laser energy absorption at deeper aspects of the root surface may also explain the different tissue responses between the root

surfaces in the LLLT group, because the energy of the laser beam decreases as the laser light passes through the tissue (165). On that basis, we surmise that the more energy absorption of our laser treatment by the target tissue, the more cementum forms over the root surface before applying the orthodontic force, and ultimately, the less OITRR occurs on that surface.

Orthodontic treatment would not be possible without the fact that teeth root surfaces are more resistant to resorption than the opposing alveolar bone. The presence of a viable cementum layer covering the root surface may primarily underlie the resistance of the root to resorption (9, 24, 91). A mild, self-limiting form of root surface injury occurs when the pressure caused by the tooth movement damages or traumatizes the outer layer of cementum, which is fully regenerated once the orthodontic force has stopped (28, 91). However, if such an injury removes the entire cementum layer, a resorption process involving the outer layers of root dentin can follow unless the stimulation caused by orthodontic pressure is removed (25-28). The resorption process is linked to multinucleated clastic cells (odontoclasts) that are found within lacunae on the unprotected root dentin surface (25-28). These cells are distinguished from other multinucleated cells by the presence of a highly ruffled border opposing the dentin surface (25-28). The ruffled border increases their secretory ability at the active resorption site between the cell and dentin surface (91). The active resorption site is effectively sealed by the firm attachment of the odontoclast to the dentin surface, which is mediated mainly by integrin receptors located on the cell surface (91).

To our knowledge, this is the first report describing the effect of increased root cementum thickness on the root resorption caused by orthodontic treatment. Based on our findings, cementum layer augmentation could provide additional protection to the dental root against resorption during orthodontic treatment. A possible simple explanation for our findings is that root resorption seems to progress more rapidly in dentin than in cementum (91, 271), and therefore adding more layers of cementum tissue over the root surface would slow down the resorption process.

Although many theories have been proposed, the exact reason why cementum tissues are inherently more resistant to resorption, compared with dentin and alveolar bone, is still unknown (91). It has long been suggested that multinucleated clastic cells are unable to resorb or attach to non-mineralized matrix (272). According to one theory, the thin zone of non-mineralized layer (precementum) covering the external surface of cementum provides a protective barrier that prevents resorbing cells from developing and gaining access to the root surface (91, 272). However, the results of our study show that increasing the entire cementum thickness enhanced its resistance against resorption. This could mean that the unique proteins comprising the cementum matrix, rather than the non-mineralized condition of its outermost layer, may be primarily responsible for the inherent resistance of this tissue to resorption.

In terms of origin, morphology and function, odontoclasts are similar to osteoclasts, which are the bone-resorbing cells (273). Therefore, disturbing the attachment abilities of osteoclasts by blocking their integrin receptors using echistatin, an arginine-glycine-aspartic acid (RGD) containing peptide, can also inhibit root resorption by odontoclasts (53). Many studies have investigated the important role of integrin in the recognition and attachment of osteoclasts to several extracellular matrix proteins containing the RGD sequence (274-276). It has been found that osteoclast activity can be suppressed or enhanced according to the protein composition of the extracellular matrix (261-263). Furthermore, compared with alveolar bone, a recent analysis of the dental cementum proteome (250) identified several unique and differentially expressed proteins in cementum tissues that can provide insight into the possible inhibitory effects of these proteins on the activity of the resorbing cells. For example, biglycan (BGN) is a small leucine-rich proteoglycan (SLRP) that has been found to be abundantly more in dental cementum than alveolar bone (250). BGN knockout mice have been used to illustrate the role of BGN in osteoclast function. Mice deficient in BGN showed increased osteoclast formation and activity (277). Moreover, an antioxidant protein called superoxide dismutase 3 (SOD3) was exclusively found in dental cementum and therefore, was identified as a biomarker for cementum tissue (250). SOD3 can protect cementum tissues against oxidative stress by preventing the accumulation of reactive oxygen species (ROS) that are produced as by-products of the mitochondrial respiratory chain reactions (250). In line with this, several studies have investigated the mechanism by which estrogen

deficiency induces bone resorption, and emerging evidence has identified the ability of this sexual hormone to act as an antioxidant that protects bone against oxidative stress (278-280). Decreasing ROS accumulation through the defensive effect of antioxidants can inhibit osteoclast formation and resorption activity (281, 282). On that basis, expression of SOD3 as an endogenous antioxidant protein may enable the dental cementum to restrict odontoclast activity by preventing the accumulation of ROS in the tissue.

Unlike measuring the cementum thickness in the first experiment, micro-CT allows for accurate and reproducible volumetric analyses of the root resorption in the second experiment because it much easier to precisely outline and segment the resorption volume from the volume of root hard tissues based on the micro-CT images (Figure 13). The small size of rat's dental root sample required high-resolution micro-CT images for an accurate visualization of an even smaller resorption lesion (263, 267). While the highest resolution possible is desirable, *ex vivo* micro-CT imaging was done for all the samples in the second experiment in order to avoid the morbidity risk associated with increasing the radiation exposure as seen in the live animal micro-CT analyses in our pilot study. For these reasons, we think that micro-CT imaging provides an excellent alternative compared to the histological evaluation of root resorption caused by orthodontic tooth movement in the second experiment.

Many studies have found that micro-CT is a tool of high value for examining the root resorption (22, 259, 260). The use of micro-CT analyses to evaluate root resorption has several benefits over using the histological evaluation in the second experiment. The three-dimensional visualization of the root sample provided by the micro-CT imaging helped to study all the aspects of root's external surfaces in order not to miss detecting any resorption lacuna. Micro-CT imaging enabled the three-dimensional volumetric analyses of root resorption and had the advantage of being accurate and reproducible without destroying the original sample (259, 262, 263). On the other hand, an accurate volumetric evaluation of the root resorption could not be attained histologically. As mentioned before, the inherent technical sensitivity of the histological studies in addition to the difficulty of repeating or reproducing their slides preparations can affect the accuracy of the histological evaluation (259-261). Moreover, due to the possible loss of root material caused by the sample physical sectioning, some resorption lacunae could be partially or totally missed during the histological slides preparation.

Although the histological evaluation of the roots in the second experiment was only descriptive in nature, the findings appear to agree with those in the histomorphometric analysis of the first experiment. The increased cementum thickness in the second experiment was apparent in every root sample that was exposed to LLLT compared with the control samples. Notably, the incremental increase in the thickness of the cellular cementum as it approached the root apex was relatively greater in the LLLT treated roots (Figure 24) compared with the

evenly increased rate of the same tissue in the control group (Figure 25). Therefore, the apparent increase in cementum thickness as demonstrated by the likely increased growth of cellular cementum, can be considered a sign of remodeling activities along the external roots surfaces exposed to LLLT immediately before applying the orthodontic force. Cellular cementum is known to play important adaptive and reparative roles due to its ability to grow faster than the other cementum type (69). Cellular cementum contains an abundant cellular material that makes it readily available not only to repair any resorptive defect, but also to adapt the shape of the external root surfaces to any mechanical stress caused by the orthodontic force (69).

As discussed earlier, the root resorption volume caused by orthodontic treatment was evaluated and analyzed more adequately by the micro-CT analysis. However, the descriptive histological evaluation showed that the initial LLLT treatment appeared to decrease the severity of OITRR. It was histologically clear that orthodontic force caused a considerable amount of resorption in both groups, demonstrated by the presence of resorption lacunae on the external root surfaces. However, on the roots surfaces that were exposed to the initial LLLT treatment, most of the resorption was confined to the outer cementum layer, with fewer deep resorption lacunae extending to the outer layer of the radicular dentin when compared with control samples. Moreover, one mesial root in the control group (Figure 25), clearly exhibited a shortened root, which is a more severe form of OITRR that results in irreparable damage to the root structure (24). Therefore, the

change in root morphology caused by the increased growth of cementum following the initial LLLT treatment could provide mechanical protection against OITRR by affecting the stress distribution of orthodontic force (16, 17, 23). In other words, besides being inherently resistant to resorption, the initial cementum overgrowth in response to LLLT may increase the root surface area, which in turn could protect the tissue mechanically by diffusing the pressure against the compressed root surface and distributing the stress along a wider area following the application of orthodontic force.

Although this research project was designed to examine the effect of increased root cementun thickness on preventing the root resorption caused by orthodontic treatment; using LLLT may offer several advantages for any related future clinical application in orthodontic treatment. Many studies have confirmed that LLLT is able to reduce the level of pain during orthodontic treatment (209-215). Moreover, positive results have been reported in studies of the effects of LLLT in accelerating tooth movement rate during orthodontic treatment (207, 208, 217-226). The mechanism that LLLT accelerates the rate of tooth movement lies in its ability to stimulate the remodeling activity of the alveolar bone surrounding the dental root (228, 229). Several studies have reported that LLLT is effective in stimulating alveolar bone resorption at the pressure side of the dental root during orthodontic treatment by increasing the activities of the multinucleated clastic cells (228, 229). However, while the root resorption process is linked to the increased activity of clastic cells in the pressure side during orthodontic treatment

(25-28), a very recent study found that the application of LLLT during tooth movement did not stimulate root surface resorption (283). These controversial findings could be explained by the distribution of the blood vessels within the periodontal region. A previous study showed that most of the periodontal blood vessels are located within the alveolar region and adjacent to the alveolar bone away from the root surface (284). This might suggest a correlation between the proximity of the blood vessels and which surface is likely to be resorbed as a result of the clastic cells activation during orthodontic tooth movement. In any event, the concept of using LLLT could be clinically useful not only in increasing the root surface resistance against reorption, but also in accelerating the rate of orthodontic tooth movement.

In conclusion, two weeks of daily low-level laser therapy (LLLT) immediately before starting an orthodontic tooth movement significantly decreased the total volume of orthodontically induced tooth root resorption (OITRR) in rats. This protective effect against root resorption, on average, was more evident in the mesial and buccal root surfaces, and was correlated with the increased cementum thickness in the same surfaces that was observed in the LLLT group in the first animal experiment. Moreover, the increase in cementum thickness induced by the initial LLLT remodeling treatment not only decreased the volume of external dental root surface resorption in rats, but also appeared to decrease the OITRR severity. The role of our LLLT intervention in humans should be explored in

future research, as extrapolation from animal studies to human trials is not always straightforward or completely accurate.

9 CONCLUSIONS

9.1 Conclusions from the First Animal Experiment

From the first animal experiment, we concluded the following:

1- Two weeks of daily LLLT treatment (Ga-Al-As at 830 nm wavelength) significantly increased the total cementum thickness in rat's dental root surfaces.

2- Our LLLT treatment significantly increased the cementum thickness on all the different aspects of the mesial root of the rat's maxillary first molar, except the distal surface, when compared with both control and CsA treatment. Moreover, the cementum thickness in LLLT group was significantly more in the mesial and buccal roots surfaces than in the distal and lingual surfaces within the same group

3- Daily dose by subcutaneous injection of 10 mg/kg of body weight CsA treatment has no effect on the normal growth of rat's dental root cementum over a two-week period.

4- Our method in utilization the micro-CT scanning as a non-invasive modality *in vivo* setting to obtain longitudinal imaging at 18 μm resolution did not accurately detect the growth in the cementum layer volume.

9.2 Conclusions from the Second Animal Experiment

From the second animal experiment, we concluded the following:

1- Remodeling the root external surfaces by inducing new cementum formation using two weeks of daily LLLT treatment (Ga-Al-As at 830 nm wavelength) immediately before starting an orthodontic tooth movement significantly decreased the total volume of OITRR in rats.

2- On average, this protective effect against root resorption was more in the root surfaces that showed more cementum growth in response to our LLLT treatment.

3- Cementum layer augmentation before the application of orthodontic force seems to decrease the severity of external root surface resorption caused by the orthodontic tooth movement.

REFERENCES

1. Ramanathan C, Hofman Z. Root resorption in relation to orthodontic tooth movement. Acta Medica (Hradec Kralove). 2006;49(2):91-5.

2. Kurol J, Owman-Moll P, Lundgren D. Time-related root resorption after application of a controlled continuous orthodontic force. Am J Orthod Dentofacial Orthop. 1996 Sep;110(3):303-10.

3. Sameshima GT, Sinclair PM. Predicting and preventing root resorption: Part I. Diagnostic factors. Am J Orthod Dentofacial Orthop. 2001 May;119(5):505-10.

4. Sameshima GT, Sinclair PM. Predicting and preventing root resorption: Part II. Treatment factors. Am J Orthod Dentofacial Orthop. 2001 May;119(5):511-5.

5. Vlaskalic V, Boyd RL, Baumrind S. Etiology and sequelae of root resorption. Semin Orthod. 1998 Jun;4(2):124-31.

6. Lupi JE, Handelman CS, Sadowsky C. Prevalence and severity of apical root resorption and alveolar bone loss in orthodontically treated adults. Am J Orthod Dentofacial Orthop. 1996 Jan;109(1):28-37.

7. Taithongchai R, Sookkorn K, Killiany DM. Facial and dentoalveolar structure and the prediction of apical root shortening. Am J Orthod Dentofacial Orthop. 1996 Sep;110(3):296-302.

8. Levander E, Malmgren O. Long-term follow-up of maxillary incisors with severe apical root resorption. Eur J Orthod. 2000 Feb;22(1):85-92.

9. Fuss Z, Tsesis I, Lin S. Root resorption--diagnosis, classification and treatment choices based on stimulation factors. Dent Traumatol. 2003 Aug;19(4):175-82.

10. Segal GR, Schiffman PH, Tuncay OC. Meta analysis of the treatment-related factors of external apical root resorption. Orthod Craniofac Res. 2004 May;7(2):71-8.

11. Pizzo G, Licata ME, Guiglia R, Giuliana G. Root resorption and orthodontic treatment. Review of the literature. Minerva Stomatol. 2007 Jan-Feb;56(1-2):31-44.

12. Parker RJ, Harris EF. Directions of orthodontic tooth movements associated with external apical root resorption of the maxillary central incisor. Am J Orthod Dentofacial Orthop. 1998 Dec;114(6):677-83.

13. Faltin RM, Faltin K, Sander FG, Arana-Chavez VE. Ultrastructure of cementum and periodontal ligament after continuous intrusion in humans: a transmission electron microscopy study. Eur J Orthod. 2001 Feb;23(1):35-49.

14. Owman-Moll P, Kurol J, Lundgren D. Continuous versus interrupted continuous orthodontic force related to early tooth movement and root resorption. Angle Orthod. 1995;65(6):395,401; discussion 401-2.

15. Mavragani M, Vergari A, Selliseth NJ, Boe OE, Wisth PL. A radiographic comparison of apical root resorption after orthodontic treatment with a standard edgewise and a straight-wire edgewise technique. Eur J Orthod. 2000 Dec;22(6):665-74.

16. Oyama K, Motoyoshi M, Hirabayashi M, Hosoi K, Shimizu N. Effects of root morphology on stress distribution at the root apex. Eur J Orthod. 2007 Apr;29(2):113-7.

17. Levander E, Bajka R, Malmgren O. Early radiographic diagnosis of apical root resorption during orthodontic treatment: a study of maxillary incisors. Eur J Orthod. 1998 Feb;20(1):57-63.

18. Levander E, Malmgren O, Stenback K. Apical root resorption during orthodontic treatment of patients with multiple aplasia: a study of maxillary incisors. Eur J Orthod. 1998 Aug;20(4):427-34.

19. Hartsfield JK,Jr, Everett ET, Al-Qawasmi RA. Genetic Factors in External Apical Root Resorption and Orthodontic Treatment. Crit Rev Oral Biol Med. 2004 Jan 1;15(2):115-22.

20. Maltha JC, van Leeuwen EJ, Dijkman GE, Kuijpers-Jagtman AM. Incidence and severity of root resorption in orthodontically moved premolars in dogs. Orthod Craniofac Res. 2004 May;7(2):115-21.

21. Casa MA, Faltin RM, Faltin K, Sander FG, Arana-Chavez VE. Root resorptions in upper first premolars after application of continuous torque moment. Intra-individual study. J Orofac Orthop. 2001 Jul;62(4):285-95.

22. Harris DA, Jones AS, Darendeliler MA. Physical properties of root cementum: part 8. Volumetric analysis of root resorption craters after application of controlled intrusive light and heavy orthodontic forces: a microcomputed tomography scan study. Am J Orthod Dentofacial Orthop. 2006 Nov;130(5):639-47.

23. Jimenez-Pellegrin C, Arana-Chavez VE. Root resorption repair in mandibular first premolars after rotation. A transmission electron microscopy analysis combined with immunolabeling of osteopontin. Am J Orthod Dentofacial Orthop. 2007 Aug;132(2):230-6.

24. Brezniak N, Wasserstein A. Orthodontically induced inflammatory root resorption. Part I: The basic science aspects. Angle Orthod. 2002 Apr;72(2):175-9.

25. Brudvik P, Rygh P. Root resorption beneath the main hyalinized zone. Eur J Orthod. 1994 Aug;16(4):249-63.

26. Brudvik P, Rygh P. Multi-nucleated cells remove the main hyalinized tissue and start resorption of adjacent root surfaces. Eur J Orthod. 1994 Aug;16(4):265-73.

27. Brudvik P, Rygh P. Non-clast cells start orthodontic root resorption in the periphery of hyalinized zones. Eur J Orthod. 1993 Dec;15(6):467-80.

28. Brudvik P, Rygh P. The initial phase of orthodontic root resorption incident to local compression of the periodontal ligament. Eur J Orthod. 1993 Aug;15(4):249-63.

29. Alhashimi N, Frithiof L, Brudvik P, Bakhiet M. Orthodontic tooth movement and de novo synthesis of proinflammatory cytokines. Am J Orthod Dentofacial Orthop. 2001 Mar;119(3):307-12.

30. Bletsa A, Berggreen E, Brudvik P. Interleukin-1alpha and tumor necrosis factor-alpha expression during the early phases of orthodontic tooth movement in rats. Eur J Oral Sci. 2006 Oct;114(5):423-9.

31. Alhashimi N, Frithiof L, Brudvik P, Bakhiet M. CD40-CD40L expression during orthodontic tooth movement in rats. Angle Orthod. 2004 Feb;74(1):100-5.

32. Brudvik P, Rygh P. The repair of orthodontic root resorption: an ultrastructural study. Eur J Orthod. 1995 Jun;17(3):189-98.

33. Owman-Moll P, Kurol J. The early reparative process of orthodontically induced root resorption in adolescents--location and type of tissue. Eur J Orthod. 1998 Dec;20(6):727-32.

34. Sameshima GT, Sinclair PM. Characteristics of patients with severe root resorption. Orthod Craniofac Res. 2004 May;7(2):108-14.

35. Brezniak N, Wasserstein A. Orthodontically induced inflammatory root resorption. Part II: The clinical aspects. Angle Orthod. 2002 Apr;72(2):180-4.

36. Luther F, Dominguez-Gonzalez S, Fayle SA. Teamwork in orthodontics: limiting the risks of root resorption. Br Dent J. 2005 Apr 9;198(7):407-11.

37. Owman-Moll P, Kurol J, Lundgren D. Repair of orthodontically induced root resorption in adolescents. Angle Orthod. 1995;65(6):403,8; discussion 409-10.

38. Krishnan V, Davidovitch Z. The effect of drugs on orthodontic tooth movement. Orthod Craniofac Res. 2006 Nov;9(4):163-71.

39. Poumpros E, Loberg E, Engstrom C. Thyroid function and root resorption. Angle Orthod. 1994;64(5):389,93; discussion 394.

40. Shirazi M, Dehpour AR, Jafari F. The effect of thyroid hormone on orthodontic tooth movement in rats. J Clin Pediatr Dent. 1999 Spring;23(3):259-64.

41. Vazquez-Landaverde LA, Rojas-Huidobro R, Alonso Gallegos-Corona M, Aceves C. Periodontal 5'-deiodination on forced-induced root resorption--the protective effect of thyroid hormone administration. Eur J Orthod. 2002 Aug;24(4):363-9.

42. Mavragani M, Brudvik P, Selvig KA. Orthodontically induced root and alveolar bone resorption: inhibitory effect of systemic doxycycline administration in rats. Eur J Orthod. 2005 Jun;27(3):215-25.

43. Golub LM, Ciancio S, Ramamamurthy NS, Leung M, McNamara TF. Low-dose doxycycline therapy: effect on gingival and crevicular fluid collagenase activity in humans. J Periodontal Res. 1990 Nov;25(6):321-30.

44. Shapira L, Soskolne WA, Houri Y, Barak V, Halabi A, Stabholz A. Protection against endotoxic shock and lipopolysaccharide-induced local inflammation by tetracycline: correlation with inhibition of cytokine secretion. Infect Immun. 1996 Mar;64(3):825-8.

45. Villa PA, Oberti G, Moncada CA, Vasseur O, Jaramillo A, Tobon D, et al. Pulp-dentine complex changes and root resorption during intrusive orthodontic tooth movement in patients prescribed nabumetone. J Endod. 2005 Jan;31(1):61-6.

46. Jerome J, Brunson T, Takeoka G, Foster C, Moon HB, Grageda E, et al. Celebrex offers a small protection from root resorption associated with orthodontic movement. J Calif Dent Assoc. 2005 Dec;33(12):951-9.

47. Fleisch H. Bisphosphonates: mechanisms of action. Endocr Rev. 1998 Feb;19(1):80-100.

48. Igarashi K, Adachi H, Mitani H, Shinoda H. Inhibitory effect of the topical administration of a bisphosphonate (risedronate) on root resorption incident to orthodontic tooth movement in rats. J Dent Res. 1996 Sep;75(9):1644-9.

49. Liu L, Igarashi K, Haruyama N, Saeki S, Shinoda H, Mitani H. Effects of local administration of clodronate on orthodontic tooth movement and root resorption in rats. Eur J Orthod. 2004 Oct;26(5):469-73.

50. Wesselink PR, Beertsen W. Ankylosis of the mouse molar after systemic administration of 1-hydroxyethylidene-1,1-bisphosphonate (HEBP). J Clin Periodontol. 1994 Aug;21(7):465-71.

51. Alatli I, Hellsing E, Hammarstrom L. Orthodontically induced root resorption in rat molars after 1-hydroxyethylidene-1,1-bisphosphonate injection. Acta Odontol Scand. 1996 Apr;54(2):102-8.

52. Jager A, Zhang D, Kawarizadeh A, Tolba R, Braumann B, Lossdorfer S, et al. Soluble cytokine receptor treatment in experimental orthodontic tooth movement in the rat. Eur J Orthod. 2005 Feb;27(1):1-11.

53. Talic NF, Evans C, Zaki AM. Inhibition of orthodontically induced root resorption with echistatin, an RGD-containing peptide. Am J Orthod Dentofacial Orthop. 2006 Feb;129(2):252-60.

54. Elliott JC. Recent progress in the chemistry, crystal chemistry and structure of the apatites. Calcif Tissue Res. 1969;3(4):293-307.

55. Brown WE, Gregory TM, Chow LC. Effects of fluoride on enamel solubility and cariostasis. Caries Res. 1977;11 Suppl 1:118-41.

56. Kato K, Nakagaki H, Robinson C, Weatherell JA. Distribution of fluoride across cementum, dentine and alveolar bone in rats. Caries Res. 1990;24(2):117-20.

57. Kato S, Nakagaki H, Toyama Y, Kanayama T, Arai M, Togari A, et al. Fluoride profiles in the cementum and root dentine of human permanent anterior teeth extracted from adult residents in a naturally fluoridated and a non-fluoridated area. Gerodontology. 1997 Jul;14(1):1-8.

58. Foo M, Jones A, Darendeliler MA. Physical properties of root cementum: Part 9. Effect of systemic fluoride intake on root resorption in rats. Am J Orthod Dentofacial Orthop. 2007 Jan;131(1):34-43.

59. van't Hof RJ, Ralston SH. Nitric oxide and bone. Immunology. 2001 Jul;103(3):255-61.

60. Mancini L, Moradi-Bidhendi N, Becherini L, Martineti V, MacIntyre I. The biphasic effects of nitric oxide in primary rat osteoblasts are cGMP dependent. Biochem Biophys Res Commun. 2000 Aug 2;274(2):477-81.

61. Shirazi M, Nilforoushan D, Alghasi H, Dehpour AR. The role of nitric oxide in orthodontic tooth movement in rats. Angle Orthod. 2002 Jun;72(3):211-5.

62. Sandy JR, Farndale RW, Meikle MC. Recent advances in understanding mechanically induced bone remodeling and their relevance to orthodontic theory and practice. Am J Orthod Dentofacial Orthop. 1993 Mar;103(3):212-22.

63. Yamasaki K, Shibata Y, Fukuhara T. The effect of prostaglandins on experimental tooth movement in monkeys (Macaca fuscata). J Dent Res. 1982 Dec;61(12):1444-6.

64. Yamasaki K, Miura F, Suda T. Prostaglandin as a mediator of bone resorption induced by experimental tooth movement in rats. J Dent Res. 1980 Oct;59(10):1635-42.

65. Yamasaki K, Shibata Y, Imai S, Tani Y, Shibasaki Y, Fukuhara T. Clinical application of prostaglandin E1 (PGE1) upon orthodontic tooth movement. Am J Orthod. 1984 Jun;85(6):508-18.

66. Leiker BJ, Nanda RS, Currier GF, Howes RI, Sinha PK. The effects of exogenous prostaglandins on orthodontic tooth movement in rats. Am J Orthod Dentofacial Orthop. 1995 Oct;108(4):380-8.

67. Boekenoogen DI, Sinha PK, Nanda RS, Ghosh J, Currier GF, Howes RI. The effects of exogenous prostaglandin E2 on root resorption in rats. Am J Orthod Dentofacial Orthop. 1996 Mar;109(3):277-86.

68. Mosby. *Mosby's Dental Dictionary*. 2nd edition ed. Elsevier, Inc; 2008.

69. Bosshardt DD, Selvig KA. Dental cementum: the dynamic tissue covering of the root. Periodontol 2000. 1997 Feb;13:41-75.

70. MacNeil RL, Somerman MJ. Development and regeneration of the periodontium: parallels and contrasts. Periodontol 2000. 1999 Feb;19:8-20.

71. Nanci A, Ten Cate AR. Ten Cate's oral histology : development, structure, and function. 7th ed. St. Louis: Mosby Elsevier; 2008.

72. Dastmalchi R, Polson A, Bouwsma O, Proskin H. Cementum thickness and mesial drift. J Clin Periodontol. 1990 Nov;17(10):709-13.

73. Saygin NE, Giannobile WV, Somerman MJ. Molecular and cell biology of cementum. Periodontol 2000. 2000 Oct;24:73-98.

74. Sperber GH. Craniofacial development. Hamilton, Ont; London: B C Decker; 2001.

75. Zeichner-David M, Oishi K, Su Z, Zakartchenko V, Chen LS, Arzate H, et al. Role of Hertwig's epithelial root sheath cells in tooth root development. Dev Dyn. 2003 Dec;228(4):651-63.

76. Zeichner-David M. Regeneration of periodontal tissues: cementogenesis revisited. Periodontol 2000. 2006;41:196-217.

77. Grzesik WJ, Narayanan AS. Cementum and periodontal wound healing and regeneration. Crit Rev Oral Biol Med. 2002;13(6):474-84.

78. Brice GL, Sampson WJ, Sims MR. An ultrastructural evaluation of the relationship between epithelial rests of Malassez and orthodontic root resorption and repair in man. Aust Orthod J. 1991 Oct;12(2):90-4.

79. Hasegawa N, Kawaguchi H, Ogawa T, Uchida T, Kurihara H. Immunohistochemical characteristics of epithelial cell rests of Malassez during cementum repair. J Periodontal Res. 2003 Feb;38(1):51-6.

80. Bosshardt DD. Are cementoblasts a subpopulation of osteoblasts or a unique phenotype? J Dent Res. 2005 May;84(5):390-406.

81. Bartold PM, Narayanan AS. Molecular and cell biology of healthy and diseased periodontal tissues. Periodontol 2000. 2006;40:29-49.

82. Ikezawa K, Hart CE, Williams DC, Narayanan AS. Characterization of cementum derived growth factor as an insulin-like growth factor-I like molecule. Connect Tissue Res. 1997;36(4):309-19.

83. Arzate H, Olson SW, Page RC, Gown AM, Narayanan AS. Production of a monoclonal antibody to an attachment protein derived from human cementum. FASEB J. 1992 Aug;6(11):2990-5.

84. Bartold PM, McCulloch CA, Narayanan AS, Pitaru S. Tissue engineering: a new paradigm for periodontal regeneration based on molecular and cell biology. Periodontol 2000. 2000 Oct;24:253-69.

85. Boyd DH, Kinirons MJ, Gregg TA. A prospective study of factors affecting survival of replanted permanent incisors in children. Int J Paediatr Dent. 2000 Sep;10(3):200-5.

86. Moradian H, Badakhsh S, Rahimi M, Hekmatfar S. Replantation of an avulsed maxillary incisor after 12 hours: three-year follow-up. Iran Endod J. 2013 Winter;8(1):33-6.

87. Poi WR, Sonoda CK, Martins CM, Melo ME, Pellizzer EP, de Mendonca MR, et al. Storage media for avulsed teeth: a literature review. Braz Dent J. 2013 Sep-Oct;24(5):437-45.

88. Wu YM, Richards DW, Rowe DJ. Production of matrix-degrading enzymes and inhibition of osteoclast-like cell differentiation by fibroblast-like cells from the periodontal ligament of human primary teeth. J Dent Res. 1999 Feb;78(2):681-9.

89. Kanzaki H, Chiba M, Shimizu Y, Mitani H. Dual regulation of osteoclast differentiation by periodontal ligament cells through RANKL stimulation and OPG inhibition. J Dent Res. 2001 Mar;80(3):887-91.

90. Tyrovola JB, Spyropoulos MN, Makou M, Perrea D. Root resorption and the OPG/RANKL/RANK system: a mini review. J Oral Sci. 2008 Dec;50(4):367-76.

91. Darcey J, Qualtrough A. Resorption: part 1. Pathology, classification and aetiology. Br Dent J. 2013 May;214(9):439-51.

92. Lindskog S, Blomlof L, Hammarstrom L. Comparative effects of parathyroid hormone on osteoblasts and cementoblasts. J Clin Periodontol. 1987 Aug;14(7):386-9.

93. Khosla S. Minireview: the OPG/RANKL/RANK system. Endocrinology. 2001 Dec;142(12):5050-5.

94. Lindskog S, Hammarstrom L. Evidence in favor of an anti-invasion factor in cementum or periodontal membrane of human teeth. Scand J Dent Res. 1980 Apr;88(2):161-3.

95. Soma S, Iwamoto M, Higuchi Y, Kurisu K. Effects of continuous infusion of PTH on experimental tooth movement in rats. J Bone Miner Res. 1999 Apr;14(4):546-54.

96. Li F, Li G, Hu H, Liu R, Chen J, Zou S. Effect of parathyroid hormone on experimental tooth movement in rats. Am J Orthod Dentofacial Orthop. 2013 Oct;144(4):523-32.

97. Emslie RD. Some considerations on the role of cementum in periodontal disease. J Clin Periodontol. 1978 Feb;5(1):1-12.

98. Robinson PJ. Possible roles of diseased cementum in periodontitis. J Prev Dent. 1975 May-Jun;2(3):3-5.

99. Chutimanutskul W, Ali Darendeliler M, Shen G, Petocz P, Swain MV. Changes in the physical properties of human premolar cementum after application of 4 weeks of controlled orthodontic forces. Eur J Orthod. 2006 Aug;28(4):313-8.

100. Rex T, Kharbanda OP, Petocz P, Darendeliler MA. Physical properties of root cementum: part 6. A comparative quantitative analysis of the mineral composition of human premolar cementum after the application of orthodontic forces. Am J Orthod Dentofacial Orthop. 2006 Mar;129(3):358-67.

101. Mirabella AD, Artun J. Prevalence and severity of apical root resorption of maxillary anterior teeth in adult orthodontic patients. Eur J Orthod. 1995 Apr;17(2):93-9.

102. Lynch SE, de Castilla GR, Williams RC, Kiritsy CP, Howell TH, Reddy MS, et al. The effects of short-term application of a combination of platelet-derived and insulin-like growth factors on periodontal wound healing. J Periodontol. 1991 Jul;62(7):458-67.

103. Rutherford RB, Niekrash CE, Kennedy JE, Charette MF. Platelet-derived and insulin-like growth factors stimulate regeneration of periodontal attachment in monkeys. J Periodontal Res. 1992 Jul;27(4 Pt 1):285-90.

104. Kuboki Y, Sasaki M, Saito A, Takita H, Kato H. Regeneration of periodontal ligament and cementum by BMP-applied tissue engineering. Eur J Oral Sci. 1998 Jan;106 Suppl 1:197-203.

105. Sato Y, Kikuchi M, Ohata N, Tamura M, Kuboki Y. Enhanced cementum formation in experimentally induced cementum defects of the root surface with the application of recombinant basic fibroblast growth factor in collagen gel in vivo. J Periodontol. 2004 Feb;75(2):243-8.

106. Bosshardt DD, Sculean A, Windisch P, Pjetursson BE, Lang NP. Effects of enamel matrix proteins on tissue formation along the roots of human teeth. J Periodontal Res. 2005 Apr;40(2):158-67.

107. Venezia E, Goldstein M, Boyan BD, Schwartz Z. The use of enamel matrix derivative in the treatment of periodontal defects: a literature review and meta-analysis. Crit Rev Oral Biol Med. 2004 Nov 1;15(6):382-402.

108. Vella JP, Sayegh MH, Turka LA. Developments in the clinical science of transplantation during the 20th century. Pediatr Transplant. 1998 Nov;2(4):257-62.

109. Denton MD, Magee CC, Sayegh MH. Immunosuppressive strategies in transplantation. Lancet. 1999 Mar 27;353(9158):1083-91.

110. Rezzani R. Cyclosporine A and adverse effects on organs: histochemical studies. Prog Histochem Cytochem. 2004;39(2):85-128.

111. Stoddard BL, Flick KE. Calcineurin-immunosuppressor complexes. Curr Opin Struct Biol. 1996 Dec;6(6):770-5.

112. Matsuda S, Shibasaki F, Takehana K, Mori H, Nishida E, Koyasu S. Two distinct action mechanisms of immunophilin-ligand complexes for the blockade of T-cell activation. EMBO Rep. 2000 Nov;1(5):428-34.

113. Thomson AW. The effects of cyclosporin A on non-T cell components of the immune system. J Autoimmun. 1992 Apr;5 Suppl A:167-76.

114. Drewe J, Beglinger C, Kissel T. The absorption site of cyclosporin in the human gastrointestinal tract. Br J Clin Pharmacol. 1992 Jan;33(1):39-43.

115. Hamel AR, Hubler F, Carrupt A, Wenger RM, Mutter M. Cyclosporin A prodrugs: design, synthesis and biophysical properties. J Pept Res. 2004 Feb;63(2):147-54.

116. Cohen SM. Current immunosuppression in liver transplantation. Am J Ther. 2002 Mar-Apr;9(2):119-25.

117. Wassef R, Cohen Z, Langer B. Pharmacokinetic profiles of cyclosporine in rats. Influence of route of administration and dosage. Transplantation. 1985 Nov;40(5):489-93.

118. Alejandro R, Cutfield R, Shienvold FL, Latif Z, Mintz DH. Successful long-term survival of pancreatic islet allografts in spontaneous or pancreatectomy-induced diabetes in dogs. Cyclosporine-induced immune unresponsiveness. Diabetes. 1985 Aug;34(8):825-8.

119. Ciavarella D, Guiglia R, Campisi G, Di Cosola M, Di Liberto C, Sabatucci A, et al. Update on gingival overgrowth by cyclosporine A in renal transplants. Med Oral Patol Oral Cir Bucal. 2007 Jan;12(1):E19-25.

120. Christians U, Sewing KF. Cyclosporin metabolism in transplant patients. Pharmacol Ther. 1993 Feb-Mar;57(2-3):291-345.

121. Yee GC. Recent advances in cyclosporine pharmacokinetics. Pharmacotherapy. 1991;11(5):130S-4S.

122. Lake KD. Management of drug interactions with cyclosporine. Pharmacotherapy. 1991;11(5):110S-8S.

123. Chen YT, Tu HP, Chin YT, Shen EC, Chiang CY, Gau CH, et al. Upregulation of transforming growth factor-beta1 and vascular endothelial growth factor gene and protein expression in cyclosporin-induced overgrown edentulous gingiva in rats. J Periodontol. 2005 Dec;76(12):2267-75.

124. Hyland PL, Traynor PS, Myrillas TT, Marley JJ, Linden GJ, Winter P, et al. The effects of cyclosporin on the collagenolytic activity of gingival fibroblasts. J Periodontol. 2003 Apr;74(4):437-45.

125. Schincaglia GP, Forniti F, Cavallini R, Piva R, Calura G, del Senno L. Cyclosporin-A increases type I procollagen production and mRNA level in human gingival fibroblasts in vitro. J Oral Pathol Med. 1992 Apr;21(4):181-5.

126. Tipton DA, Stricklin GP, Dabbous MK. Fibroblast heterogeneity in collagenolytic response to cyclosporine. J Cell Biochem. 1991 Jun;46(2):152-65.

127. Buduneli N, Kutukculer N, Aksu G, Atilla G. Evaluation of transforming growth factor-beta 1 level in crevicular fluid of cyclosporin A-treated patients. J Periodontol. 2001 Apr;72(4):526-31.

128. Cotrim P, de Andrade CR, Martelli-Junior H, Graner E, Sauk JJ, Coletta RD. Expression of matrix metalloproteinases in cyclosporin-treated gingival fibroblasts is regulated by transforming growth factor (TGF)-beta1 autocrine stimulation. J Periodontol. 2002 Nov;73(11):1313-22.

129. Iacopino AM, Doxey D, Cutler CW, Nares S, Stoever K, Fojt J, et al. Phenytoin and cyclosporine A specifically regulate macrophage phenotype and expression of platelet-derived growth factor and interleukin-1 in vitro and in vivo: possible molecular mechanism of drug-induced gingival hyperplasia. J Periodontol. 1997 Jan;68(1):73-83.

130. Chin YT, Chen YT, Tu HP, Shen EC, Chiang CY, Gau CH, et al. Upregulation of the expression of epidermal growth factor and its receptor in gingiva upon cyclosporin A treatment. J Periodontol. 2006 Apr;77(4):647-56.

131. Gau CH, Chou TC, Chiu HC, Shen EC, Nieh S, Chiang CY, et al. Effect of cyclosporin A on the expression of inducible nitric oxide synthase in the gingiva of rats. J Periodontol. 2005 Dec;76(12):2260-6.

132. Noguchi K, Shitashige M, Ishikawa I. Involvement of cyclooxygenase-2 in interleukin-1alpha-induced prostaglandin production by human periodontal ligament cells. J Periodontol. 1999 Aug;70(8):902-8.

133. Chiang CY, Chen YT, Hung FM, Tu HP, Fu MM, Fu E. Cyclosporin-A inhibits the expression of cyclooxygenase-2 in gingiva. J Periodontal Res. 2007 Oct;42(5):443-9.

134. Tipton DA, Pabst MJ, Dabbous MK. Interleukin-1 beta- and tumor necrosis factor-alpha-independent monocyte stimulation of fibroblast collagenase activity. J Cell Biochem. 1990 Dec;44(4):253-64.

135. Tannirandorn P, Epstein S. Drug-induced bone loss. Osteoporos Int. 2000;11(8):637-59.

136. Russell RG, Graveley R, Skjodt H. The effects of cyclosporin A on bone and cartilage. Br J Rheumatol. 1993 Mar;32 Suppl 1:42-6.

137. del Pozo E, Lippuner K, Ruch W, Casez JP, Payne T, MacKenzie A, et al. Different effects of cyclosporin A on bone remodeling in young and adult rats. Bone. 1995 Apr;16(4 Suppl):271S-5S.

138. Erben RG, Brunner KS, Breig B, Eberle J, Goldberg M, Hofbauer LC. Skeletal effects of cyclosporin A are gender related in rats. Endocrinology. 2003 Jan;144(1):40-9.

139. Fu E, Hsieh YD, Mao TK, Shen EC. A histomorphological investigation of the effect of cyclosporin on trabecular bone of the rat mandibular condyle. Arch Oral Biol. 2001 Dec;46(12):1105-10.

140. Shen EC, Fu E, Hsieh YD. Effects of cyclosporin A on dental alveolar bone: a histomorphometric study in rats. J Periodontol. 2001 May;72(5):659-65.

141. Cetinkaya BO, Acikgoz G, Keles GC, Ayas B, Korkmaz A. The effect of cyclosporin A on alveolar bone in rats subjected to experimental periodontal disease. Toxicol Pathol. 2006;34(6):716-22.

142. Gau CH, Hsieh YD, Shen EC, Lee S, Chiang CY, Fu E. Healing following tooth extraction in cyclosporine-fed rats. Int J Oral Maxillofac Surg. 2005 Oct;34(7):782-8.

143. Ayanoglou CM, Lesty C. New cementum formation induced by cyclosporin A: a histological, ultrastructural and histomorphometric study in the rat. J Periodontal Res. 1997 Aug;32(6):543-56.

144. Ayanoglou CM, Lesty C. Maintenance of new cementum formed during cyclosporin A administration after suspension of the treatment. J Periodontal Res. 1997 Oct;32(7):614-8.

145. Ayanoglou CM. Evidence that cyclosporin A administration induces the formation of new cementum-like islets inside the gingival connective tissue. J Periodontal Res. 1998 Apr;33(3):166-71.

146. Shen EC, Fu E, Gau CH, Hsieh YD, Chiang CY. Effect of cyclosporin A on the mineral apposition rate of cementum and dentin in growing rats. J Periodontol. 2005 Jun;76(6):936-40.

147. Spolidorio LC, Spolidorio DM, Holzhausen M, Nassar CA, Nassar PO. Cyclosporin A-induced new cementum formation: a morphometric evaluation in the periapical region of rats. Braz Dent J. 2007;18(1):24-8.

148. Jayasheela M, Mehta DS. The role of cyclosporine A on the periodontal tissues. Dent Res J (Isfahan). 2013 Nov;10(6):802-8.

149. Daley TD, Wysocki GP, Mamandras AH. Orthodontic therapy in the patient treated with cyclosporine. Am J Orthod Dentofacial Orthop. 1991 Dec;100(6):537-41.

150. Walker MR, Lovel SF, Melrose CA. Orthodontic treatment of a patient with a renal transplant and drug-induced gingival overgrowth: a case report. J Orthod. 2007 Dec;34(4):220-8.

151. Pöntinen PJ. Low level laser therapy as a medical treatment modality : a manual for physicians, dentists, physiotherapists and veterinary surgeons. Tampere: Art Urpo Ltd.; 1992.

152. Andersen K. Laser technology--a surgical tool of the past, present, and future. AORN J. 2003 Nov;78(5):794,802, 805-7.

153. Wigdor H. Basic physics of laser interaction with vital tissue. Alpha Omegan. 2008 Sep;101(3):127-32.

154. Gross AJ, Herrmann TR. History of lasers. World J Urol. 2007 Jun;25(3):217-20.

155. Miller M, Truhe T. Lasers in dentistry: an overview. J Am Dent Assoc. 1993 Feb;124(2):32-5.

156. Walsh LJ. The current status of laser applications in dentistry. Aust Dent J. 2003 Sep;48(3):146,55; quiz 198.

157. Shi XQ, Welander U, Angmar-Mansson B. Occlusal caries detection with KaVo DIAGNOdent and radiography: an in vitro comparison. Caries Res. 2000 Mar-Apr;34(2):151-8.

158. Cobb DS, Dederich DN, Gardner TV. In vitro temperature change at the dentin/pulpal interface by using conventional visible light versus argon laser. Lasers Surg Med. 2000;26(4):386-97.

159. Dougherty TJ. An update on photodynamic therapy applications. J Clin Laser Med Surg. 2002 Feb;20(1):3-7.

160. Dederich DN, Bushick RD, ADA Council on Scientific Affairs and Division of Science, Journal of the American Dental Association. Lasers in dentistry: separating science from hype. J Am Dent Assoc. 2004 Feb;135(2):204,12; quiz 229.

161. Sgolastra F, Petrucci A, Gatto R, Monaco A. Efficacy of Er:YAG laser in the treatment of chronic periodontitis: systematic review and meta-analysis. Lasers Med Sci. 2012 May;27(3):661-73.

162. Dederich DN. Laser curettage: an overview. Compend Contin Educ Dent. 2002 Nov;23(11A):1097-103.

163. Dederich DN. Laser/tissue interaction: what happens to laser light when it strikes tissue? J Am Dent Assoc. 1993 Feb;124(2):57-61.

164. Ohshiro T, Calderhead RG. Low level laser therapy : a practical introduction. Chichester; New York: Wiley; 1988.

165. Kutsch VK. Lasers in dentistry: comparing wavelengths. J Am Dent Assoc. 1993 Feb;124(2):49-54.

166. Ohshiro T. Low reactive-level laser therapy : practical application. Chichester; New York: Wiley; 1991.

167. Peavy GM. Lasers and laser-tissue interaction. Vet Clin North Am Small Anim Pract. 2002 May;32(3):517,34, v-vi.

168. Niemz MH. Laser-Tissue Interactions: Fundamentals and Applications. 3rd Edition ed. Berlin; New York: Springer-Verlag; 2007.

169. Basford JR. Low intensity laser therapy: still not an established clinical tool. Lasers Surg Med. 1995;16(4):331-42.

170. Anderson RR, Parrish JA. The optics of human skin. J Invest Dermatol. 1981 Jul;77(1):13-9.

171. Bjordal JM, Couppe C, Chow RT, Tuner J, Ljunggren EA. A systematic review of low level laser therapy with location-specific doses for pain from chronic joint disorders. Aust J Physiother. 2003;49(2):107-16.

172. Esnouf A, Wright PA, Moore JC, Ahmed S. Depth of penetration of an 850nm wavelength low level laser in human skin. Acupunct Electrother Res. 2007;32(1-2):81-6.

173. Kolari PJ. Penetration of unfocused laser light into the skin. Arch Dermatol Res. 1985;277(4):342-4.

174. Kolarova H, Ditrichova D, Wagner J. Penetration of the laser light into the skin in vitro. Lasers Surg Med. 1999;24(3):231-5.

175. Tuner J HL. Laser Therapy - Clinical Practice and Scientific Background. Grangesburg, Sweden: Prima Books; 2002.

176. Sun G, Tuner J. Low-level laser therapy in dentistry. Dent Clin North Am. 2004 Oct;48(4):1061,76, viii.

177. Walsh LJ. The current status of low level laser therapy in dentistry. Part 1. Soft tissue applications. Aust Dent J. 1997 Aug;42(4):247-54.

178. American National Standard for Safe Use of Lasers in Health Care, ANSI Z136-3 [Internet]. Available from: http://www.lia.org/publications/ansi/Z136-3.

179. Mester E, Spiry T, Szende B, Tota JG. Effect of laser rays on wound healing. Am J Surg. 1971 Oct;122(4):532-5.

180. Mester E, Mester AF, Mester A. The biomedical effects of laser application. Lasers Surg Med. 1985;5(1):31-9.

181. Brugnera AJ. Atlas of laser therapy applied to clinical dentistry. Chicago: Quintessance Editora Ltda.; 2006.

182. Harazaki M, Isshiki Y. Soft laser irradiation effects on pain reduction in orthodontic treatment. Bull Tokyo Dent Coll. 1997 Nov;38(4):291-5.

183. Fujiyama K, Deguchi T, Murakami T, Fujii A, Kushima K, Takano-Yamamoto T. Clinical effect of CO(2) laser in reducing pain in orthodontics. Angle Orthod. 2008 Mar;78(2):299-303.

184. Hudson DE, Hudson DO, Wininger JM, Richardson BD. Penetration of laser light at 808 and 980 nm in bovine tissue samples. Photomed Laser Surg. 2013 Apr;31(4):163-8.

185. Spencer P, Cobb CM, McCollum MH, Wieliczka DM. The effects of CO2 laser and Nd:YAG with and without water/air surface cooling on tooth root structure: correlation between FTIR spectroscopy and histology. J Periodontal Res. 1996 Oct;31(7):453-62.

186. Lins RD, Dantas EM, Lucena KC, Catao MH, Granville-Garcia AF, Carvalho Neto LG. Biostimulation effects of low-power laser in the repair process. An Bras Dermatol. 2010 Nov-Dec;85(6):849-55.

187. Arany PR, Nayak RS, Hallikerimath S, Limaye AM, Kale AD, Kondaiah P. Activation of latent TGF-beta1 by low-power laser in vitro correlates with increased TGF-beta1 levels in laser-enhanced oral wound healing. Wound Repair Regen. 2007 Nov-Dec;15(6):866-74.

188. Pyo SJ, Song WW, Kim IR, Park BS, Kim CH, Shin SH, et al. Low-level laser therapy induces the expressions of BMP-2, osteocalcin, and TGF-beta1 in hypoxic-cultured human osteoblasts. Lasers Med Sci. 2013 Feb;28(2):543-50.

189. Yu W, Naim JO, Lanzafame RJ. The effect of laser irradiation on the release of bFGF from 3T3 fibroblasts. Photochem Photobiol. 1994 Feb;59(2):167-70.

190. Sakurai Y, Yamaguchi M, Abiko Y. Inhibitory effect of low-level laser irradiation on LPS-stimulated prostaglandin E2 production and cyclooxygenase-2 in human gingival fibroblasts. Eur J Oral Sci. 2000 Feb;108(1):29-34.

191. Gavish L, Perez L, Gertz SD. Low-level laser irradiation modulates matrix metalloproteinase activity and gene expression in porcine aortic smooth muscle cells. Lasers Surg Med. 2006 Sep;38(8):779-86.

192. Blaya DS, Guimaraes MB, Pozza DH, Weber JB, de Oliveira MG. Histologic study of the effect of laser therapy on bone repair. J Contemp Dent Pract. 2008 Sep 1;9(6):41-8.

193. Merli LA, Santos MT, Genovese WJ, Faloppa F. Effect of low-intensity laser irradiation on the process of bone repair. Photomed Laser Surg. 2005 Apr;23(2):212-5.

194. Medina-Huertas R, Manzano-Moreno FJ, De Luna-Bertos E, Ramos-Torrecillas J, Garcia-Martinez O, Ruiz C. The effects of low-level diode laser irradiation on differentiation, antigenic profile, and phagocytic capacity of osteoblast-like cells (MG-63). Lasers Med Sci. 2014 Jul;29(4):1479-84.

195. Takeda Y. Irradiation effect of low-energy laser on alveolar bone after tooth extraction. Experimental study in rats. Int J Oral Maxillofac Surg. 1988 Dec;17(6):388-91.

196. Trelles MA, Mayayo E. Bone fracture consolidates faster with low-power laser. Lasers Surg Med. 1987;7(1):36-45.

197. Karu T, Pyatibrat L, Kalendo G. Irradiation with He-Ne laser increases ATP level in cells cultivated in vitro. J Photochem Photobiol B. 1995 Mar;27(3):219-23.

198. Garavello-Freitas I, Baranauskas V, Joazeiro PP, Padovani CR, Dal Pai-Silva M, da Cruz-Hofling MA. Low-power laser irradiation improves histomorphometrical parameters and bone matrix organization during tibia wound healing in rats. J Photochem Photobiol B. 2003 May-Jun;70(2):81-9.

199. Marquezan M, Bolognese AM, Araujo MT. Evaluation of two protocols for low-level laser application in patients submitted to orthodontic treatment. Dental Press J Orthod. 2013 Feb 15;18(1):33.e1,33.e9.

200. Pretel H, Lizarelli RF, Ramalho LT. Effect of low-level laser therapy on bone repair: histological study in rats. Lasers Surg Med. 2007 Dec;39(10):788-96.

201. Miloro M, Miller JJ, Stoner JA. Low-level laser effect on mandibular distraction osteogenesis. J Oral Maxillofac Surg. 2007 Feb;65(2):168-76.

202. Kreisner PE, Blaya DS, Gaiao L, Maciel-Santos ME, Etges A, Santana-Filho M, et al. Histological evaluation of the effect of low-level laser on distraction osteogenesis in rabbit mandibles. Med Oral Patol Oral Cir Bucal. 2010 Jul 1;15(4):e616-8.

203. Ozawa Y, Shimizu N, Kariya G, Abiko Y. Low-energy laser irradiation stimulates bone nodule formation at early stages of cell culture in rat calvarial cells. Bone. 1998 Apr;22(4):347-54.

204. Shimizu N, Mayahara K, Kiyosaki T, Yamaguchi A, Ozawa Y, Abiko Y. Low-intensity laser irradiation stimulates bone nodule formation via insulin-like growth factor-I expression in rat calvarial cells. Lasers Surg Med. 2007 Jul;39(6):551-9.

205. Kiyosaki T, Mitsui N, Suzuki N, Shimizu N. Low-level laser therapy stimulates mineralization via increased Runx2 expression and ERK phosphorylation in osteoblasts. Photomed Laser Surg. 2010 Aug;28 Suppl 1:S167-72.

206. Hamajima S, Hiratsuka K, Kiyama-Kishikawa M, Tagawa T, Kawahara M, Ohta M, et al. Effect of low-level laser irradiation on osteoglycin gene expression in osteoblasts. Lasers Med Sci. 2003;18(2):78-82.

207. Dominguez A, Gomez C, Palma JC. Effects of low-level laser therapy on orthodontics: rate of tooth movement, pain, and release of RANKL and OPG in GCF. Lasers Med Sci. 2013 Dec 18.

208. Genc G, Kocadereli I, Tasar F, Kilinc K, El S, Sarkarati B. Effect of low-level laser therapy (LLLT) on orthodontic tooth movement. Lasers Med Sci. 2013 Jan;28(1):41-7.

209. Turhani D, Scheriau M, Kapral D, Benesch T, Jonke E, Bantleon HP. Pain relief by single low-level laser irradiation in orthodontic patients undergoing fixed appliance therapy. Am J Orthod Dentofacial Orthop. 2006 Sep;130(3):371-7.

210. Kim WT, Bayome M, Park JB, Park JH, Baek SH, Kook YA. Effect of frequent laser irradiation on orthodontic pain. A single-blind randomized clinical trial. Angle Orthod. 2013 Jul;83(4):611-6.

211. Eslamian L, Borzabadi-Farahani A, Hassanzadeh-Azhiri A, Badiee MR, Fekrazad R. The effect of 810-nm low-level laser therapy on pain caused by orthodontic elastomeric separators. Lasers Med Sci. 2014 Mar;29(2):559-64.

212. Li FJ, Zhang JY, Zeng XT, Guo Y. Low-level laser therapy for orthodontic pain: a systematic review. Lasers Med Sci. 2014 Sep 26.

213. Lim HM, Lew KK, Tay DK. A clinical investigation of the efficacy of low level laser therapy in reducing orthodontic postadjustment pain. Am J Orthod Dentofacial Orthop. 1995 Dec;108(6):614-22.

214. Artes-Ribas M, Arnabat-Dominguez J, Puigdollers A. Analgesic effect of a low-level laser therapy (830 nm) in early orthodontic treatment. Lasers Med Sci. 2013 Jan;28(1):335-41.

215. Dominguez A, Velasquez SA. Effect of low-level laser therapy on pain following activation of orthodontic final archwires: a randomized controlled clinical trial. Photomed Laser Surg. 2013 Jan;31(1):36-40.

216. Shimizu N, Yamaguchi M, Goseki T, Shibata Y, Takiguchi H, Iwasawa T, et al. Inhibition of prostaglandin E2 and interleukin 1-beta production by low-power laser irradiation in stretched human periodontal ligament cells. J Dent Res. 1995 Jul;74(7):1382-8.

217. Torri S, Weber JB. Influence of low-level laser therapy on the rate of orthodontic movement: a literature review. Photomed Laser Surg. 2013 Sep;31(9):411-21.

218. Carvalho-Lobato P, Garcia VJ, Kasem K, Ustrell-Torrent JM, Tallon-Walton V, Manzanares-Cespedes MC. Tooth movement in orthodontic treatment with low-level laser therapy: a systematic review of human and animal studies. Photomed Laser Surg. 2014 May;32(5):302-9.

219. Ge MK, He WL, Chen J, Wen C, Yin X, Hu ZA, et al. Efficacy of low-level laser therapy for accelerating tooth movement during orthodontic treatment: a systematic review and meta-analysis. Lasers Med Sci. 2014 Feb 20.

220. Kawasaki K, Shimizu N. Effects of low-energy laser irradiation on bone remodeling during experimental tooth movement in rats. Lasers Surg Med. 2000;26(3):282-91.

221. Yoshida T, Yamaguchi M, Utsunomiya T, Kato M, Arai Y, Kaneda T, et al. Low-energy laser irradiation accelerates the velocity of tooth movement via stimulation of the alveolar bone remodeling. Orthod Craniofac Res. 2009 Nov;12(4):289-98.

222. Altan BA, Sokucu O, Ozkut MM, Inan S. Metrical and histological investigation of the effects of low-level laser therapy on orthodontic tooth movement. Lasers Med Sci. 2012 Jan;27(1):131-40.

223. Huang TH, Liu SL, Chen CL, Shie MY, Kao CT. Low-level laser effects on simulated orthodontic tension side periodontal ligament cells. Photomed Laser Surg. 2013 Feb;31(2):72-7.

224. Kim SJ, Kang YG, Park JH, Kim EC, Park YG. Effects of low-intensity laser therapy on periodontal tissue remodeling during relapse and retention of orthodontically moved teeth. Lasers Med Sci. 2013 Jan;28(1):325-33.

225. Cruz DR, Kohara EK, Ribeiro MS, Wetter NU. Effects of low-intensity laser therapy on the orthodontic movement velocity of human teeth: a preliminary study. Lasers Surg Med. 2004;35(2):117-20.

226. Youssef M, Ashkar S, Hamade E, Gutknecht N, Lampert F, Mir M. The effect of low-level laser therapy during orthodontic movement: a preliminary study. Lasers Med Sci. 2008 Jan;23(1):27-33.

227. Kim YD, Kim SS, Kim SJ, Kwon DW, Jeon ES, Son WS. Low-level laser irradiation facilitates fibronectin and collagen type I turnover during tooth movement in rats. Lasers Med Sci. 2008 Jul 4.

228. Fujita S, Yamaguchi M, Utsunomiya T, Yamamoto H, Kasai K. Low-energy laser stimulates tooth movement velocity via expression of RANK and RANKL. Orthod Craniofac Res. 2008 Aug;11(3):143-55.

229. Yamaguchi M, Hayashi M, Fujita S, Yoshida T, Utsunomiya T, Yamamoto H, et al. Low-energy laser irradiation facilitates the velocity of tooth movement and the expressions of matrix metalloproteinase-9, cathepsin K, and alpha(v) beta(3) integrin in rats. Eur J Orthod. 2010 Apr;32(2):131-9.

230. Franzen TJ, Zahra SE, El-Kadi A, Vandevska-Radunovic V. The influence of low-level laser on orthodontic relapse in rats. Eur J Orthod. 2014 Oct 6.

231. Saito S, Shimizu N. Stimulatory effects of low-power laser irradiation on bone regeneration in midpalatal suture during expansion in the rat. Am J Orthod Dentofacial Orthop. 1997 May;111(5):525-32.

232. Seifi M, Shafeei HA, Daneshdoost S, Mir M. Effects of two types of low-level laser wave lengths (850 and 630 nm) on the orthodontic tooth movements in rabbits. Lasers Med Sci. 2007 Nov;22(4):261-4.

233. Limpanichkul W, Godfrey K, Srisuk N, Rattanayatikul C. Effects of low-level laser therapy on the rate of orthodontic tooth movement. Orthod Craniofac Res. 2006 Feb;9(1):38-43.

234. Brin I, Tulloch JF, Koroluk L, Philips C. External apical root resorption in Class II malocclusion: a retrospective review of 1- versus 2-phase treatment. Am J Orthod Dentofacial Orthop. 2003 Aug;124(2):151-6.

235. Brudvik P, Rygh P. Root resorption after local injection of prostaglandin E2 during experimental tooth movement. Eur J Orthod. 1991 Aug;13(4):255-63.

236. Ong CK, Walsh LJ, Harbrow D, Taverne AA, Symons AL. Orthodontic tooth movement in the prednisolone-treated rat. Angle Orthod. 2000 Apr;70(2):118-25.

237. Sekhavat AR, Mousavizadeh K, Pakshir HR, Aslani FS. Effect of misoprostol, a prostaglandin E1 analog, on orthodontic tooth movement in rats. Am J Orthod Dentofacial Orthop. 2002 Nov;122(5):542-7.

238. Seifi M, Eslami B, Saffar AS. The effect of prostaglandin E2 and calcium gluconate on orthodontic tooth movement and root resorption in rats. Eur J Orthod. 2003 Apr;25(2):199-204.

239. Verna C, Hartig LE, Kalia S, Melsen B. Influence of steroid drugs on orthodontically induced root resorption. Orthod Craniofac Res. 2006 Feb;9(1):57-62.

240. Gameiro GH, Nouer DF, Pereira-Neto JS, de Araujo Magnani MB, de Andrade ED, Novaes PD, et al. Histological analysis of orthodontic root resorption in rats treated with the cyclooxygenase-2 (COX-2) inhibitor celecoxib. Orthod Craniofac Res. 2008 Aug;11(3):156-61.

241. Sainani K. The importance of accounting for correlated observations. PM R. 2010 Sep;2(9):858-61.

242. Friedmann H, Lubart R, Laulicht I, Rochkind S. A possible explanation of laser-induced stimulation and damage of cell cultures. J Photochem Photobiol B. 1991 Oct;11(1):87-91.

243. Karu TI, Pyatibrat LV, Afanasyeva NI. A novel mitochondrial signaling pathway activated by visible-to-near infrared radiation. Photochem Photobiol. 2004 Sep-Oct;80(2):366-72.

244. Gao X, Xing D. Molecular mechanisms of cell proliferation induced by low power laser irradiation. J Biomed Sci. 2009 Jan 12;16:4,0127-16-4.

245. Morimoto Y, Arai T, Kikuchi M, Nakajima S, Nakamura H. Effect of low-intensity argon laser irradiation on mitochondrial respiration. Lasers Surg Med. 1994;15(2):191-9.

246. Karu TI. Mitochondrial signaling in mammalian cells activated by red and near-IR radiation. Photochem Photobiol. 2008 Sep-Oct;84(5):1091-9.

247. Stroud DA, Ryan MT. Mitochondria: organization of respiratory chain complexes becomes cristae-lized. Curr Biol. 2013 Nov 4;23(21):R969-71.

248. McBride HM, Neuspiel M, Wasiak S. Mitochondria: more than just a powerhouse. Curr Biol. 2006 Jul 25;16(14):R551-60.

249. Brookes PS, Yoon Y, Robotham JL, Anders MW, Sheu SS. Calcium, ATP, and ROS: a mitochondrial love-hate triangle. Am J Physiol Cell Physiol. 2004 Oct;287(4):C817-33.

250. Salmon CR, Tomazela DM, Ruiz KG, Foster BL, Paes Leme AF, Sallum EA, et al. Proteomic analysis of human dental cementum and alveolar bone. J Proteomics. 2013 Oct 8;91:544-55.

251. Li S, Ge S, Yang P. Immunohistochemical localization of connective tissue growth factor, transforming growth factor-beta1 and phosphorylated-smad2/3 in the developing periodontium of rats. J Periodontal Res. 2014 Oct;49(5):624-33.

252. Thomas HF. Root formation. Int J Dev Biol. 1995 Feb;39(1):231-7.

253. Lester KS. The unusual nature of root formation in molar teeth of the laboratory rat. J Ultrastruct Res. 1969 Sep;28(5):481-506.

254. Toomarian L, Fekrazad R, Tadayon N, Ramezani J, Tuner J. Stimulatory effect of low-level laser therapy on root development of rat molars: a preliminary study. Lasers Med Sci. 2012 May;27(3):537-42.

255. Foster BL, Nagatomo KJ, Nociti FH,Jr, Fong H, Dunn D, Tran AB, et al. Central role of pyrophosphate in acellular cementum formation. PLoS One. 2012;7(6):e38393.

256. Klein L, Lemel MS, Wolfe MS, Shaffer J. Cyclosporin A does not affect the absolute rate of cortical bone resorption at the organ level in the growing rat. Calcif Tissue Int. 1994 Oct;55(4):295-301.

257. Peli JF, Oriez D. Rate and growth pattern of radicular apical third tissue apposition in tetracycline-labeled rats. J Endod. 1999 Apr;25(4):251-6.

258. Pinzon RD, Kozlov M, Burch WP. Histology of rat molar pulp at different ages. J Dent Res. 1967 Jan-Feb;46(1):202-8.

259. Chan EK, Darendeliler MA. Exploring the third dimension in root resorption. Orthod Craniofac Res. 2004 May;7(2):64-70.

260. Gonzales C, Hotokezaka H, Darendeliler MA, Yoshida N. Repair of root resorption 2 to 16 weeks after the application of continuous forces on maxillary first molars in rats: a 2- and 3-dimensional quantitative evaluation. Am J Orthod Dentofacial Orthop. 2010 Apr;137(4):477-85.

261. Chan EK, Darendeliler MA, Petocz P, Jones AS. A new method for volumetric measurement of orthodontically induced root resorption craters. Eur J Oral Sci. 2004 Apr;112(2):134-9.

262. Kuhn G, Schultz M, Muller R, Ruhli FJ. Diagnostic value of micro-CT in comparison with histology in the qualitative assessment of historical human postcranial bone pathologies. Homo. 2007;58(2):97-115.

263. Bouxsein ML, Boyd SK, Christiansen BA, Guldberg RE, Jepsen KJ, Muller R. Guidelines for assessment of bone microstructure in rodents using micro-computed tomography. J Bone Miner Res. 2010 Jul;25(7):1468-86.

264. Particelli F, Mecozzi L, Beraudi A, Montesi M, Baruffaldi F, Viceconti M. A comparison between micro-CT and histology for the evaluation of cortical bone: effect of polymethylmethacrylate embedding on structural parameters. J Microsc. 2012 Mar;245(3):302-10.

265. Hara T, Tanck E, Homminga J, Huiskes R. The influence of microcomputed tomography threshold variations on the assessment of structural and mechanical trabecular bone properties. Bone. 2002 Jul;31(1):107-9.

266. Hangartner TN. Thresholding technique for accurate analysis of density and geometry in QCT, pQCT and microCT images. J Musculoskelet Neuronal Interact. 2007 Jan-Mar;7(1):9-16.

267. Cooper D, Turinsky A, Sensen C, Hallgrimsson B. Effect of voxel size on 3D micro-CT analysis of cortical bone porosity. Calcif Tissue Int. 2007 Mar;80(3):211-9.

268. Colby LA, Morenko BJ. Clinical considerations in rodent bioimaging. Comp Med. 2004 Dec;54(6):623-30.

269. Proffit WR, editor. Contemporary Orthodontics. 5th ed ed. St. Louis, Mo.: Elsevier/Mosby; 2013.

270. Pandis N, Walsh T, Polychronopoulou A, Katsaros C, Eliades T. Split-mouth designs in orthodontics: an overview with applications to orthodontic clinical trials. Eur J Orthod. 2013 Dec;35(6):783-9.

271. Lindskog S, Pierce AM, Blomlof L, Hammarstrom L. The role of the necrotic periodontal membrane in cementum resorption and ankylosis. Endod Dent Traumatol. 1985 Jun;1(3):96-101.

272. Trope M. Root resorption of dental and traumatic origin: classification based on etiology. Pract Periodontics Aesthet Dent. 1998 May;10(4):515-22.

273. Wang Z, McCauley LK. Osteoclasts and odontoclasts: signaling pathways to development and disease. Oral Dis. 2011 Mar;17(2):129-42.

274. Rodan SB, Rodan GA. Integrin function in osteoclasts. J Endocrinol. 1997 Sep;154 Suppl:S47-56.

275. Fuller K, Ross JL, Szewczyk KA, Moss R, Chambers TJ. Bone is not essential for osteoclast activation. PLoS One. 2010 Sep 17;5(9):10.1371/journal.pone.0012837.

276. Chambers TJ, Fuller K. How are osteoclasts induced to resorb bone? Ann N Y Acad Sci. 2011 Dec;1240:1-6.

277. Bi Y, Nielsen KL, Kilts TM, Yoon A, A Karsdal M, Wimer HF, et al. Biglycan deficiency increases osteoclast differentiation and activity due to defective osteoblasts. Bone. 2006 Jun;38(6):778-86.

278. Baek KH, Oh KW, Lee WY, Lee SS, Kim MK, Kwon HS, et al. Association of oxidative stress with postmenopausal osteoporosis and the effects of hydrogen peroxide on osteoclast formation in human bone marrow cell cultures. Calcif Tissue Int. 2010 Sep;87(3):226-35.

279. Cervellati C, Bonaccorsi G, Cremonini E, Bergamini CM, Patella A, Castaldini C, et al. Bone mass density selectively correlates with serum markers of oxidative damage in post-menopausal women. Clin Chem Lab Med. 2013 Feb;51(2):333-8.

280. Cervellati C, Bonaccorsi G, Cremonini E, Romani A, Fila E, Castaldini MC, et al. Oxidative stress and bone resorption interplay as a possible trigger for postmenopausal osteoporosis. Biomed Res Int. 2014;2014:569563.

281. Bartell SM, Kim HN, Ambrogini E, Han L, Iyer S, Serra Ucer S, et al. FoxO proteins restrain osteoclastogenesis and bone resorption by attenuating H2O2 accumulation. Nat Commun. 2014 Apr 30;5:3773.

282. Jin Z, Li X, Wan Y. Nuclear Receptor Regulation of Osteoclast and Bone Remodeling. Mol Endocrinol. 2014 Dec 30:me20141316.

283. Altan AB, Bicakci AA, Mutaf HI, Ozkut M, Inan VS. The effects of low-level laser therapy on orthodontically induced root resorption. Lasers Med Sci. 2015 Jan 30.

284. Murrell EF, Yen EH, Johnson RB. Vascular changes in the periodontal ligament after removal of orthodontic forces. Am J Orthod Dentofacial Orthop. 1996 Sep;110(3):280-6.

APPENDICES

Extra Analyses of the First Animal Experiment Results

According to the study design of the first animal experiment, different statistical analyses were applicable. In the body of our thesis (see Results 7.1), we chose the most appropriate statistical model. However, based on the statistical assumptions, the following are all the possible tests that are still valid to perform on the data of the first animal experiment.

Additional Analyses for the Micro-CT Data

Several statistical tests were possible to perform on the data set obtained from the micro-CT analyses of the first animal experiment. Because there is a relationship between root-volume immediately before treatment start (Time 0) and at the end of the two-week treatment (Time 1), ANCOVA test was used to measure the effect of each treatment on the root volume change from Time 0 to Time 1, using the root-volume at Time 0 as a covariate factor that could affect the treatment outcome. Moreover, the repeated measure ANOVA test was also used in this data set since each root volume value was measured at multiple times. On the other hand, by ignoring the root-volume at Time 0 as a covariate, additional non-parametric analyses were done on another set of values that created mathematically to directly compare the root volume difference between Time 1 and Time 0.

Parametric Statistical Tests

ANCOVA

Analysis of Covariance (ANCOVA) was considered to be a good tool for this data set because there is a relationship between root-volume at Time 0 and root-volume after two weeks of treatment (Time 1); therefore it is possible that the root-volume at Time 0 (covariate) could be a strong predictive factor of the root-volume after two weeks of treatment. Moreover, including root-volume at Time 0 factor as a predictor along with the treatment factor, will give us a smaller error term and a larger F ratio for assessment of the main effect of each treatment factor.

The most appropriate ANCOVA model was calculated by removing the highest non-significant interaction one at a time (only if the variable was not included in any significant interaction). This process can be followed from the first model in the first Table 24, to the final one in the second following Tables 25:

Dependent Variable: root-volume at Time1						
Source	Type III Sum of Squares	df	Mean Square	F	Sig.	Partial Eta Squared
Corrected Model	.284	5	.057	11.413	.000	.826
Intercept	.076	1	.076	15.348	.002	.561
Treatment	.009	2	.005	.932	.420	.134
Time0	.079	1	.079	15.902	.002	.570
Treatment * Time0	.001	2	.000	.096	.909	.016
Error	.060	12	.005			
Total	23.308	18				
Corrected Total	.344	17				

Table 24: first table of ANCOVA test of between subjects effect.

Dependent Variable: root-volume at Time1						
Source	Type III Sum of Squares	df	Mean Square	F	Sig.	Partial Eta Squared
Corrected Model	.283	3	.094	21.769	.000	.823
Intercept	.199	1	.199	45.773	.000	.766
Treatment	.104	2	.052	12.019	.001	.632
Time0	.176	1	.176	40.588	.000	.744
Error	.061	14	.004			
Total	23.308	18				
Corrected Total	.344	17				

Table 25: final table of ANCOVA test of between subjects effects.

From the first ANCOVA model (Table 24), the interaction (Treatment by root-volume at Time0) was not significant (p=0.909) which mean that there is no (Treatment by root-volume at Time0) effect on the final root-volume after two weeks treatment. This is also means that the homogeneity of regression assumption is met for these data.

From the final ANCOVA model (Table 25), Treatment factor had a statistically significant effect (p=0.001) on the difference of the mean root-volume after two weeks of treatment once we've controlled for the root-volume at time zero. Moreover, 63% of the variability in the root-volume after two weeks could be accounted for the Treatment factor.

Table 26 shows the root-volume means, after two weeks of each treatment, once they adjusted for the covariate factor, which is root-volume at Time 0.

Dependent Variable: root-volume at Time1				
Treatment	Mean	Std. Error	95% Confidence Interval	
			Lower Bound	Upper Bound
Control	1.152[a]	.027	1.094	1.210
CsA	1.027[a]	.027	.969	1.085
LLLT	1.210[a]	.027	1.152	1.267
a. Covariates appearing in the model are evaluated at the following values: root-volume at Time0 = 0.7309.				

Table 26: estimated means adjusted for the covariate factor.

Table 27 compares the root-volume means between the treatment groups, after two weeks, once they adjusted for the covariate factor (root-volume at Time 0).

Dependent Variable: root-volume at Time1						
(I) Treatment	(J) Treatment	Mean Difference (I-J)	Std. Error	Sig.	95% Confidence Interval for Difference	
					Lower Bound	Upper Bound
Control	CsA	.125	.038	.006	.043	.207
	LLLT	-.058	.038	.155	-.140	.025
CsA	Control	-.125	.038	.006	-.207	-.043
	LLLT	-.182	.038	.000	-.264	-.101
LLLT	Control	.058	.038	.155	-.025	.140
	CsA	.182	.038	.000	.101	.264
Based on estimated marginal means						

Table 27: pairwise comparisons once adjusted for the covariate factor.

LLLT treatment has a significant effect on the root-volume change between Time 0 and Time 1 compared with the CsA treatment. The root-volume increased significantly from time-zero to two-weeks ($p<0.001$) on the LLLT group compared with the CsA treatment.

However, there is no significant difference effect on root-volume change between time-zero and two-weeks when compare between LLLT treatment and control groups. On the other hand, during two weeks period, the root volume increased significantly on control group compare to CsA treatment (p=0.006)

Dependent Variable: root-volume at Time1							
Parameter	B	Std. Error	t	Sig.	95% Confidence Interval		Partial Eta Squared
					Lower Bound	Upper Bound	
Intercept	.666	.087	7.629	.000	.479	.854	.806
[Treatment=Control]	-.058	.038	-1.504	.155	-.140	.025	.139
[Treatment=CSA]	-.182	.038	-4.794	.000	-.264	-.101	.621
[Treatment=LLLT]	0[a]	.	.	.	.	.	.
Time0	.743	.117	6.371	.000	.493	.993	.744
a. This parameter is set to zero because it is redundant.							

Table 28: parameter estimates.

From the previous Table 28, the estimated regression equations of root volume for each treatment was calculated as following formulas:

Time-1-root-volume = (B0 + B1 Treatment) + B2*Time-0-root-volume

Control

Time-1-root-volume = (B0 + B1 Treatment) + B2*Time-0-root-volume

= (0.666 – 0.058) + 0.743 *Time-0-root-volume

= 0.608 + 0.743 *Time-0-root-volume

CsA

Time-1-root-volume = (B0 + B1 Treatment) + B2*Time-0-root-volume

= (0.666 – 0.182) + 0.743 *Time-0-root-volume

= 0.484 + 0.743 *Time-0-root-volume

LLLT

Time-1-root-volume = (B0 + B1 Treatment) + B2*Time-0-root-volume

= (0.666 + 0) + 0.743 *Time-0-root-volume

= 0.666 + 0.743 *Time-0-root-volume

The following scatter plot (Figure 24) represents the estimated regression equation of root volume for each treatment

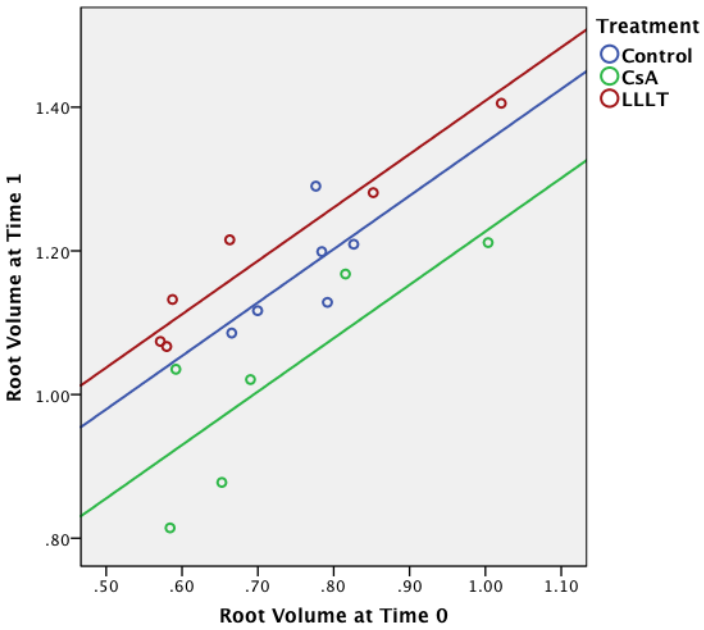

Figure 26: estimated regression of root volume for each treatment.

Repeated Measure ANOVA

In a repeated measure, or within subject factor, each root volume value was measured at multiple times. Examining the within subject factor by comparing means of root volume values at two different times, immediately before treatment start (Time 0) and at the end of the two-week treatment (Time 1); and the effect of time on mean root volume between treatment groups. The between subject factor effect is the comparison between the overall mean root-volume of different treatment groups.

Within-subject factor: Two level time root-volume

Between- subject factor: Treatment (LLLT, CsA and control)

Null hypotheses for repeated measure ANOVA

(1) Hypothesis for the within-subject factor:

Ho: mean root-volume is the same in Time 0 and Time 1

(2) Hypothesis for between-subject factor:

Ho: the main effects of LLLT, CsA and control are the same on overall mean root volume

(3) Hypothesis for interaction:

Ho: the effect of time on mean root volume is the same between LLLT, CsA and control

The sample is too small to evaluate if the assumption of multivariate normality is satisfied.

Source		Type III Sum of Squares	df	Mean Square	F	Sig.
Root Volume	Sphericity Assumed	1.430	1	1.430	524.565	.000
	Greenhouse-Geisser	1.430	1.00	1.430	524.565	.000
	Huynh-Feldt	1.430	1.00	1.430	524.565	.000
	Lower-bound	1.430	1.00	1.430	524.565	.000
Root Volume * Treatment	Sphericity Assumed	.052	2	.026	9.627	.002
	Greenhouse-Geisser	.052	2.00	.026	9.627	.002
	Huynh-Feldt	.052	2.00	.026	9.627	.002
	Lower-bound	.052	2.00	.026	9.627	.002
Error(Root Volume)	Sphericity Assumed	.041	15	.003		
	Greenhouse-Geisser	.041	15.00	.003		
	Huynh-Feldt	.041	15.00	.003		
	Lower-bound	.041	15.00	.003		

Table 29: repeated measure ANOVA test of within-subject effect.

From the previous Table 29, mean root volume is not the same ($p<0.001$) across the two time points, meaning that the null hypothesis for the within-subject factor should be rejected. Therefore, the mean root-volume is the significantly different between Time 0 and Time 1 regardless of the treatment effect.

Moreover, the effect of time on mean root volume is not the same ($p=0.002$) between the treatment groups; which mean that the null hypothesis for the interaction should be rejected. Therefore, the treatment factor caused a significant effect on the change of mean root volume between Time 0 and Time 1. In other words, there is a significant difference between treatment groups in the amount of change in mean root volume between Time 0 and Time 1

Source	Type III Sum of Squares	df	Mean Square	F	Sig.
Intercept	31.149	1	31.149	907.545	.000
Treatment	.061	2	.031	.894	.430
Error	.515	15	.034		

Table 30: repeated measure ANOVA test of between-subject effect.

The test of between-subject effect (Table 30) shows no significant difference (p=0.430) between groups on their overall mean root-volume. The null hypothesis for the between-subject factor was accepted, meaning that, when neglecting the effect of time, there is no main effect of treatment on overall mean root volume.

The following plot (Figure 25) summarizes the effect of time on mean root volume between the different treatments.

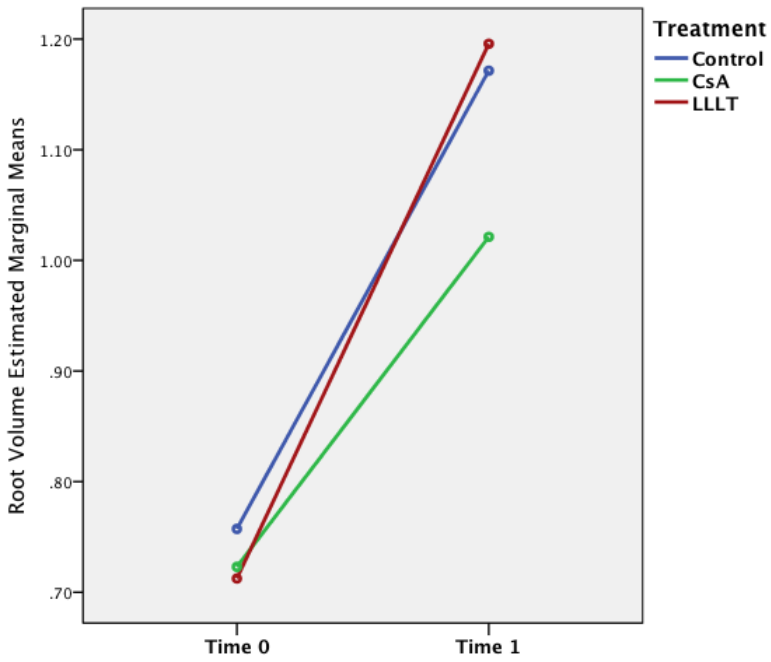

Figure 27: effect of time on mean root volume between the different treatments.

Pearson Correlation

The following Table 31 shows the Pearson correlation between the root-volume difference (difference between Time 1 and Time 0 volume) and between the baseline root volume (at Time 0). The correlation is not strongly negative, which could mean that the difference of the root volume at the base line between the treatment groups is not strongly affecting the outcome root volume of each treatment.

		Time0	Root volume difference
Root volume at Time0	Pearson Correlation	1	-.341
	Sig.		.166
	Number of sample	18	18
Root Volume Difference	Pearson Correlation	-.341	1
	Sig.	.166	
	Number of sample	18	18

Table 31: correlation between the root-volume difference the baseline root volume.

In summary: either ANCOVA or Repeated Measure ANOVA can be used to analyze this pre-test / post-test type of data. In ANCOVA, when we take into account baseline root volume (at Time 0) as covariate, we found that mean root volume after two weeks is significantly different ($p=0.001$) between all treatment groups. The root volume increased significantly on the control group compared with the CsA treatment ($p=0.006$), but there was no significant difference when compared the LLLT group with the control. This finding was also supported by Repeated Measure ANOVA as there was a significant interaction value between time and treatment, which means that the effect of time on mean root volume is not the same ($p=0.002$) between the treatment groups.

Although both analyses gave slightly different results, both ANCOVA and Repeated Measure ANOVA point to the same pattern of group differences in this study. Moreover, there is no strong correlation between the root-volume difference and the baseline root-volume (at Time 0). In this scenario the choice between both parametric analyses methods did not appear to make a substantial difference in the nature of the conclusions about the outcome results.

Non-Parametric Statistical Tests

Compare root volume difference

Another value was created, from this type of data, and subjected to non-parametric analyses. Root-Volume-Difference (RVD) values were calculated by mathematic subtracting of the root volume value, obtained from micro-CT analyses, at the end of the two-week treatment (Time 1), from the volume value of the same root immediately before treatment start (Time 0).

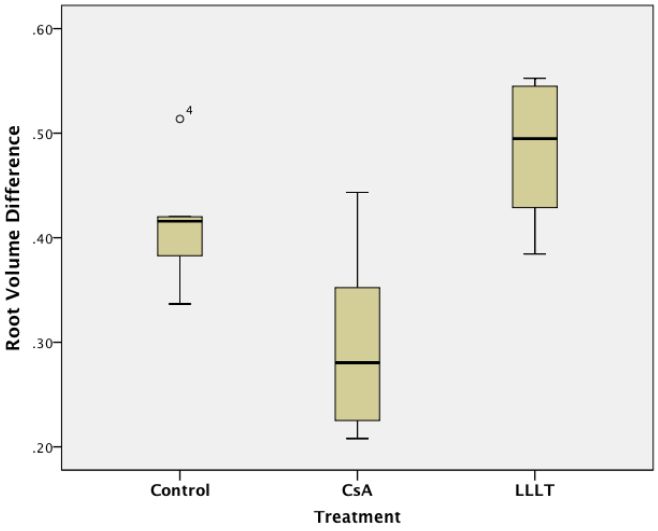

Figure 28: Root-Volume-Difference of each treatment group.

The previous box-plot (Figure 26) compares Root-Volume-Difference (RVD) of the three treatment groups (CsA, LLLT treatment and control).

Kruskal-Wallis test (Table 32) shows that the mean Root-Volume-Difference (RVD) is not the same (p-value=0.012) between treatment groups, which indicates a significant difference on mean RVD between the three treatment groups.

Null Hypothesis	Test	Sig.	Decision
The distribution of **root volume difference** is the same across categories of all treatment groups	Independent-Samples Kruskal-Wallis Test	0.012	**Reject** the null hypothesis
The significant level is 0.05			

Table 32: Kruskal-Wallis test of RVD between all groups.

To identify where the difference was, three different Mann-Whitney tests (the following tables) were done to compare Root-Volume-Difference (RVD) between every two distinct treatment groups.

According to Mann-Whitney test (Table 33), LLLT treatment has a significant effect on the RVD between Time 0 and Time 1 compared with the CsA treatment. The root-volume of LLLT groups increased significantly in two weeks (p=0.009) compared with the CsA group.

Null Hypothesis	Test	Sig.	Decision
The distribution of **root volume difference** is the same across categories of LLLT and CsA treatment groups	Independent-Samples Mann-Whitney U Test	0.009	**Reject** the null hypothesis
The significant level is 0.05			

Table 33 Mann-Whitney test of RVD between LLLT and CsA groups.

Another Mann-Whitney test (Table 34) compares root-volume-difference of two treatment groups (CsA treatment and control). There is no significant difference between the two weeks CsA treatment and the control group regarding the root-volume-difference.

Null Hypothesis	Test	Sig.	Decision
The distribution of **root volume difference** is the same across categories of CsA treatment and Control groups	Independent-Samples Mann-Whitney U Test	0.065	**Retain** the null hypothesis
The significant level is 0.05			

Table 34: Mann-Whitney test of RVD between CsA group and control.

Moreover, another Mann-Whitney test was done (Table 35) to compare root-volume-difference of two treatment groups (LLLT treatment and control). There is no significant difference between the two weeks LLLT treatment and the control group regarding the root-volume-difference.

Null Hypothesis	Test	Sig.	Decision
The distribution of **root volume difference** is the same across categories of LLLT treatment and Control groups	Independent-Samples Mann-Whitney U Test	0.093	**Retain** the null hypothesis
The significant level is 0.05			

Table 35: Mann-Whitney test of RVD between LLLT group and control.

Parametric Analyses of the Histomorphometric Data

The data obtained from the histomorphometric analyses of the first experiment had met the statistical assumptions to allow the application of the following parametric test.

ANOVA

In order to test and compare the total cementum thickness in all the treatment groups at the same time, one-way ANOVA test was performed with the following null hypothesis:

Ho: the mean amount of total cementum thickness formed by each treatment is the same.

Total Cementum thickness					
	Sum of Squares	df	Mean Square	F	Sig.
Between Groups	15897.704	2	7948.852	9.973	.002
Within Groups	11955.521	15	797.035		
Total	27853.225	17			

Table 36: one-way ANOVA test of total cementum thickness.

One-way ANOVA (Table 36) shows a significant value (p=0.002), which indicates strong evidence against the null hypothesis. Therefore, at least one of the treatments has a significant effect on the mean amount of cementum formation in rat's dental root surfaces.

A multiple comparison test (Table 37) was done for further investigations about the effect of the different treatments in the mean amount of cementum thickness on rat's dental root surfaces. In conclusion, two weeks of LLLT treatment had significantly increased the amount of cementum thickness on rat's dental root surfaces in comparison to both CsA treatment (p=0.002) and control (p=0.001).

Dependent Variable: Total Cementum thickness LSD Test						
(I) Treatment	(J) Treatment	Mean Difference (I-J)	Std. Error	Sig.	95% Confidence Interval	
					Lower Bound	Upper Bound
Control	CsA	-3.304	16.300	.842	-38.046	31.438
	LLLT	-64.630	16.300	.001	-99.372	-29.888
CsA	Control	3.304	16.300	.842	-31.438	38.046
	LLLT	-61.326	16.300	.002	-96.068	-26.584
LLLT	Control	64.630	16.300	.001	29.888	99.372
	CsA	61.326	16.300	.002	26.584	96.068

Table 37 multiple comparisons of total cementum thickness between groups.

On the other hand, there is no difference between the two weeks CsA treatment and the control group regarding the cementum thickness on rat's dental root surfaces. It could be concluded that, two weeks of CsA treatment has no significant effect on the cementum formation in rat's dental root surfaces in comparison to control group.

Extra Analyses of the Second Animal Experiment Results

The following supplementary statistical tests were performed on the data obtained from the micro-CT analyses of the second animal experiment.

Additional Analyses for the Micro-CT Data

The Paired Samples t-test was consider the appropriate statistical model to investigate the effect cementum remodeling on the root resorption caused by orthodontic tooth movement (see Results 7.2). However, the violation of normality assumption necessitates the performing of the following tests in order to validate the results that used in the body of our thesis.

Paired Samples t-test of Log Transformed Data

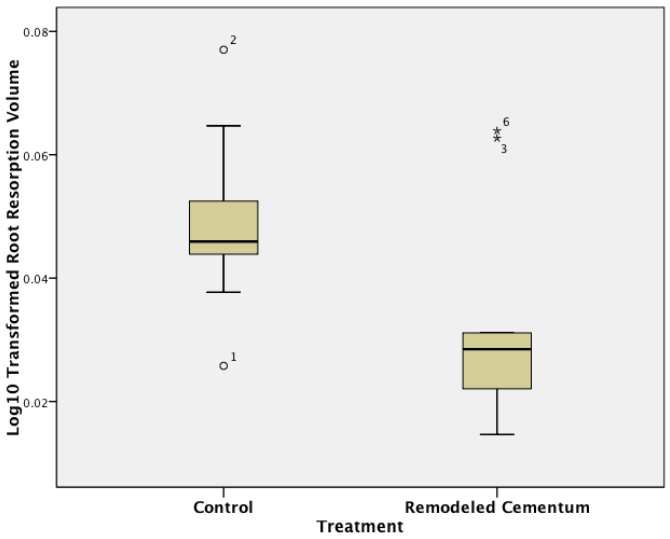

Figure 29: log-transformed data of total root resorption volume in both treatment groups.

Due to the presence of positive skewness and multiple outliers in total root resorption volume data of the Remodeled-Cementum group, a log transformation on the raw data was performed. The previous box-plot (Figure 27) compares the

log-transformed data of total resorption volume of the mesial root, caused by the orthodontic tooth movement, between both groups.

Both groups showed considerable enhancement regarding the normality of the transformed data, however, the Remodeled-Cementum group still showing positive skewness and multiple outliers. Moreover, the Kolmogorov-Smirnov and Shapiro-Wilk tests are still showing significant p-values for the Remodeled-Cementum group (Table 38).

	Kolmogorov-Smirnov			Shapiro-Wilk		
	Statistic	df	Sig.	Statistic	df	Sig.
log10_Control	.193	9	.200	.962	9	.823
log10_Remodeled Cementum	.334	9	.005	.800	9	.021

Table 38: tests of normality of log-transformed total resorption volume data.

The results of Paired Samples t-tests on the log-transformed data were similar to the one on the raw data (Table 39). There is a significant difference (p=0.025) in the total amount of root resorption volume caused by orthodontic tooth movement between the former LLLT treated roots and control. Therefore, roots that received LLLT treatment for two weeks showed significantly less root resorption due to the subsequent orthodontic tooth movement when compared with the control.

Pair 1	Paired Differences					t	df	Sig.
	Mean	Std. Deviation	Std. Error Mean	95% Confidence Interval of the Difference				
				Lower	Upper			
(log10)Control – (log10)Remodeled Cement	.0157	.0172	.0057	.0025	.0289	2.745	8	.025

Table 39 Paired Samples t-test of log-transformed total resorption volume data.

Moreover, two different Paired Samples t-tests (Table 40) showed no significant difference on the amount the orthodontically induced resorption volumes when comparing the log-transformed data of both roots' two halves: the mesial-buccal (p=0.055) and the distal-lingual (p=0.150) aspects, between the Remodeled-Cementum group and control. These results were similar to the analyses of the raw data.

		Paired Differences					t	df	Sig. (2-tailed)
		Mean	Std. Deviation	Std. Error Mean	95% Confidence Interval of the Difference				
					Lower	Upper			
Pair 1	log10_DL_Control - log10_DL_Remodeled	.0058	.0109	.0036	-.0026	.0142	1.592	8	.150
Pair 2	log10_MB_Control - log_MB_Remodeled	.0106	.0142	.0047	-.0003	.0215	2.245	8	.055

Table 40 Paired Samples t-test of log-transformed data at mesial-buccal (MB), and distal-lingual (DL) surfaces.

Non-Parametric Tests

Due to the presence of positive skewness and multiple outliers in Remodeled-Cementum group in both raw and log-transformed data, the following non-parametric test on the raw data was performed.

Null Hypothesis	Test	Sig.	Decision
The median of differences of **total root resorption** between **Control** and **Remodeled Cementum** groups equals 0	Related-Samples Wilcoxon Signed Rank Test	0.028	**Reject** the null hypothesis
The significant level is 0.05			

Table 41 Wilcoxon Signed Rank test of total root resorption volume.

Non-parametric Wilcoxon Signed Rank test (Table 41) showed a significant difference (p=0.028) in the total amount of root resorption volume caused by orthodontic tooth movement between the former LLLT treated roots and control. This result was similar to the parametric analyses; therefore, roots that received LLLT treatment for two weeks showed significantly less root resorption due to the subsequent orthodontic tooth movement when compared with the control. In other words, the preexisting root surfaces remodeling caused by two weeks LLLT treatment has a significant protective effects against root resorption due to the four weeks orthodontic tooth movement.

Moreover, two different non-parametric Wilcoxon Signed Rank tests showed no significant difference on the amount the orthodontically induced resorption volumes when comparing the Remodeled-Cementum group and control in regard to both roots' two halves: the mesial-buccal (p=0.066) and the distal-lingual (p=0.110) aspects, as shown respectively in the following table (Tables 42). These results were also similar to the parametric analyses.

Null Hypothesis	Test	Sig.	Decision
The median of differences of **Mesial-Buccal root resorption** between **Control** and **Remodeled Cementum** groups equals 0	Related-Samples Wilcoxon Signed Rank Test	0.066	**Retain** the null hypothesis
The median of differences of **Distal-Lingual root resorption** between **Control** and **Remodeled Cementum** groups equals 0	Related-Samples Wilcoxon Signed Rank Test	0.110	**Retain** the null hypothesis
The significant level is 0.05			

Table 42 Wilcoxon Signed Rank test of both mesial-buccal and distal-lingual root surfaces resorption volume.